SYNTHESES, CHARACTERIZATION AND OPTICAL PROPERTIES OF FLUORINE CONTAINING BENZIMIDAZOLE DERIVATIVES

A THESIS SUBMITTED TO
THE GRADUATE SCHOOL OF NATURAL AND APPLIED SCIENCES
OF
MIDDLE EAST TECHNICAL UNIVERSITY

BY

MERVE İLERİ

IN PARTIAL FULFILLMENT OF THE REQUIREMENTS
FOR
THE DEGREE OF MASTER OF SCIENCE
IN
CHEMISTRY

JANUARY 2015

Approval of the thesis:

SYNTHESES, CHARACTERIZATION AND OPTICAL PROPERTIES OF FLUORINE CONTAINING BENZIMIDAZOLE DERIVATIVES

submitted by **MERVE İLERİ** in partial fulfillment of the requirements for the degree of **Master of Science in Chemistry Department, Middle East Technical University** by,

Prof. Dr. Gülbin Dural Ünver _____
Dean, Graduate School of **Natural and Applied Sciences**

Prof. Dr. İlker Özkan _____
Head of Department, **Chemistry**

Prof. Dr. Levent Toppare _____
Supervisor, **Chemistry Dept., METU**

Assoc. Prof. Dr. Ali Çırpan _____
Co-Supervisor, **Chemistry Dept., METU**

Examining Committee Members:

Assoc. Prof. Dr. Metin Ak _____
Chemistry Dept., Pamukkale University

Prof. Dr. Levent Toppare _____
Chemistry Dept., METU

Assoc. Prof. Dr. Ali Çırpan _____
Chemistry Dept., METU

Assoc. Prof. Dr. Emren Nalbant Esentürk _____
Chemistry Dept., METU

Dr. Görkem Günbaş _____
Chemistry Dept., METU

Date: 09.01.2015

I hereby declare that all information in this document has been obtained and presented in accordance with academic rules and ethical conduct. I also declare that, as required by these rules and conduct, I have fully cited and referenced all material and results that are not original to this work.

Name, Last Name: Merve İLERİ

Signature:

ABSTRACT

SYNTHESES, CHARACTERIZATION AND OPTICAL PROPERTIES OF FLUORINE CONTAINING BENZIMIDAZOLE DERIVATIVES

İleri, Merve

M. S., Department of Chemistry

Supervisor: Prof. Dr. Levent Toppare

Co-Supervisor: Assoc. Prof. Dr. Ali Çırpan

January 2015, 99 pages

In the last decades use of conducting polymers as electrochromic materials attracted tremendous attention all over the world due to properties like processability, high optical contrasts, fast switching times and tuning band gap via structural modifications. Low band gap polymers are pursued in order to increase the conductivity. For that matter donor – acceptor – donor theory is the most effective and commonly used method. The donor – acceptor – donor approach is not only used for obtaining low band gap polymers, but also for producing polymers with improved optical, mechanical and electronic properties. Based on donor – acceptor – donor approach, the electron donating groups raise the highest occupied molecular orbital level and electron withdrawing groups lower the lowest unoccupied molecular orbital level. In this study, novel donor – acceptor – donor type monomers were designed,

synthesized and polymerized electrochemically. In the first part of the thesis study, para- and meta- substituted fluorine containing benzimidazole derivatives as an acceptor moiety and thiophene as the donor moiety were used. Monomers, 2-(4-fluorophenyl)-4,7-di(thiophen-2-yl)-1H-benzo[d]imidazole (M1) and 2-(3-fluorophenyl)-4,7-di(thiophen-2-yl)-1H-benzo[d]imidazole (M2) were synthesized via Stille coupling and electrochemically polymerized. The position of fluorine was varied from para- to meta- in order to investigate position effects on the electrochemical and optical properties of electrochemically synthesized polymers. Both polymers were p-dopable and switched between orange and blue color during doping/dedoping. In the second part of this study, synthesis of two novel monomers including perfluorophenyl containing benzimidazole as the acceptor unit and thiophene and 3,4-ethylenedioxythiophene as the donor units were performed. 2-(Perfluorophenyl)-4,7-di(thiophen-2-yl)-1H-benzo[d]imidazole (M3) and 4,7-bis(2,3-dihydrothieno[3,4-b][1,4]dioxin-5-yl)-2-(perfluorophenyl)-1H-benzo[d]imidazole (M4) were synthesized and polymerized electrochemically. The effect of electron donating moieties on the optical properties of electrochemically polymerized polymers was investigated.

Keywords: Conducting polymers, benzimidazole, electrochromism, donor–acceptor theory, substitution effect, fluorine, donor effect.

ÖZ

FLOR İÇEREN BENZİMİDAZOL TÜREVLERİNİN SENTEZİ, KARAKTERİZASYONU VE OPTİK ÖZELLİKLERİ

İleri, Merve
Yüksek Lisans, Kimya Bölümü
Tez Yöneticisi: Prof. Dr. Levent Toppare
Ortak Tez Yöneticisi: Doç. Dr. Ali Çırpan

Ocak 2015, 99 sayfa

İletken polimerlerin elektrokromik materyal olarak kullanımı; işlenebilirlik, yüksek optik contrast, hızlı dönüşüm zamanı ve yapısal modifikasyonlarla ayarlanabilen bant aralığı gibi özelliklerinden dolayı tüm dünyada son birkaç on yıl içinde büyük ilgi çekmektedirler. İletkenliği artırmak amacıyla düşük bant aralığına sahip polimerler elde edilmeye çalışılmaktadır. Bunun için en etkili ve yaygın kullanılan yöntem donör – akseptör – donör teorisidir. Verici – alıcı – verici yaklaşımı sadece düşük bant aralığına sahip polimerleri elde etmek için kullanılmaz, aynı zamanda geliştirilmiş optik, mekanik ve elektronik özelliklere sahip polimerlerin üretilmesi için kullanılır. Verici – alıcı – verici yaklaşımına dayanarak; elektron verici gruplar, dolu olan en yüksek enerjili moleküler orbital seviyesini yükseltirler ve elektron alıcı gruplar, boş olan en düşük enerjili moleküler orbital seviyesini düşürürler. Bu

çalışmada, yeni donör – akseptör – donör türdeki monomerler dizayn edildi, sentezlendi ve elektrokimyasal yöntemle polimerleştirildi. Tez çalışmasının ilk kısmında; akseptör ünitesi olarak para- ve meta- pozisyonunda flor içeren benzimidazol türevleri ve donör ünitesi olarak tiyofen kullanılmıştır. Monomerler, 2-(4-florofenil)-4,7-di(tiyofen-2-il)-1H-benzo[d]imidazol (M1) ve 2-(3-florofenil)-4,7-di(tiyofen-2-il)-1H-benzo[d]imidazol (M2) sentezlendi ve elektrokimyasal olarak polimerleştirildi. Sübstitüent olarak kullanılan florun para- meta- pozisyon etkisini incelemek amacıyla, elektrokimyasal olarak sentezlenen polimerlerin elektrokimyasal ve optik özellikleri çalışılmıştır. Her iki polimerde de p- tipi katkılanma ve "doping / dedoping" sırasında turuncu ve mavi renk arasında geçiş gözlenmiştir. Bu çalışmanın ikinci kısmında, akseptör ünitesi olarak perflorofenil içeren benzimidazol ve donör olarak tiyofen ve 3,4- etilendioksitiyofen içeren yeni monomerlerin sentezi yapılmıştır. 2-(Perflorofenil)-4,7-di(tiyofen-2-yl)-1H-benzo[d]imidazol (M3) ve 4,7-bis(2,3-dihidrotieno[3,4-b][1,4]dioksin-5-yl)-2-(perflorofenil)-1H-benzo[d]imidazol (M4) sentezlenmiştir ve elektrokimyasal olarak polimerleştirilmiştir. Elektron verici grupların, elektrokimyasal olarak sentezlenen polimerlerin optik özelliklerinin üzerindeki etkisi incelenmiştir.

Anahtar kelimeler: İletken polimerler, benzimidazol, elektrokromism, donör – akseptör teorisi, sübstitüent etkisi, flor, donör etkisi.

to my precious family and Cem..

ACKNOWLEDGMENTS

I would like to thank my supervisor Prof. Dr. Levent Toppare for his aspiring guidance, endless support, invaluable constructive criticism, patience, suggestions and encouragement. His advices on my research as well as my life have been priceless for me and I believe that his words will remain in a corner of my mind throughout my life.

I would like to express my thanks to my co-supervisor Assoc. Prof. Dr. Ali Çırpan for his understanding, support and funny jokes. He always gives nice energy to the laboratory environment.

I would like to thank Assoc. Prof. Dr. Yasemin Arslan Udum for her help and valuable discussions on electrochemistry.

I would like to express the deepest appreciation to Dr. Görkem Günbaş for endless support and motivation in my research and career. He always shares his boundless knowledge with me and it has been an honor for me to work with him in the same project.

I would like to express my special thanks to Şerife Özdemir Hacıoğlu for teaching me both organic synthesis and electrochemical studies. She has been not only a guide for me in the laboratory but also caring me like a mother at all times. Words cannot express my feelings. She will always remain as a private person in all my life.

I would like to thank Ebru Işık for being one of my best friends since undergraduate years, her real friendship, precious memories and happy times. I know she will always be there for me and support me when I need.

I would like to thank Pelin Erdek and Nur Çiçek Kekeç for their nice friendships, always being together with me and long phone calls. They always support and encourage me even if they are far away.

I would like to thank Seza Göker for helping me in all times, make me laugh with funny jokes, coffee breaks and numerous shopping. She has supported me in all aspects of my life and provided me an excellent working environment in D-156 Laboratory.

I would like to thank Melis Kesik for her friendship, non-continuous diets and enjoyable moments.

I would like to thank Çağla İstanbulluoğlu for her kind friendship, working with her until midnights, sharing a lot of things and making a smile on my face.

I would like to thank Seda Çömez for her friendship and colorimetric experiments.

I would like to express my thanks to my home mate Esra Özdemir for spending excellent times with me, her nice friendship and being thoughtful.

I would like to thank Nehir Utku for her kind friendship, wonderful voice and giving me the most suitable nickname.

I would like to thank Esra Öğün for being my friend, moral support and fun times. I believe long distances cannot break our nice friendship.

I would like to express my thanks to Şevki Can Cevher, Gönül Hızalan Özsoy and Saniye Söylemez for their kind friendships and spending good times in the working environment.

I would like to thank Emre Ataoğlu and Janset Turan for their nice friendships, coffee breaks and for being a lovely couple.

I would like to express my special appreciation to my precious family for believing me without any questioning, supporting me throughout my life spiritually and giving me a chance under all circumstances. Without their support I would not have come to these days.

I would like to express my deepest thanks and appreciation to Cem Özcan for his true great love, endless support, being understanding and being always there for me in all times. For five years, he has been a romantic and made wonderful surprises for me. He always creates a big smile on my face even if in my miserable and desperate moments. Words cannot express my thoughts. I would not succeed and complete my thesis study without him and his support.

TABLE OF CONTENTS

ABSTRACT v
ÖZ vii
ACKNOWLEDGMENTS x
TABLE OF CONTENTS xiii
LIST OF TABLES xvi
LIST OF FIGURES xvii
LIST OF ABBREVIATIONS xxi
CHAPTERS
1 INTRODUCTION 1
1.1 Conjugated Polymers 1
1.2 Band Theory 2
1.3 Conduction Mechanism in Conducting Polymers 6
1.3.1 Solitons, Polarons, Bipolarons 6
1.3.2 Doping Process in Conducting Polymers 7
1.4 Synthesis of Conducting Polymers 9
1.4.1 Mechanism of Electropolymerization 11
1.4.2 Factors Affecting Electrochemical Polymerization 14
1.5 Characterization Methods of Electrochromic Polymers 15
1.6 Electrochromism 15
1.7 Electrochromic Devices 16
1.7.1 Construction of Electrochromic Devices 16
1.7.2 Preparation of the gel electrolyte 17
1.7.3 Characterization of Electrochromic Devices 18
1.8 Low Band Gap Polymers 19
1.9 Benzimidazole Derivatives as an Acceptor Moiety in Conducting Polymers 21
1.10 Aim of This Work 22

2 EXPERIMENTAL 23
2.1 Materials 23
2.2 Methods and Equipments 23
2.3 Syntheses of Monomers 24
2.3.1 Synthesis of 4,7-dibromobenzo[c][1,2,5]thiadiazole 24
2.3.2 Synthesis of 3,6-dibromo-1,2-phenylenediamine 25
2.3.3 Synthesis of 4,7-dibromo-2-(4-fluorophenyl)-1H-benzo[d]imidazole 26
2.3.4 Synthesis of tributyl(thiophene-2-yl)stannane 28
2.3.5 Synthesis of 2-(4-fluorophenyl)-4,7-di(thiophen-2-yl)-1H-benzo[d]imidazole 29
2.3.6 Synthesis of 4,7-dibromo-2-(3-fluorophenyl)-1H-benzo[d]imidazole 31
2.3.7 Synthesis of 2-(3-fluorophenyl)-4,7-di(thiophen-2-yl)-1H-benzo[d]imidazole 32
2.3.8 Synthesis of 4,7-dibromo-2-(perfluorophenyl)-1H-benzo[d]imidazole 34
2.3.9 Synthesis of 2-(perfluorophenyl)-4,7-di(thiophen-2-yl)-1H-benzo[d]imidazole 35
2.3.10 Synthesis of tributyl(2,3-dihydrothieno[3,4-b][1,4]dioxin-5-yl)stannane 37
2.3.11 Synthesis of 4,7-bis(2,3-dihydrothieno[3,4-b][1,4]dioxin-5-yl)-2-(perfluorophenyl)-1H-benzo[d]imidazole 38
3 RESULTS AND DISCUSSION 41
3.1 Electrochemical Properties of Donor – Acceptor – Donor Type Polymers 41
3.1.1 Electrochemical and Optical Properties of M1 and M2 41
3.1.1.1 Electrochemical Polymerization of M1 and M2 41
3.1.1.2 Scan rate dependence of M1 and M2 45
3.1.1.3 Spectroelectrochemical and Colorimetric Studies of P1 and P2 47
3.1.1.4 Electrochromic contrast and switching studies of P1 and P2 52
3.1.2 Electrochemical and Optical Properties of M3 and M4 55
3.1.2.1 Electrochemical Polymerization of M3 and M4 55
3.1.2.2 Scan rate dependence of M3 and M4 59
3.1.2.3 Spectroelectrochemical and Colorimetric Studies of P3 and P4 60

3.1.2.4 Electrochromic contrast and switching studies of P3 and P4 65
4 CONCLUSION 69
REFERENCES 73
APPENDICES
A. NMR SPECTRA OF SYNTHESIZED MONOMERS 81

LIST OF TABLES

TABLES

Table 3.1 Summary of electrochemical and spectroelectrochemical properties of P1 and P2 48

Table 3.2 Colorimetry results of P1 and P2 51

Table 3.3 Summary of kinetic and optic studies of P1 and P2 54

Table 3.4 Summary of electrochemical and spectroelectrochemical properties of P3 and P4 63

Table 3.5 Colorimetry results of P3 and P4 65

Table 3.6 Summary of percent transmittance changes and switching times of P3 and P4 at corresponding wavelengths 67

LIST OF FIGURES

FIGURES

Figure 1.1 Common conducting polymer structures: (a) polyacetylene, (b) polythiophene, (c) polyaniline, (d) poly(3,4-ethylenedioxythiophene), (e) polyfuran, (f) polypyrrole, (g) polycarbazole, (h) polyphenylene .. 2

Figure 1.2 The band structure in conducting polymers 3

Figure 1.3 Band structures of conductors, semiconductors and insulators..... 4

Figure 1.4 The generation of band structures in conjugated polymers..... 5

Figure 1.5 Representation of charge carriers 7

Figure 1.6 The formation of charge carriers in polythiophene upon oxidation 8

Figure 1.7 Chemical synthesis of polythiophene by means of metal catalyzed coupling 10

Figure 1.8 Oxidative chemical polymerization of thiophene via iron (III) chloride 10

Figure 1.9 Electrochemical polymerization of thiophene..... 11

Figure 1.10 Electropolymerization mechanism of heterocycles X = O, S or N-R) (ECE)..... 13

Figure 1.11 Schematic illustration of dual type transmissive /absorptive electrochromic devices 17

Figure 1.12 The methods for the alteration of the band gap..... 20

Figure 1.13 Common benzazole derivatives: (a) benzothiadiazole, (b) benzimidazole, (c) benzotriazole, (d) benzoselenadiazole, (e) benzooxadiazole 21

Figure 2.1 Synthetic route for 4,7-dibromobenzo[c][1,2,5]thiadiazole..... 25

Figure 2.2 Synthetic route for 3,6-dibromo-1,2-phenylenediamine 26

Figure 2.3 Synthetic route for 4,7-dibromo-2-(4-fluorophenyl)-1H-benzo[d]imidazole 27

Figure 2.4 Synthetic route for tributyl(thiophene-2-yl)stannane 29
Figure 2.5 Synthetic route for 2-(4-fluorophenyl)-4,7-di(thiophen-2-yl)-1H-benzo[d]imidazole 30
Figure 2.6 Synthetic route for 4,7-dibromo-2-(3-fluorophenyl)-1H-benzo[d]imidazole 32
Figure 2.7 Synthetic route for 2-(3-fluorophenyl)-4,7-di(thiophen-2-yl)-1H-benzo[d]imidazole 33
Figure 2.8 Synthetic route for 4,7-dibromo-2-(perfluorophenyl)-1H-benzo[d]imidazole 35
Figure 2.9 Synthetic route for 2-(perfluorophenyl)-4,7-di(thiophen-2-yl)-1H-benzo[d]imidazole 36
Figure 2.10 Synthetic route for tributyl(2,3-dihydrothieno[3,4-b][1,4]dioxin-5-yl)stannane 38
Figure 2.11 Synthetic route for 4,7-bis(2,3-dihydrothieno[3,4-b][1,4]dioxin-5-yl)-2-(perfluorophenyl)-1H-benzo[d]imidazole 39
Figure 3.1 Electropolymerization of M1 and M2 42
Figure 3.2 Repeated potential scan polymerization of (a) M1 and (b) M2 at 100 mV s^{-1} in 0.1 M $LiClO_4$/$NaClO_4$ CH_2Cl_2/ACN (5:95, v:v) solution on an ITO electrode 43
Figure 3.3 Single scan cyclic voltammograms of (a) P1 and (b) P2 in a monomer free 0.1 M $LiClO_4$/$NaClO_4$ ACN solution 44
Figure 3.4 Scan rate dependence of (a) P1 film and (b) P2 film in a monomer free 0.1 M $NaClO_4$ - $LiClO_4$ / ACN solution at 50, 100, 150, 200, 250 and 300 mV.s^{-1}. 46
Figure 3.5 Electronic absorption spectra for (a) P1 and (b) P2 films in 0.1 M $NaClO_4$–$LiClO_4$/ACN solution between 0.0 V and 1.2 V for P1 , 0.0 V and 1.15 V for P2. 48
Figure 3.6 Structures of the polymers and their colors at their neutral and different oxidized states 50

Figure 3.7 Optical contrasts and switching times monitored at different wavelengths for (a) P1 and (b) P2 in 0.1 M $NaClO_4$–$LiClO_4$/ACN solution 53
Figure 3.8 Electropolymerization of M3 and M4 56
Figure 3.9 Repeated potential scan polymerization of (a) M3 and (b) M4 at 100 mV s^{-1} in 0.1 M $LiClO_4$/$NaClO_4$ CH_2Cl_2/ACN (5:95, v:v) solution on an ITO electrode 57
Figure 3.10 Single scan cyclic voltammograms of (a) P3 and (b) P4 in a monomer free 0.1 M $LiClO_4$/$NaClO_4$ ACN solution..... 58
Figure 3.11 Scan rate dependence of (a) P3 film and (b) P4 film in a monomer free 0.1 M $NaClO_4$ - $LiClO_4$ / ACN solution at 50, 100, 150, 200, 250 and 300 $mV.s^{-1}$ 60
Figure 3.12 Electronic absorption spectra for (a) P3 and (b) P4 films in 0.1 M $NaClO_4$–$LiClO_4$ / ACN solution between 0.5 and 1.2 V for P3, 0.2 and 1.1 V for P4..... 62
Figure 3.13 Structures of the polymers and their colors at their neutral and different oxidized states..... 64
Figure 3.14 Optical contrasts and switching times monitored at different wavelengths for (a) P3 and (b) P4 in a monomer free 0.1 M $NaClO_4$–$LiClO_4$/ACN solution 66
Figure A. 1 ^{1}H-NMR spectrum of 4,7-dibromobenzo[c][1,2,5]thiadiazole 81
Figure A. 2 ^{13}C-NMR spectrum of 4,7-dibromobenzo[c][1,2,5]thiadiazole 82
Figure A. 3 ^{1}H-NMR spectrum of 3,6-dibromo-1,2-phenylenediamine..... 83
Figure A. 4 ^{13}C-NMR spectrum of 3,6-dibromo-1,2-phenylenediamine 84
Figure A. 5 ^{1}H-NMR spectrum of 4,7-dibromo-2-(4-fluorophenyl)-1H-benzo[d]imidazole 85
Figure A. 6 ^{13}C-NMR spectrum of 4,7-dibromo-2-(4-fluorophenyl)-1H-benzo[d]imidazole 86
Figure A. 7 ^{1}H-NMR spectrum of tributyl(thiophene-2-yl)stannane 87
Figure A. 8 ^{13}C-NMR spectrum of tributyl(thiophene-2-yl)stannane 88

Figure A. 9 ^{1}H-NMR spectrum of 2-(4-fluorophenyl)-4,7-di(thiophen-2-yl)-1H-benzo[d]imidazole 89
Figure A. 10 ^{13}C-NMR spectrum of 2-(4-fluorophenyl)-4,7-di(thiophen-2-yl)-1H-benzo[d]imidazole 90
Figure A. 11 ^{1}H-NMR spectrum of 4,7-dibromo-2-(3-fluorophenyl)-1H-benzo[d]imidazole 91
Figure A. 12 ^{13}C-NMR spectrum of 4,7-dibromo-2-(3-fluorophenyl)-1H-benzo[d]imidazole 92
Figure A. 13 ^{1}H-NMR spectrum of 2-(3-fluorophenyl)-4,7-di(thiophen-2-yl)-1H-benzo[d]imidazole 93
Figure A. 14 ^{13}C-NMR spectrum of 2-(3-fluorophenyl)-4,7-di(thiophen-2-yl)-1H-benzo[d]imidazole 94
Figure A. 15 ^{1}H-NMR spectrum of 4,7-dibromo-2-(perfluorophenyl)-1H-benzo[d]imidazole 95
Figure A. 16 ^{1}H-NMR spectrum of 2-(perfluorophenyl)-4,7-di(thiophen-2-yl)-1H-benzo[d]imidazole 96
Figure A. 17 ^{1}H-NMR spectrum of tributyl(2,3-dihydrothieno[3,4-b][1,4]dioxin-5-yl)stannane 97
Figure A. 18 ^{13}C-NMR spectrum of tributyl(2,3-dihydrothieno[3,4-b][1,4]dioxin-5-yl)stannane 98
Figure A. 19 ^{1}H-NMR spectrum of 4,7-bis(2,3-dihydrothieno[3,4-b][1,4]dioxin-5-yl)-2-(perfluorophenyl)-1H-benzo[d]imidazole 99

LIST OF ABBREVIATIONS

A	Acceptor
ACN	Acetonitrile
AFM	Atomic Force Microscopy
Ag	Silver
BIm	Benzimidazole
CB	Conduction Band
$CDCl_3$	Deuterated chloroform
CE	Counter Electrode
$CHCl_3$	Chloroform
CIE	La Commission Internationale de l'Eclairage
CP	Conducting Polymer
CV	Cyclic Voltammetry
D	Donor
DCM	Dichloromethane
d-DMSO	Deuterated dimethyl sulfoxide
DSC	Differential Scanning Calorimetry
ECD	Electrochromic device
EDOT	3,4-Ethylenedioxythiophene
E_g	Band gap
E_g^{op}	Optical band gap
EtOH	Ethanol
Fc	Ferrocene
$FeCl_3$	Iron (III) chloride
FTIR	Fourier Transform Infrared Spectroscopy
GPC	Gel Permeation Chromatography
HOMO	Highest Occupied Molecular Orbital

HRMS	High Resolution Mass Spectrometer
ITO	Indium Tin Oxide
L, a, b	Luminance, hue, saturation
$LiClO_4$	Lithium perchlorate
LUMO	Lowest Unoccupied Molecular Orbital
$NaClO_4$	Sodium perchlorate
NIR	Near Infrared
NMR	Nuclear Magnetic Resonance Spectrometer
OFET	Organic Field Effect Transistor
OLED	Organic Light Emitting Diode
PA	Polyacetylene
PAn	Polyaniline
PC	1,2-propylenecarbonate
PMMA	Poly(methyl methacrylate)
Pt	Platinum
R_s	Sheet Resistance
SEM	Scanning Electron Microscopy
SHE	Standard Hydrogen Electrode
$TBAPF_6$	Tetrabutylammonium hexafluorophosphate
TGA	Thermal Gravimetric Analysis
THF	Tetrahydrofuran
TLC	Thin Layer Chromatography
TMS	Trimethylsilane
UV	Ultraviolet
VB	Valence Band
Vis	Visible
WO_3	Tungsten trioxide

CHAPTER 1

INTRODUCTION

1.1 Conjugated Polymers

Conjugated polymers have drawn considerable interest in the last decades due to properties like ease of processability, light weight, high optical contrast, low cost, wide range of colors, fast switching times and ability to tune the band gap via structural modifications [1-4]. This research area began with the studies of Henry Letheby in 1862. The anodic oxidation of aniline under acidic conditions onto platinum electrode was carried out and the electrochemical polymerization of aniline was performed [5]. After that, Alan MacDiarmid, Alan Heeger and Hideki Shirakawa found that polyacetylene acquired 10^9 times more conductivity than its original form by means of oxidation with iodine vapor. As a result, three scientists were awarded with the Nobel Prize in Chemistry for the discovery and development of conductive polymers in 2000 [6-9]. After that discovery, the area of conducting polymers had been increasing day by day and other aromatic and heterocyclic molecules were examined (Figure 1.1). The novel application fields like electrochromic devices (ECDs) [10-15], organic photovoltaics (OPVs) [16-20], biosensors [21-23], organic field effect transistors (OFETs) [24, 25] and organic light emitting diodes (OLEDs) [26, 27] have been actively pursued in the last few decades.

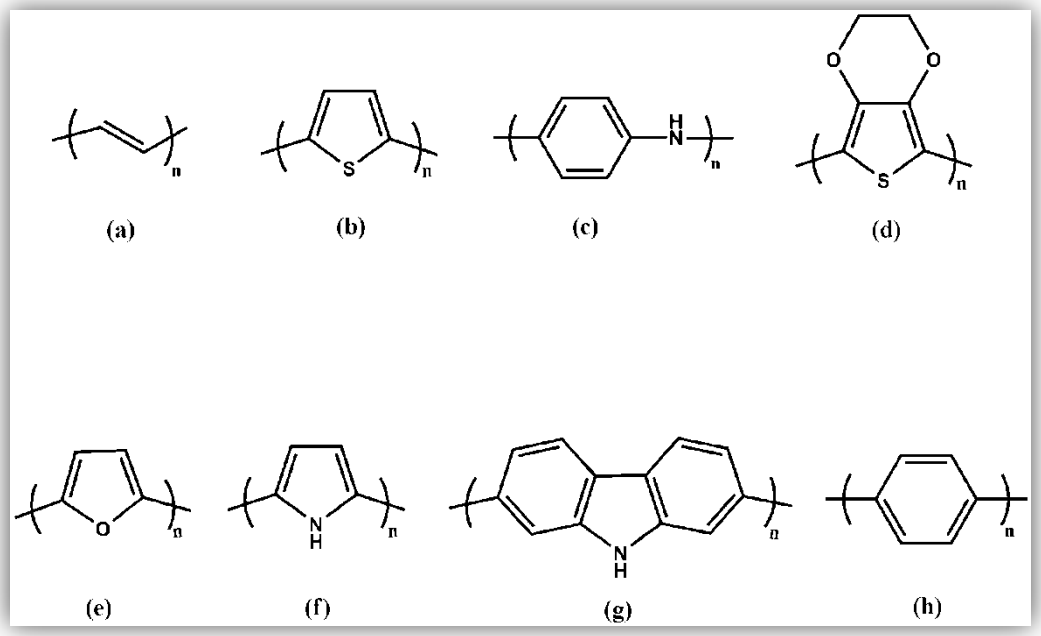

Figure 1.1 Common conducting polymer structures: (a) polyacetylene, (b) polythiophene, (c) polyaniline, (d) poly(3,4-ethylenedioxythiophene), (e) polyfuran, (f) polypyrrole, (g) polycarbazole, (h) polyphenylene

1.2 Band Theory

The band gap is the energy difference between valence band and conduction band and has tremendous effect on electronic and optical properties of the conjugated polymers [28, 29]. In literature, valence band is known as the highest occupied molecular orbital (HOMO) and conduction band is known as the lowest unoccupied molecular orbital (LUMO). Additionally, the band theory examines the properties of conductors, semiconductors and insulators. Based on this theory, conducting polymers belong to the class of semiconductors. In conductors, there is no difference between valence band and conduction band hence electrons can move easily. On the

contrary, in insulators, there is large spacing between valence band and conduction band hence there is no flow of electrons between VB and CB. In semiconductors, the band gap is smaller than insulators thus the valence band is partially empty and the conduction band is partially filled via few electrons.

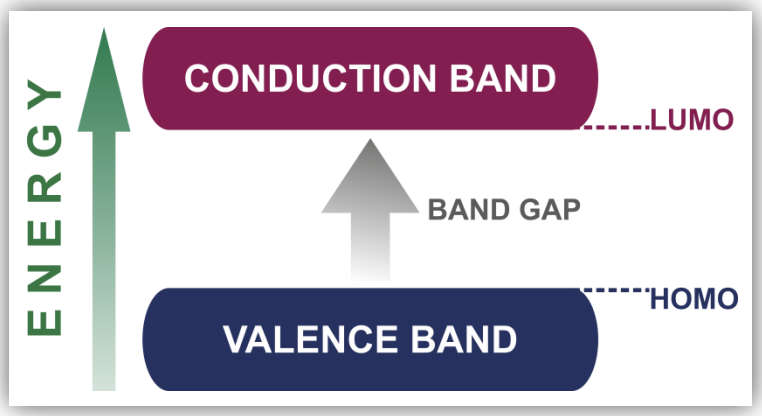

Figure 1.2 The band structure in conducting polymers

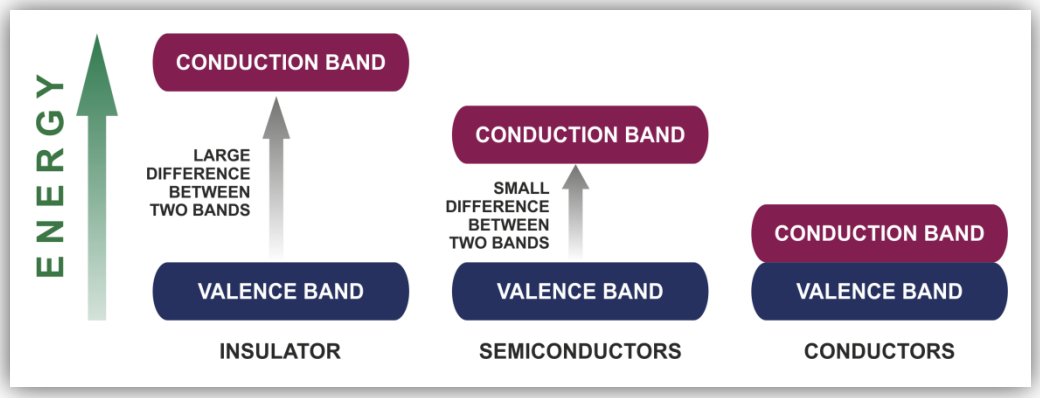

Figure 1.3 Band structures of conductors, semiconductors and insulators

So as to increase the conductivity, semiconductors can be doped with charge carriers which can be electrons (n-type) or holes (p-type). Moreover, the conductivity increases as the conjugation length increases. Hence the band gap decreases. Figure 1.4 illustrates the band structures of pyrrole and polypyrrole whereas conjugation increases a lower band gap is obtained.

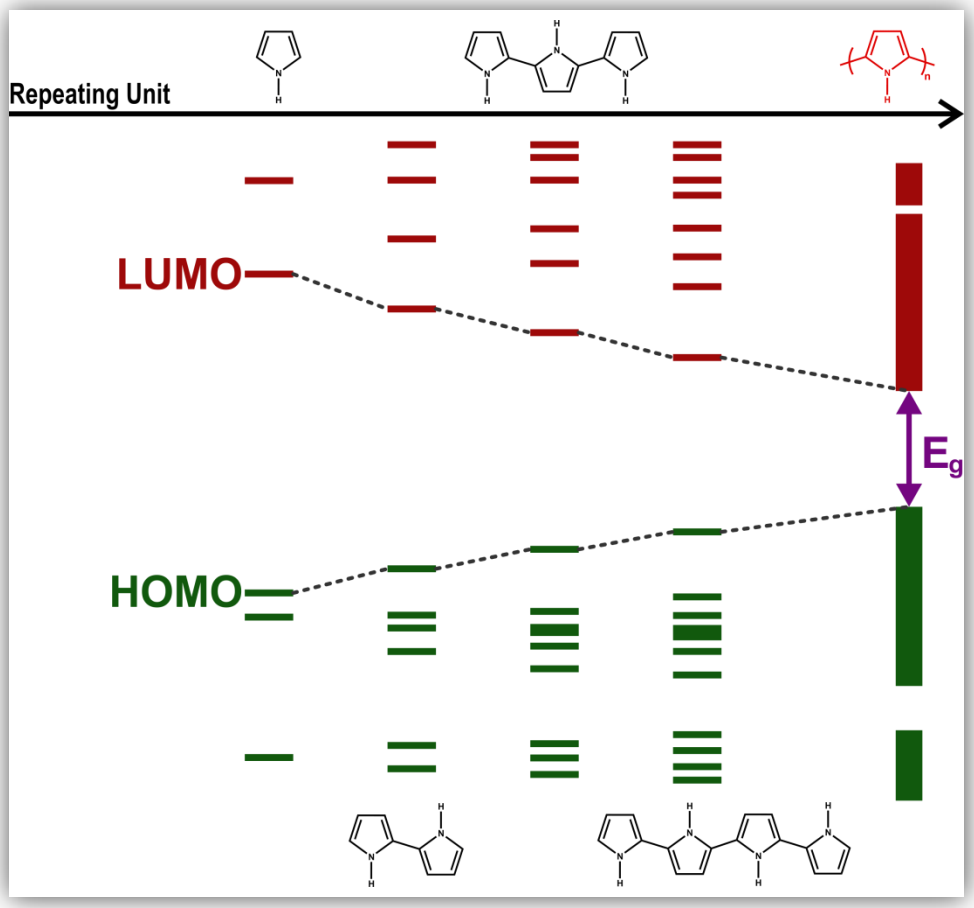

Figure 1.4 The generation of band structures in conjugated polymers

The band gap can be calculated from the onset of π- π^* transition in the UV-vis spectrum. On the other hand, from the difference between the onset of oxidation and reduction potentials in the cyclic voltammogram the band gap can be calculated.

1.3 Conduction Mechanism in Conducting Polymers

Conjugated polymers can be more conductive upon doping. The doped structures are different from that of neutral ones. In other words, the doped species of conducting polymers can be solitons, polarons and bipolarons which possess higher energy than the undoped polymer.

1.3.1 Solitons, Polarons, Bipolarons

Solitons, polarons and bipolarons which are conjugational defects are generated when the conjugated polymers are doped. As a result of the oxidation or reduction of the polymer, the charge carriers as p-type or n-type are produced. In other words, positive charge carriers (p-type) are generated when the polymer is oxidized where an electron is removed from the polymer. Polarons, radical cation, are formed after removal of an electron from the backbone of the polymer. Additionally, bipolarons are generated after removal of a second electron with further oxidation. On the other hand, negative charge carriers (n-type) are generated when the polymer is reduced where an electron is infused to the polymer.

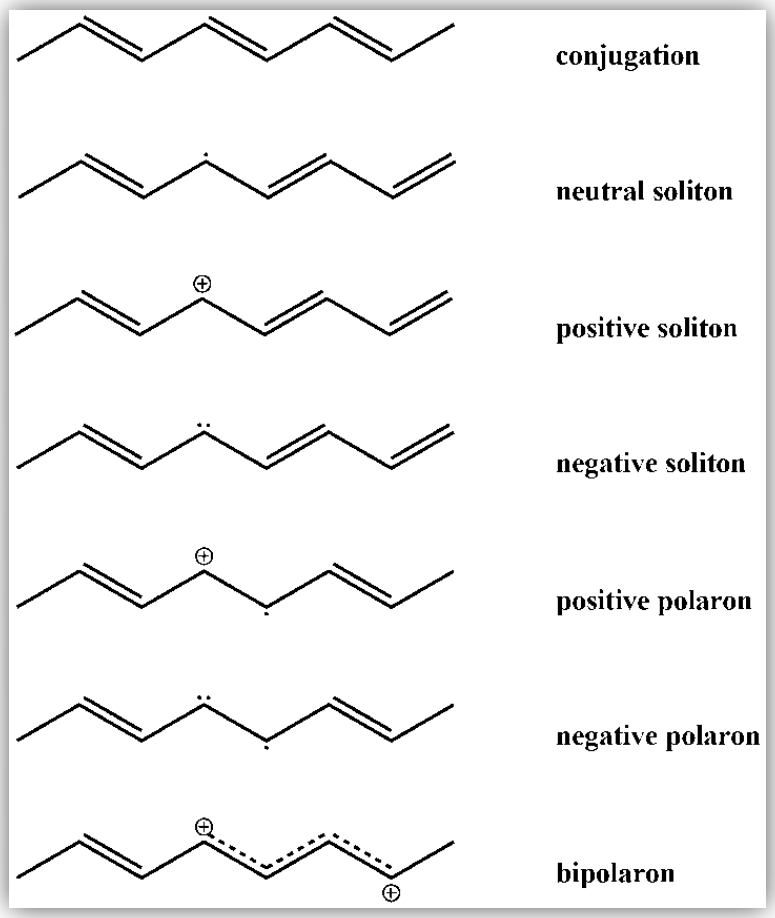

Figure 1.5 Representation of charge carriers

1.3.2 Doping Process in Conducting Polymers

The conductivity in conducting polymers can be increased upon doping. With the redox process, the doping process has been achieved by removal of an electron from the polymer backbone or injection of an electron to the backbone of the polymer. Figure 1.6 shows the charge carriers in the backbone of polythiophene when thiophene is oxidized with a suitable oxidant. Furthermore, the process of doping /

dedoping is reversible thus; the chemical characteristic of the polymer backbone does not vary.

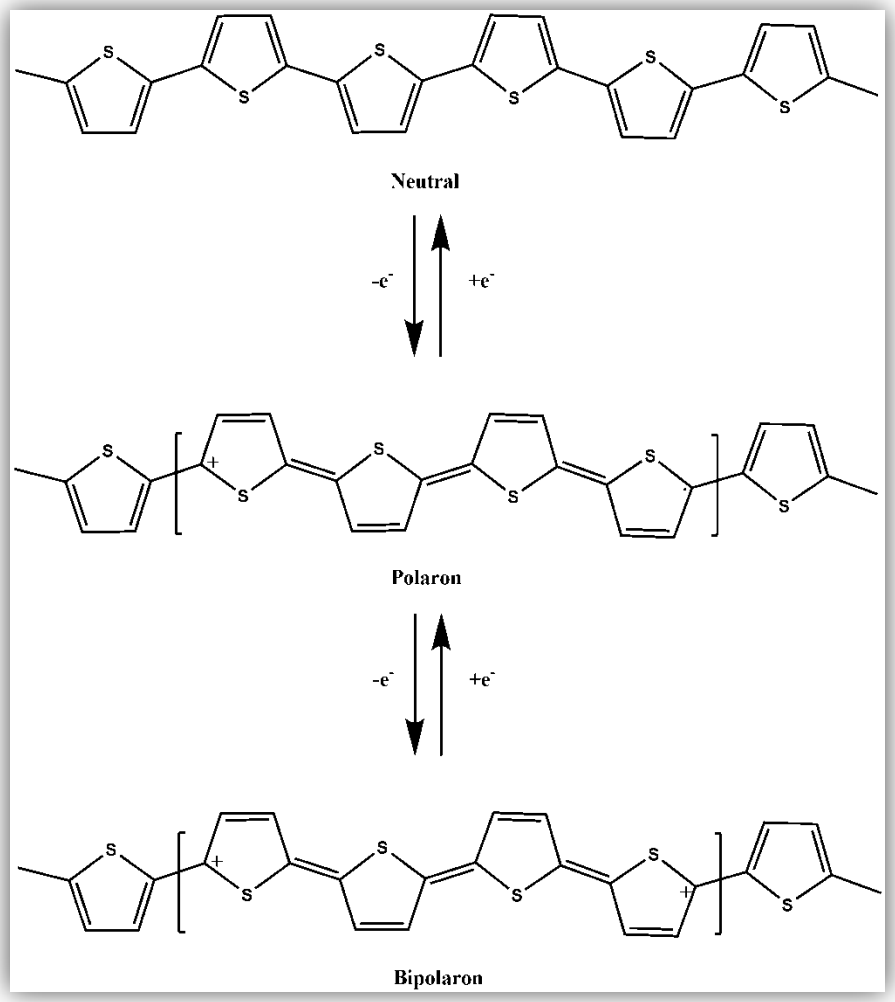

Figure 1.6 The formation of charge carriers in polythiophene upon oxidation

Electrochemical doping is the most useful method for examining doping process. In a convenient solvent system, the polymer film is biased with a suitable potential by means of electrochemical doping. The optical, mechanical and magnetic properties of the polymers can be varied by means of doping process.

1.4 Synthesis of Conducting Polymers

In the synthesis of conducting polymers, chemical and electrochemical polymerization techniques are mostly performed [30-32]. In fact, there are specific routes for the synthesis of conducting polymers such as metathesis polymerization, photochemical polymerization, Grignard reaction, solid-state polymerization and ring-opening metathesis. In chemical polymerization, polymers are generated as insulating in the neutral state and can be converted to a conducting regime by chemically or electrochemically. On the contrary, electrochemically synthesized polymers are obtained as conducting in the oxidized state.

In chemical polymerization, oxidation of monomer can be achieved using transition metal halides such as $FeCl_3$ or metal catalyzed coupling. Yamamoto reported the chemical synthesis of polythiophene via metal catalyzed coupling of 2,5-dibromothiophene in 1980 as shown in Figure 1.7 [33-35]. Additionally, Lin and Dudek stated another method of polymerization of thiophene in the presence of transition metal halides; nickel, palladium and iron etc. in same year as indicated in Figure 1.8 [36].

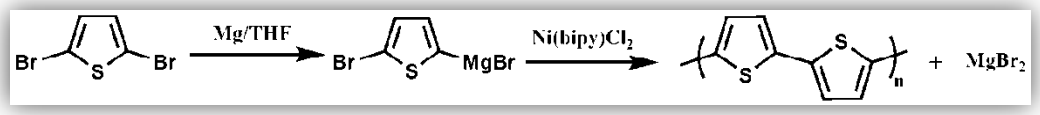

Figure 1.7 Chemical synthesis of polythiophene by means of metal catalyzed coupling

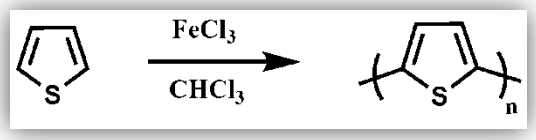

Figure 1.8 Oxidative chemical polymerization of thiophene via iron (III) chloride

In electrochemical polymerization method, a three electrode system which includes working, reference and counter electrodes is utilized. The solution contains monomer, organic solvent and supporting electrolyte. Polymers are coated onto working electrode in a monomer solution by applying suitable potentials. The electrochemical polymerization mechanism is shown in Figure 1.9.

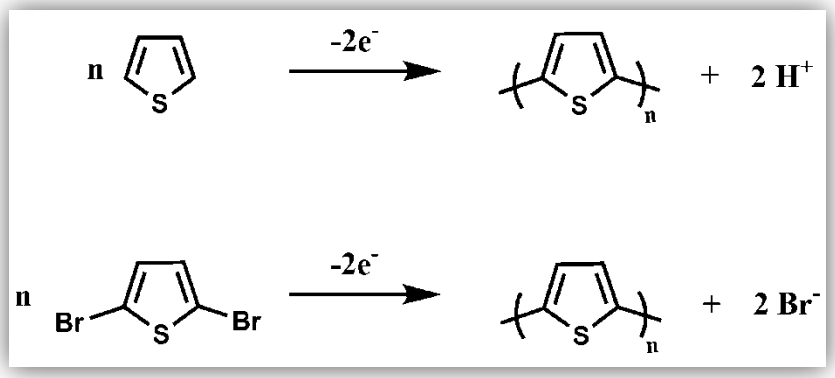

Figure 1.9 Electrochemical polymerization of thiophene

Despite the fact that chemical polymerization is commonly used for industry, electrochemical polymerization possesses a number of advantages; performing the synthesis in a short time and a simple way. Also small amounts of monomer; 5-50 mg, are enough for electrochemical polymerization and there is no need for further purification. The common drawback of electrochemical polymerization is that the polymer on working electrode is generally insoluble and it is difficult to characterize polymers via GPC and NMR.

1.4.1 Mechanism of Electropolymerization

Proposed mechanism for electropolymerization of heterocycles in which X may be O, S or N-R is represented in Figure 1.10. In the first step of electropolymerization, the oxidation of the monomer takes place and a radical cation is produced. As diffusion of the monomer from bulk occurs slower than the electron transfer reaction, high concentration of radicals is generated continuously near electrode area. In the

second step, coupling can occur in two ways, addition of radical cation to heterocyclic monomer or combination of two radical cations. In mechanism of radical – monomer coupling, the radical cation reacts with heterocyclic monomer so as to generate a neutral dimer via loss of two protons. After that, oxidized dimer radical cation and monomer react with each other and a trimer is produced. Propagation maintains respectively in order to generate a polymer. Based on ECE mechanism, electropolymerization takes place on sequential electrochemical and chemical routes up to insoluble oligomer in electrolyte solution and precipitation of oligomer on electrode surface. In a radical – radical coupling mechanism, two radicals couple with each other in order to form dihydro dimer dication by loss of two protons and rearomatization. As the dimer can be easily oxidized than monomer upon applied potential, it becomes in radical form and undergoes additional coupling with monomeric radical [37, 38].

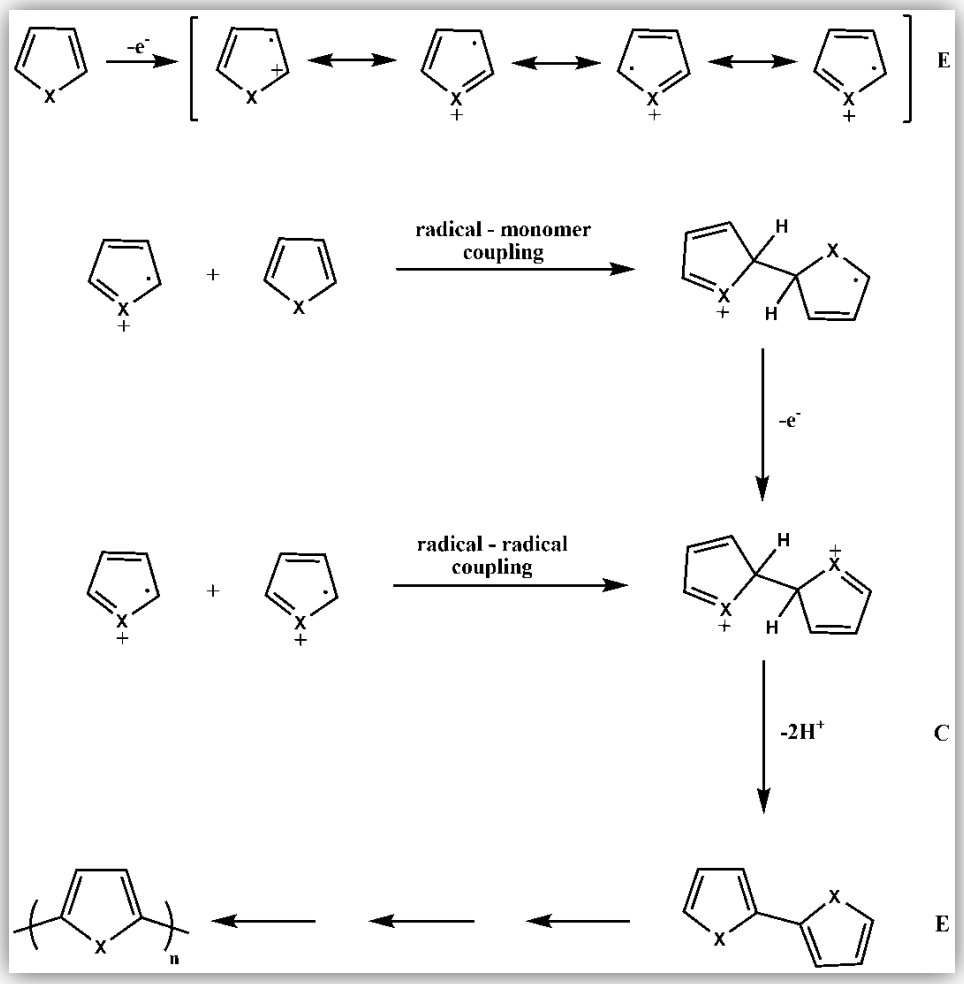

Figure 1.10 Electropolymerization mechanism of heterocycles X = O, S or N-R) (ECE)

1.4.2 Factors Affecting Electrochemical Polymerization

The influence of several parameters such as solvent, temperature, type of electrolyte and applied potential on electrical and morphological features of electrochemically synthesized polymers has been investigated.

The type of solvent is crucial for the electrochemical polymerization since it affects the electrical and physical properties of polymer. For efficient electropolymerization, a solvent should have high dielectric constant so as to provide ionic conductivity of the electrolytic medium and dissolve the supporting electrolyte. In addition, it should be highly resistant towards applied potential in terms of decomposition. To illustrate; acetonitrile, propylene carbonate, benzonitrile and nitrobenzene are commonly used solvents in electrochemical polymerization.

Supporting electrolyte provides electrical conductivity and doping of the polymer as one of ions of supporting electrolyte couples with a monomer. To achieve electrochemical polymerization, supporting electrolyte should not become electro active and nucleophilic. For instance, hexafluorophosphates and tetrafluoroborates, lithium or tetraalkylammonium salts of perchlorates are generally used as supporting electrolytes in electrochemical polymerization. As reported in literature, the conductivity of polypyrrole was found higher with perchlorate anions compare to one doped with tetrafluoroborate anions [39].

Working electrode plays an important role in polymerization process and features of resultant polymer. In general, polymers are coated onto noble metals like gold, platinum, titanium or optically transparent electrodes such as indium tin oxide coated glass slide.

The influence of temperature on electropolymerization is significant in terms of kinetics of polymerization and conductivity of the polymer. Based on stated papers, high temperature causes lower conductivity [40].

To avoid side reactions of oxidized polymer or radical cations, monomer concentration should be kept high (0.1 M).

1.5 Characterization Methods of Electrochromic Polymers

For characterization of conducting polymers, several analytical methods can be utilized. The more common technique is cyclic voltammetry indicating oxidation-reduction processes and providing HOMO and LUMO levels. Gel permeation chromatography (GPC) ensures an assumption about molecular weight of the conducting polymer. Moreover, structure conformation can be detected via nuclear magnetic resonance (NMR) spectrometry. For functional groups Fourier transform infrared (FTIR) spectrometry can be used. Surface roughness and morphology of conducting polymers can be determined by atomic force microscopy (AFM) and scanning electron microscopy (SEM), respectively. Furthermore, differential scanning calorimetry (DSC) and thermal gravimetric analysis (TGA) give information about glass-transition, melting and decomposition temperatures of conducting polymers.

1.6 Electrochromism

The reversible and visible change in transmittance upon applied potential is defined as electrochromism [41]. This results in formation of different absorption bands between redox states in visible region. Between either one transparent and one colored state or two colored states the color change is generally observed. Some electrochromic materials may possess several colors upon applied potentials and these are called as multichromic [42, 43].

Viologens, metal oxides, metal coordination complexes, metal hexacyanometallates and conjugated conducting polymers are commonly known examples of electrochromic materials. Among metal oxides, a well-known example is tungsten trioxide, WO_3, which is transparent in neutral state and converted to blue via reduction. Additionally, among conjugated conducting polymers, organic molecules are more favorable due to ease of processability, low cost, lightweight, high optical

contrast ratios, wide range of colors, fast switching times and ability to tune the band gap via structural modifications. Especially in industry, electrochromism is widely used including computer data storage, rear-view mirrors, smart windows, displays and sunglasses. The most crucial properties of electrochromic materials are good stability, long term open circuit memory, short switching times, high optical contrast and high coloration efficiency.

1.7 Electrochromic Devices

An electrochromic device is a type of a battery consisting of an electrochromic electrode and a charge balancing counter electrode separated from each other with a convenient solid or liquid. The color change is observed by charging and discharging upon applied suitable potentials [42]. The electrochromic devices have drawn considerable interest on account of properties like high optical contrast, high coloration efficiency, long term open circuit memory, short switching times and good stability. There are two types electrochromic devices; dual type transmissive /absorptive and reflective devices.

In dual type transmissive /absorptive devices, anodically and cathodically colored electrochromic polymers are coated onto ITO coated glass electrodes, then sandwiched and separated with a thin layer of gel electrolyte. These type devices provide colored and transparent states. On the contrary, in reflective devices, one of the transparent electrodes of dual type transmissive /absorptive devices is replaced via metallic reflector.

1.7.1 Construction of Electrochromic Devices

As shown in Figure 1.11 the dual type transmissive /absorptive devices are fabricated based on configuration of sandwich cell device. The anodically colored polymer in

fully reduced state and the cathodically colored polymer in fully oxidized state are spray coated on ITO coated glass electrodes. These two electrodes are separated from each other via gel electrolyte providing ionic conductivity.

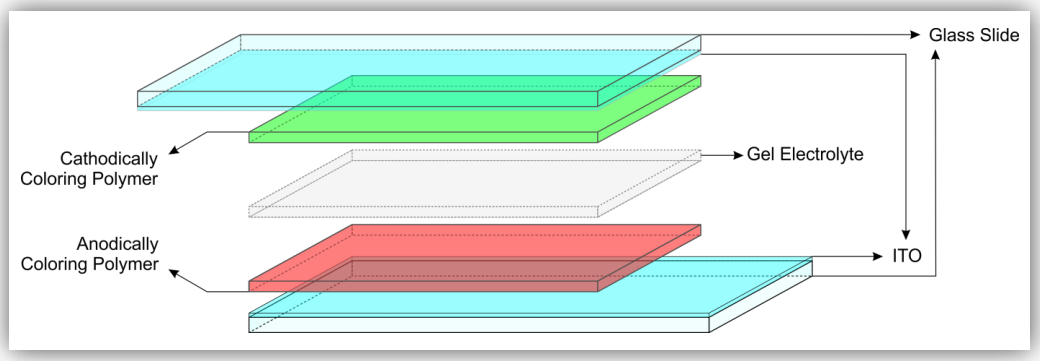

Figure 1.11 Schematic illustration of dual type transmissive /absorptive electrochromic devices

1.7.2 Preparation of the gel electrolyte

The gel electrolyte for electrochromic devices was prepared via using $TBAPF_6$: ACN : PMMA : PC in the ratio of 3:70:7:20 by weight. Tetrabutylammonium hexafluorophosphate ($TBAPF_6$) was dissolved in acetonitrile (ACN) and poly(methyl methacrylate) (PMMA, M: 120000 g/mol) was added to the mixture. The requirements of dissolving PMMA are the vigorous stirring and heating. After all PMMA was dissolved, 1,2-propylenecarbonate (PC), plasticizer, was added to the

mixture. Until enhanced transparent gel was obtained, the mixture was stirred and heated [44].

1.7.3 Characterization of Electrochromic Devices

Characterization of electrochromic devices has been performed in terms of optical contrast ratio, coloration efficiency, open circuit memory, switching time and stability. The optical contrast ratio is determined by percent transmittance changes between polymers' neutral and fully oxidized states at a specified wavelength. The coloration efficiency is optical absorbance change divided by electrochemical charge density at a described wavelength. The open circuit memory is the capacity to remember its colored state with no applied external potential. The switching time is defined as the period required for the color change of a material between its neutral and oxidized states. The stability is the ability to maintain its electrochromic features after a lot of switching cycles.

In order to observe the electrochromic behaviors of devices, cyclic voltammetry can be commonly used. The oxidation – reduction potentials, degree of reversibility and scan rate dependence on diffusion can be determined via CV under external voltages. By repeated chronoamperometry, the electrochromic devices are operated via suitable potentials to observe color changes. Spectroelectrochemical studies are performed to investigate the absorption behavior of electrochemically deposited polymer films in ECDs via applied potentials. The colorimetry experiments are done to describe the color of ECDs. In the CIE system; luminance (L), hue (a) and saturation (b) which are the attributes of color are recorded. A hue is dominant wavelength in which maximum contrast exists, saturation is the intensity of color and luminance is the brightness [45, 46].

1.8 Low Band Gap Polymers

Band gap affects both conductivity and color of polymers. There are several parameters to obtain low band gap polymers as seen in Figure 1.12 which are increasing planarity of the system, bond – length alternation, synthesis of donor – acceptor type polymers, inter chain effects and achieving good stability via resonance [47-50]. Among them, donor–acceptor theory is the most efficient and commonly used method. In donor–acceptor theory, alternating electron-rich (donor) and electron-deficient (acceptor) units were combined in the polymer backbone to achieve desired band gap [51-53]. Besides, the D–A approach is not only used for obtaining low band gap polymers, but also for producing polymers with improved optical, mechanical and electronic properties [54, 55].

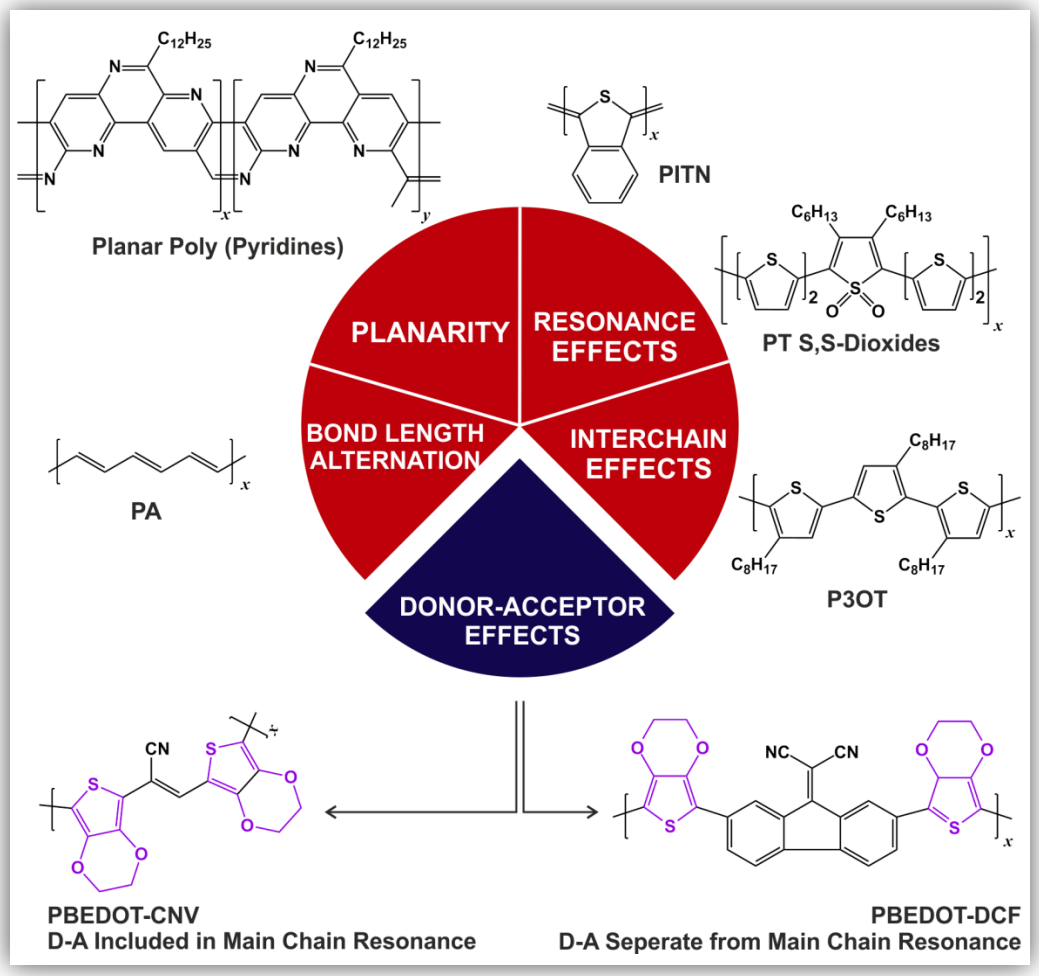

Figure 1.12 The methods for the alteration of the band gap

The type of donor and acceptor moieties should be selected carefully in the synthesis of donor – acceptor type polymers in terms of good match of donor and acceptor units. The electron donating groups raise the HOMO (Highest Occupied Molecular Orbital) level and electron withdrawing groups lower the LUMO (Lowest Unoccupied Molecular Orbital) level.

1.9 Benzimidazole Derivatives as an Acceptor Moiety in Conducting Polymers

Benzazole derivatives which possess two fused rings are admirable candidates for synthesis of conducting polymers. As shown in Figure 1.13 most usual acceptor unities for electrochromic applications are benzothiadiazole, benzotriazole, benzimidazole, benzooxadiazole and benzoselenadiazole.

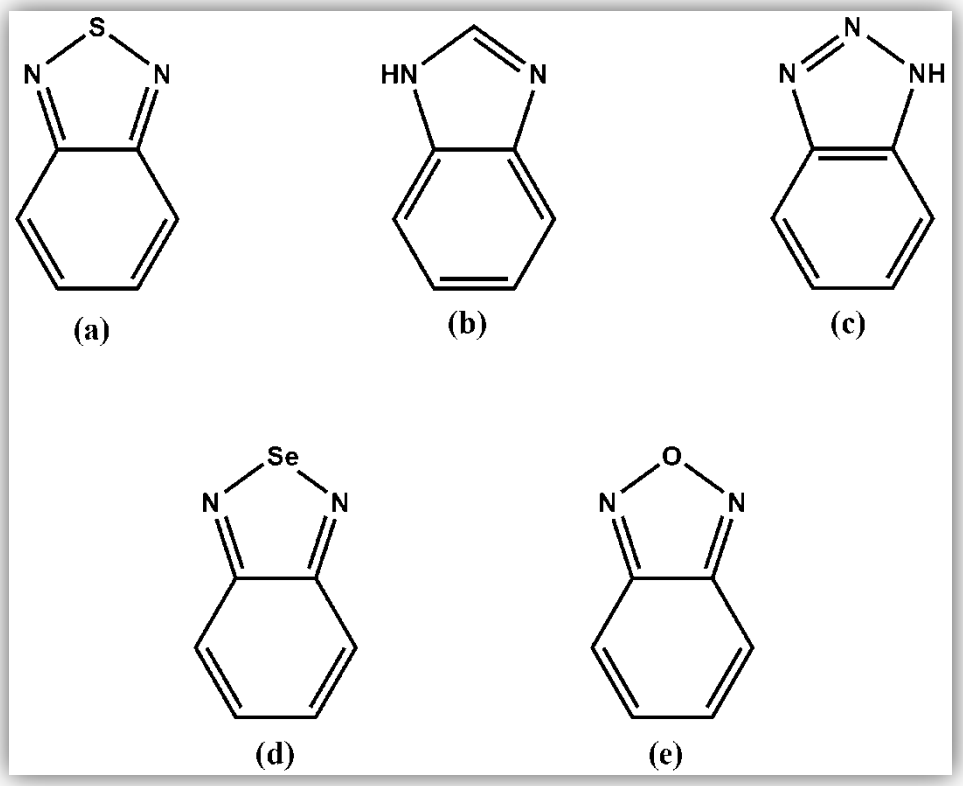

Figure 1.13 Common benzazole derivatives: (a) benzothiadiazole, (b) benzimidazole, (c) benzotriazole, (d) benzoselenadiazole, (e) benzooxadiazole

Of late years, the scientists began to concentrate on the benzimidazole derivatives like other benzazole derivatives. Benzimidazole is a heterocyclic aromatic compound including benzene and imidazole.

As benzimidazole exhibits antiviral, anticancer and antibacterial activities thus it can be utilized in medical fields [56, 57]. Moreover, BIm derivatives have been widely used in account of their promising and enhanced optical properties and good thermal stability [58]. Hence benzimidazole derivatives have been used in solar cell applications and aerospace fields reported in literature [59-61].

1.10 Aim of This Work

In this study, novel donor – acceptor – donor type monomers containing benzimidazole derivatives were designed, synthesized and electrochemically polymerized. The study consists of two parts; in the first part, the position of fluorine as a substituent was varied from para- to meta- in order to investigate position effects on the electrochemical and optical properties of electrochemically synthesized polymers. 4,7-Dibromo-2-(4-fluorophenyl)-1H-benzo[d]imidazole and 4,7-dibromo-2-(3-fluorophenyl)-1H-benzo[d]imidazole unit was used as the acceptor and these moieties were combined with thiophene unit as the donor via Stille coupling. Electrochemical, spectroelectrochemical and colorimetric studies of electrochemically synthesized polymers were performed. In second part of this study, the effect of electron donating moieties on the optical properties of electrochemically polymerized polymers was investigated. 4,7-Dibromo-2-(perfluorophenyl)-1H-benzo[d]imidazole was used as an acceptor moiety and coupled with thiophene and 3,4-ethylenedioxythiophene as the donor units by Stille coupling. The electrochemical and optical properties of electrochromic polymers were examined.

CHAPTER 2

EXPERIMENTAL

2.1 Materials

All chemicals and reagents were obtained from commercial sources and used without further purification unless mentioned otherwise. All chemicals were purchased from Aldrich except THF which was purchased from Acros and dried over sodium – benzophenone before use. All reactions were performed under argon atmosphere unless mentioned otherwise. 4,7-Dibromobenzo[c][1,2,5]thiadiazole [62], 3,6-dibromo-1,2-phenylenediamine [63], tributyl(thiophene-2-yl)stannane [64] and tributyl(2,3-dihydrothieno[3,4-b][1,4]dioxin-5-yl)stannane [65] were synthesized according to previously published procedures.

2.2 Methods and Equipments

Electrochemical studies were performed in a three-electrode cell consisting of an indium tin oxide (ITO) doped glass slide as the working electrode, platinum wire as the counter electrode, and Ag wire as the pseudo reference electrode using a Gamry Reference 600 Potentiostat. The reference electrode was subsequently calibrated to Fc/Fc^+ (0.35 V) and the band energies (HOMO and LUMO) were calculated relative to the vacuum level taking the value of SHE is −4.75 eV vs. vacuum. Varian Cary 5000 UV–Vis spectrophotometer was used to investigate the spectroelectrochemical studies of polymers. Colorimetry measurements were performed using Konica Minolta CS-100A spectrophotometer. ^{1}H NMR and ^{13}C NMR spectra were recorded

on a Bruker Spectrospin Avance DPX-400 Spectrometer with tetramethylsilane (TMS) as the internal standard and $CDCl_3$ and d-DMSO as the solvent. All shifts were given in ppm downfield from TMS. High resolution mass spectroscopy results were performed via Waters SYNAPT MS System.

2.3 Syntheses of Monomers

2.3.1 Synthesis of 4,7-dibromobenzo[c][1,2,5]thiadiazole

4,7-Dibromobenzo[c][1,2,5]thiadiazole was synthesized using previously published procedure [62]. Benzothiadiazole (5.00 g, 36.7 mmol) was dissolved in hydrogen bromide (90 mL, 47 %). A solution of bromine (4.0 mL) and hydrogen bromide (40 mL, 47 %) was prepared and added to the mixture drop wise. After the addition was complete, the mixture was refluxed for 6 hours. The mixture was cooled to room temperature. The resultant precipitate was filtered and washed with saturated $NaHSO_3$ in order to remove excess bromine. Then, the precipitate was dissolved in dichloromethane and washed with water several times. Organic layer was dried over $MgSO_4$ and the mixture was concentrated on the rotary evaporator to get rid of the solvent. Yellow solid product (10.2 g) was obtained in yield of 95 %.

^{1}H NMR (400 MHz, $CDCl_3$): δ (ppm) 7.66 (s, 2H).

^{13}C NMR (100 MHz, $CDCl_3$): δ (ppm) 152.9, 132.4, 113.9.

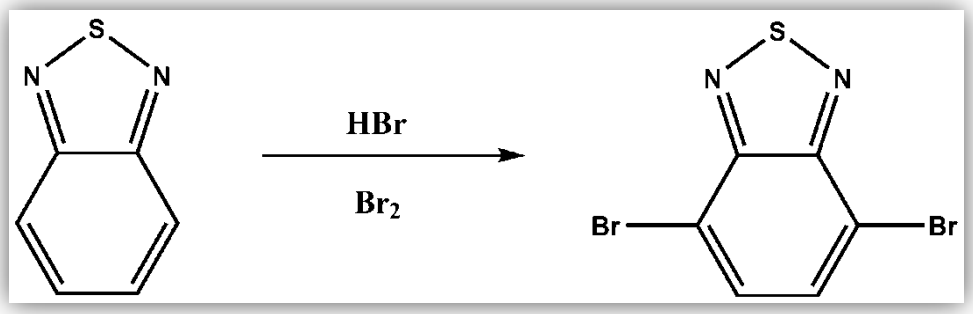

Figure 2.1 Synthetic route for 4,7-dibromobenzo[c][1,2,5]thiadiazole

2.3.2 Synthesis of 3,6-dibromo-1,2-phenylenediamine

3,6-Dibromobenzene-1,2-diamine was synthesized according to previously published procedure [63]. 4,7-Dibromobenzo[c][1,2,5]thiadiazole (2.00 g, 6.80 mmol) was dissolved in ethanol (70 mL) in 1000 mL flask. The mixture was placed in an ice bath. After that $NaBH_4$ under argon gas was added to the mixture in small portions. After the completion of addition of $NaBH_4$, the mixture was stirred overnight at room temperature. Ethanol was removed under vacuum and the product was dissolved in diethyl ether. The mixture was washed with brine and water. The organic layer was dried over $MgSO_4$ and the mixture was concentrated under reduced pressure to obtain yellowish white solid (1.50 g). Yield: 85 %.

^{1}H NMR (400MHz, $CDCl_3$): δ (ppm) 6.78 (s, 2H), 3.83 (s, 4H).

^{13}C NMR (100MHz, $CDCl_3$): δ (ppm) 131.7, 121.2, 107.7.

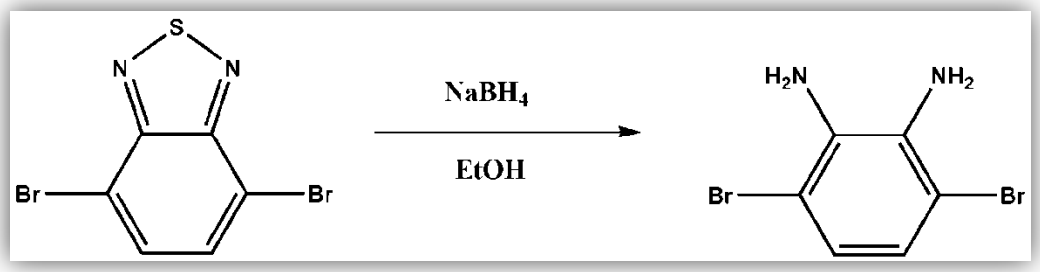

Figure 2.2 Synthetic route for 3,6-dibromo-1,2-phenylenediamine

2.3.3 Synthesis of 4,7-dibromo-2-(4-fluorophenyl)-1H-benzo[d]imidazole

4,7-Dibromo-2-(4-fluorophenyl)-1H-benzo[d]imidazole was synthesized by the modification of a previously published procedure [66]. 3,6-Dibromo-1,2-phenylenediamine (400 mg, 1.50 mmol) was dissolved in 4.0 mL acetonitrile. And hydrogen peroxide (0.8 mL, 8 mmol) was added to the mixture directly. Then, 4-fluorobenzaldehyde (0.2 mL, 1.50 mmol) was added to the mixture drop wise. After that, ammonium cerium (IV) nitrate (90 mg, 0.16 mmol) was added and the mixture was stirred overnight at room temperature. 4,7-Dibromo-2-(4-fluorophenyl)-1H-

benzo[d]imidazole was purified by means of recrystallization with cold water and hexane. The resultant product was obtained as a beige solid.

^{1}H NMR (400 MHz, d-DMSO) δ 13.33 (s, 1 H), 8.39 (dd, *J* = 3.1, 5.5, 8.6 Hz, 2H), 7.45-7.39 (m, 4H).

^{13}C NMR (100 MHz, d-DMSO) δ 130.0, 129.9, 126.5, 125.9, 116.0, 115.8, 111.2, 102.4.

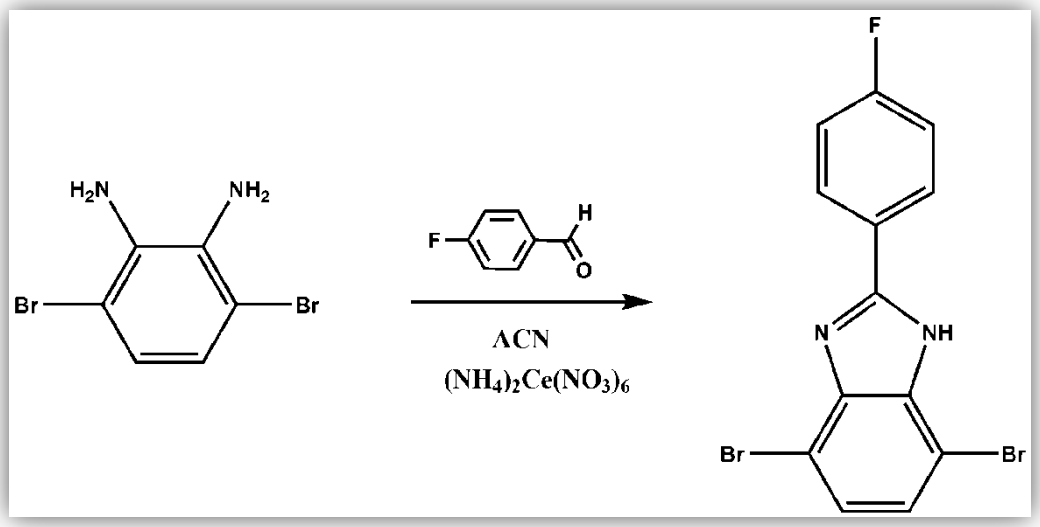

Figure 2.3 Synthetic route for 4,7-dibromo-2-(4-fluorophenyl)-1H-benzo[d]imidazole

2.3.4 Synthesis of tributyl(thiophene-2-yl)stannane

The synthesis of tributyl(thiophene-2-yl)stannane was performed based on methodology previously published in literature [64]. Thiophene (3.0 g, 30 mmol) was dissolved in dry THF (42.0 mL) in a three-necked flask under argon atmosphere. After the solution was cooled to -78 ^{o}C, n-butyl lithium (17.0 mL 2.5 M in hexane, 184 mmol) was added to the mixture dropwise. After the completion of the addition of n-butyl lithium, tributyltin chloride (11.7 mL, 43.0 mmol) was added to the mixture drop wise. Then, the mixture was allowed to reach to room temperature and stirred overnight. The solvent was removed under vacuum and the crude product was dissolved in dichloromethane and washed with NH_4Cl, brine and water. The organic layer was dried over $MgSO_4$ and the mixture was concentrated on rotary evaporator so as to get rid of the solvent. The product, yellow in color, was obtained (10.4 g) in 93 % yield.

^{1}H NMR (400 MHz, $CDCl_3$): δ (ppm) 7.57 (d, J=4.7 Hz, 1H), 7.19 (t, J= 3.3 Hz, 1H), 7.12 (d, J= 3.2 Hz, 1H), 1.50 (m, J=7.8 Hz, 6H), 1.28 (m, J= 7.3 Hz, 6H), 1.03 (t, J= 8.4 Hz, 6H), 0.82 (t, J= 7.3 Hz, 9H).

^{13}C NMR (100 MHz, $CDCl_3$): δ (ppm) 136.2, 135.2, 130.6, 127.8, 28.9, 27.3, 13.7, 10.8.

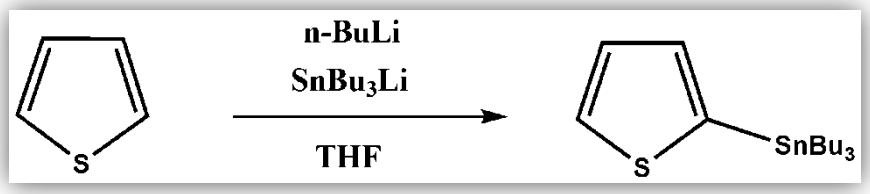

Figure 2.4 Synthetic route for tributyl(thiophene-2-yl)stannane

2.3.5 Synthesis of 2-(4-fluorophenyl)-4,7-di(thiophen-2-yl)-1H-benzo[d]imidazole

A solution of tributyl(thiophen-2-yl)stannane (1.01 g, 2.70 mmol) and 4,7-dibromo-2-(4-fluorophenyl)-1H-benzo[d]imidazole (200 mg, 0.540 mmol) and bis(triphenylphosphine)palladium (II) dichloride in dry tetrahydrofuran (40.0 mL, 0.490 mmol) was refluxed overnight under argon atmosphere. The mixture was cooled and concentrated on the rotary evaporator before purification. Column chromatography on silica gel (hexane : EtOAc 2:1) followed by preparative thin layer chromatography (silica, hexane : ethyl acetate 4:1) to purify 2-(4-fluorophenyl)-4,7-di(thiophen-2-yl)-1H-benzo[d]imidazole completely as a yellow solid (75 mg) in 37 % yield.

^{1}H NMR (400 MHz, $CDCl_3$) δ 9.57 (s, 1H), 8.16 (dd, J =1.2, 3.7 Hz, 1H), 8.04 (dd, J = 3.7, 5.2, 8.9 Hz, 2H), 7.53- 7.55 (m, 1H), 7. 37- 7.31 (m, 4H), 7.16- 7.12 (m, 4H).

^{13}C NMR (100 MHz, $CDCl_3$) δ 149.6, 139.4, 127.7, 127.6, 127.3, 126.7, 125.7, 124.6, 124.1, 123.5, 121.7, 119.3.

HRMS (EI) for $C_{21}H_{13}FN_2S_2$, calculated 377. 0582, found 377. 0557.

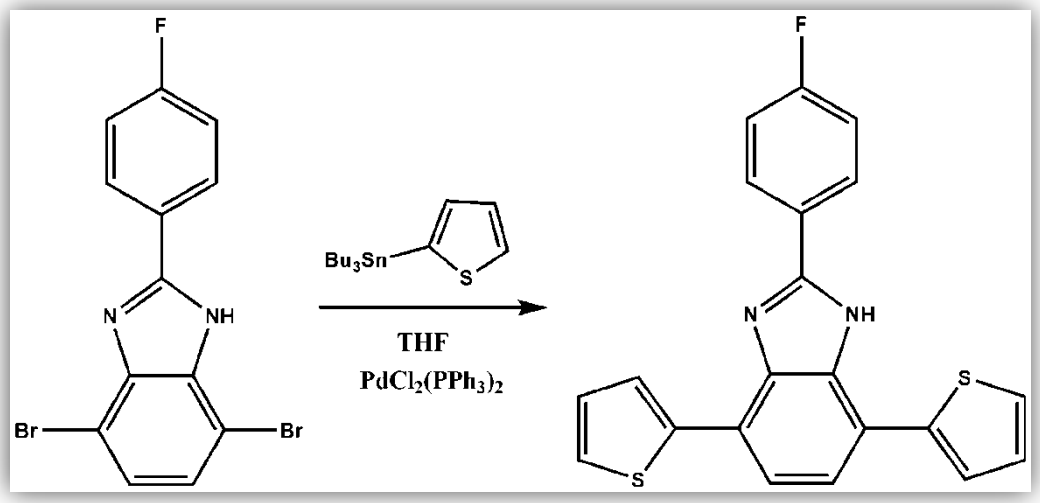

Figure 2.5 Synthetic route for 2-(4-fluorophenyl)-4,7-di(thiophen-2-yl)-1H-benzo[d]imidazole

2.3.6 Synthesis of 4,7-dibromo-2-(3-fluorophenyl)-1H-benzo[d]imidazole

4,7-Dibromo-2-(3-fluorophenyl)-1H-benzo[d]imidazole was synthesized by the modification of a previously published procedure [66]. 3,6-Dibromo-1,2-phenylenediamine (600 mg, 2.25 mmol) was dissolved in 4.0 mL ACN. H_2O_2 (1.2 mL, 12 mmol) was added to the mixture directly. 3-Fluorobenzaldehyde (0.30 mL, 0.225 mmol) was added to the mixture dropwise. After that, ammonium cerium (IV) nitrate (120 mg, 0.21 mmol) was added to the mixture and stirred overnight at room temperature. Recrystallization with cold water and hexane was used in order to purify the compound. As a result, compound was obtained as a bejge solid.

^{1}H NMR (400 MHz, d-DMSO) δ 8.20- 8.15 (m, 4H), 7.64 (dd, J = 6.6, 7.6, 14.2 Hz, 2H).

^{13}C NMR (100 MHz, d-DMSO) δ 131.1, 131.0, 130.9, 126.4, 123.7, 123.6, 117.5, 117.3, 114.1, 113.9.

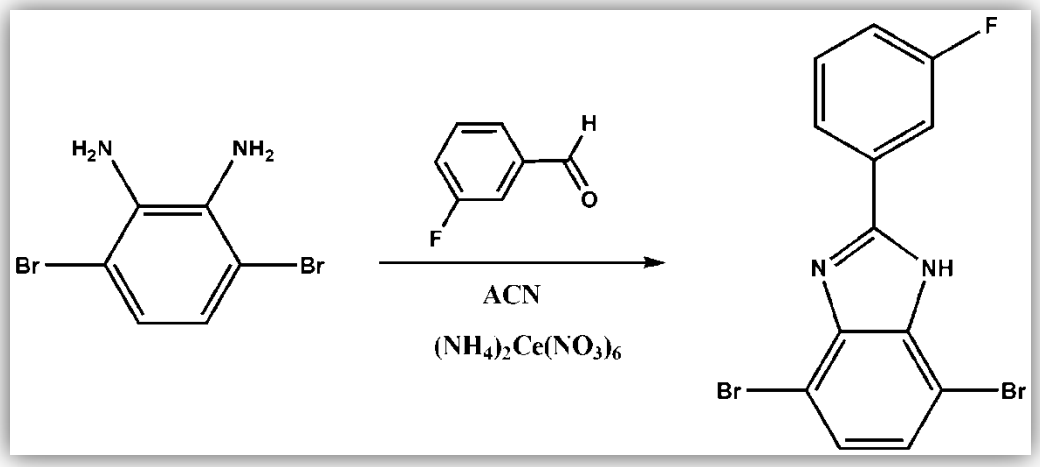

Figure 2.6 Synthetic route for 4,7-dibromo-2-(3-fluorophenyl)-1H-benzo[d]imidazole

2.3.7 Synthesis of 2-(3-fluorophenyl)-4,7-di(thiophen-2-yl)-1H-benzo[d]imidazole

A solution of tributyl(thiophen-2-yl)stannane (867 mg, 2.32 mmol) and 4,7-dibromo-2-(3-fluorophenyl)-1H-benzo[d]imidazole (170 mg, 0.46 mmol) in tetrahydrofuran (40.0 mL, 0.49 mmol) was refluxed overnight under argon atmosphere. Bis(triphenylphosphine)palladium (II) dichloride was added to the mixture as the catalyst. The reaction was concentrated on the rotary evaporator and for purifation of 2-(3-fluorophenyl)-4,7-di(thiophen-2-yl)-1H-benzo[d]imidazole the

residue was subjected to column chromatography technique (silica gel, hexane : EtOAc 3:1). After that, preparative thin layer chromatography (silica, hexane : ethyl acetate 4:1) was carried out to get the monomer totally as a yellow solid (73 mg) in 42 % yield .

^{1}H NMR (400 MHz, $CDCl_3$) δ 9.64 (s, 1H), 8.17 (dd, J = 1.1, 2.5, 3.6 Hz, 1H), 7.82-7.81 (m, 1H), 7.79- 7.75 (m, 1H), 7.55- 7.53 (m, 1H), 7.44- 7.32 (m, 5H), 7.14- 7.08 (m, 3H).

^{13}C NMR (100 MHz, $CDCl_3$) δ 162.4, 160.5, 148.7, 148.6, 138.9, 129.3, 129.2, 126.9, 124.3, 120.6, 115.9, 115.7, 112.6, 112.3.

HRMS (EI) for $C_{21}H_{13}FN_2S_2$, calculated 377. 0582 found 377. 0558.

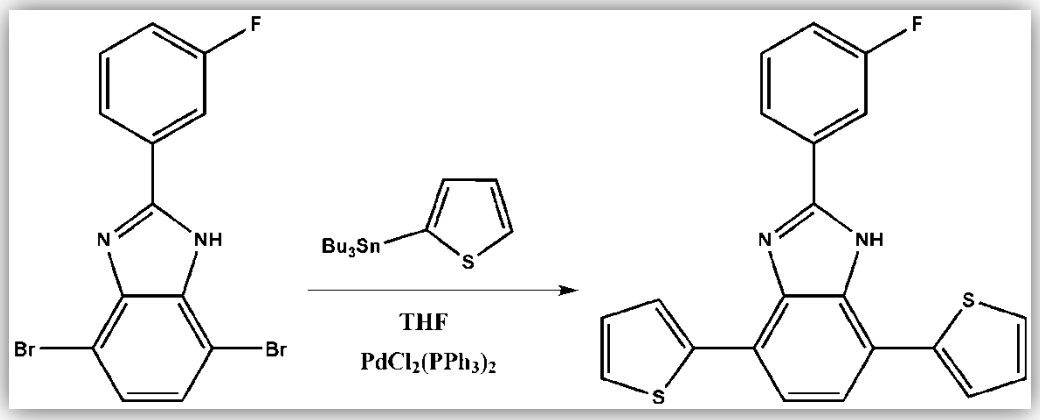

Figure 2.7 Synthetic route for 2-(3-fluorophenyl)-4,7-di(thiophen-2-yl)-1H-benzo[d]imidazole

2.3.8 Synthesis of 4,7-dibromo-2-(perfluorophenyl)-1H-benzo[d]imidazole

The brominated acceptor unit; 4,7-dibromo-2-(perfluorophenyl)-1H-benzo[d]imidazole, was synthesized with inspiration from previously stated procedures [67]. 3,6-Dibromo-1,2-phenylenediamine (500 mg, 1.88 mmol) was dissolved in 3.0 mL acetonitrile. Then, hydrogen peroxide was directly added to the mixture (0.8 mL, 8 mmol) and 2,3,4,5,6-pentafluorobenzaldehyde (0.2 mL, 1.88 mmol) was added drop wise. A clear solution was achieved, and ammonium cerium (IV) nitrate (80 mg, 0.14 mmol) was added to the mixture and stirred at room temperature for overnight. The precipitate was purified by recrystallization in cold distilled water and cold hexane. The residue was left to dry. The product was light orange in color.

^{1}H NMR (400 MHz, d-DMSO): δ 13.97 (s, 1H), 7.51 (s, 2H).

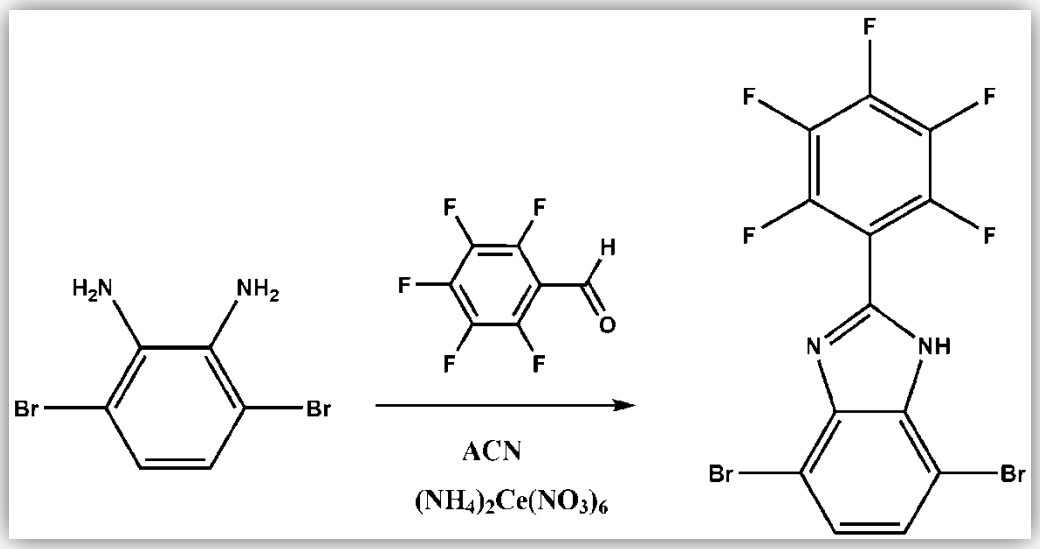

Figure 2.8 Synthetic route for 4,7-dibromo-2-(perfluorophenyl)-1H-benzo[d]imidazole

2.3.9 Synthesis of 2-(perfluorophenyl)-4,7-di(thiophen-2-yl)-1H-benzo[d]imidazole

Tributyl(thiophen-2-yl)stannane (1.28 g, 3.42 mmol) and 4,7-dibromo-2-(4-fluorophenyl)-1H-benzo[d]imidazole (300 mg, 0.69 mmol) were dissolved in tetrahydrofuran (60.0 mL, 0.74 mmol) which was dried over sodium and benzophenone. After that bis(triphenylphosphine)palladium (II) dichloride was added to the mixture. The mixture was left to reflux overnight at 130 ^{o}C under argon atmosphere. In the following day, the solvent was removed under reduced pressure.

Column chromatography was done (silica gel, hexane: ethyl acetate 3:1) for purification. However, this technique was not sufficient to purify monomer hence we performed preparative thin layer chromatography (silica, hexane: ethyl acetate 3:1). As a result the monomer (orange in color) was obtained (150 mg) successfully. Yield: 49%.

^{1}H NMR (400 MHz, $CDCl_3$): δ 10.04 (s, 1H), 8.17 (dd, J = 3.6 Hz, 2H), 7.61 (d, J = 7.9 Hz, 1H), 7.47 (d, J = 7.9 Hz, 1H), 7.38 (dd, J = 5.1 Hz, 2H), 7.33 (t, J = 6.1 Hz, 2H).

HRMS (ESI) for $C_{21}H_{10}N_2F_5S_2$ calculated 449.0206, found 449.0201.

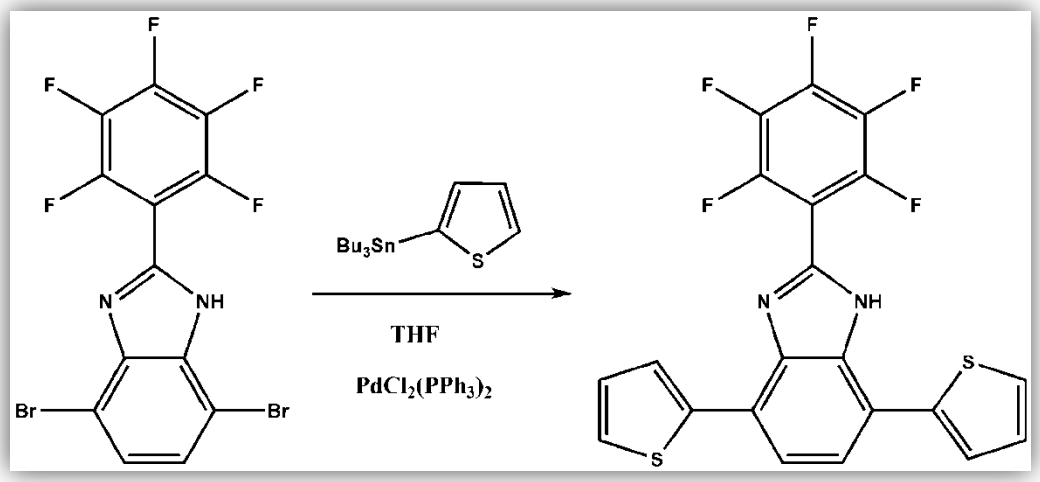

Figure 2.9 Synthetic route for 2-(perfluorophenyl)-4,7-di(thiophen-2-yl)-1H-benzo[d]imidazole

2.3.10 Synthesis of tributyl(2,3-dihydrothieno[3,4-b][1,4]dioxin-5-yl)stannane

Tributyl(2,3-dihydrothieno[3,4-b][1,4]dioxin-5-yl)stannane was synthesized based on previously stated methods in literature [65]. 3,4-Ethylenedioxythiophene (2.00 g, 14.0 mmol) was dissolved in dry THF (50 mL) in a three-neck flask under argon atmosphere. After the solution was cooled to -78 ^{o}C, n-butyl lithium (5.8 mL 2.5 M in hexane, 63.0 mmol) was added to the mixture drop wise. After the addition of n-butyl lithium completely, tributyltin chloride (3.83 mL, 14.0 mmol) was added to the mixture in small portions. The mixture was allowed to reach to room temperature and stirred overnight. In next day, the solvent was removed under vacuum. The crude product was dissolved in dichloromethane and extracted with NH_4Cl, brine and water. The organic part of extraction was dried over $MgSO_4$ and the mixture was concentrated on rotary evaporator so as to get rid of the solvent. The crude product (yellow in color) was obtained (5.4 g) in 90 % yield.

^{1}H NMR (400 MHz, $CDCl_3$): δ (ppm) 6.25 (s, 1H), 4.08 (m, 4H), 1.79 (m, J= 6.6 Hz, 6H), 1.02 (t, J= 8.3 Hz, 6H), 1.40- 1.59 (m, 6H) 0.82 (t, J= 7.3 Hz, 9H).

^{13}C NMR (100 MHz, $CDCl_3$): δ (ppm) 146.1, 104.2, 98.1, 63.1, 63.0, 27.4, 25.6, 12.1.

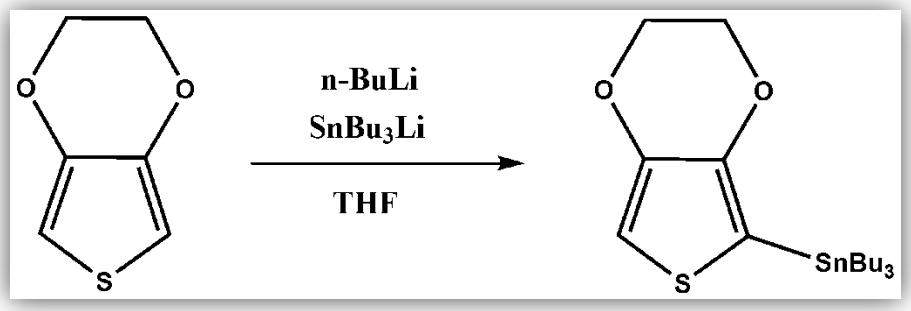

Figure 2.10 Synthetic route for tributyl(2,3-dihydrothieno[3,4-b][1,4]dioxin-5-yl)stannane

2.3.11 Synthesis of 4,7-bis(2,3-dihydrothieno[3,4-b][1,4]dioxin-5-yl)-2-(perfluorophenyl)-1H-benzo[d]imidazole

4,7-Dibromo-2-(2,3,4,5,6-pentafluorophenyl)-1H-benzo[d]imidazole (300 mg, 0.69 mmol) was dissolved in tetrahydrofuran (60 mL, 0.74 mmol) at 120 ^{o}C under argon atmosphere. Tributyl(2,3-dihydrothieno[3,4-b][1,4]dioxin-5-yl)stannane was added to the mixture directly. Then, the catalyst, bis(triphenylphosphine)palladium (II) dichloride, was added to the mixture. The mixture was refluxed overnight at 120 ^{o}C under argon atmosphere. It was concentrated on rotary evaporator to get rid of the solvent and the residue was recrystallized in cold hexane. So as to purify the monomer, column chromatography was performed (silica gel, hexane : ethyl acetate 3:1), following, the preparative thin layer chromatography (silica, hexane : ethyl

acetate 3:1) was also done. The monomer was obtained (145 mg) successfully. Yield: % 37.

^{1}H NMR (400 MHz, $CDCl_3$): δ 11.3 (s, 1H), 8.04 (d, J = 8.1 Hz, 1H), 7.42 (d, J = 8.1 Hz, 1H), 6.46 (s, 1H), 6.38 (s, 1H), 4.44-4.22 (m, J = 3.8 Hz, 8H).

HRMS (ESI) for $C_{25}H_{14}N_2O_4F_5S_2$ calculated 565.0315, found 565.0309.

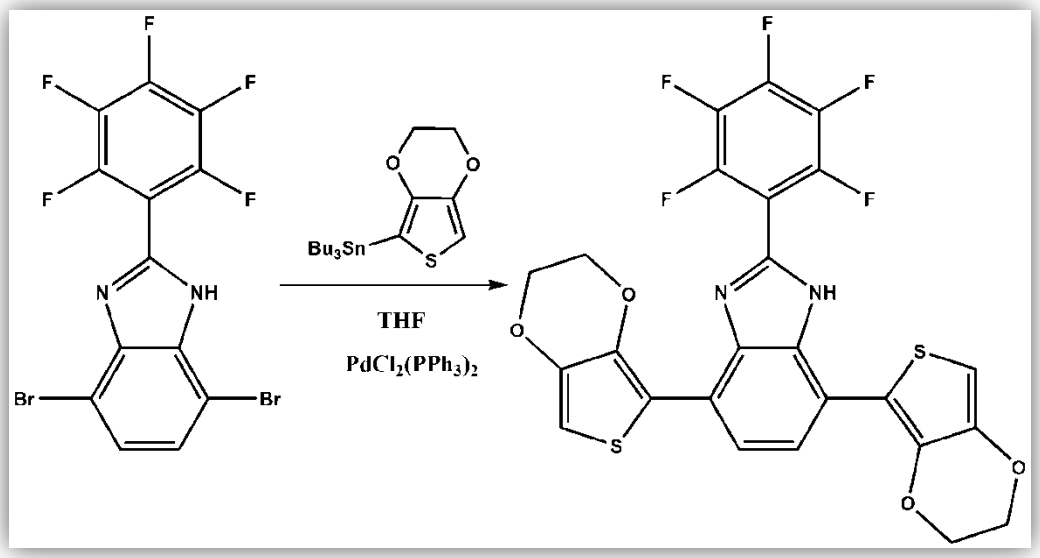

Figure 2.11 Synthetic route for 4,7-bis(2,3-dihydrothieno[3,4-b][1,4]dioxin-5-yl)-2-(perfluorophenyl)-1H-benzo[d]imidazole

CHAPTER 3

RESULTS AND DISCUSSION

3.1 Electrochemical Properties of Donor – Acceptor – Donor Type Polymers

3.1.1 Electrochemical and Optical Properties of M1 and M2

3.1.1.1 Electrochemical Polymerization of M1 and M2

The electrochemical studies were performed in a three electrode cell containing ITO coated glass slide (7 x 50 x 0.7 mm, R_s = 5 – 15 Ω) as the working electrode, a platinum wire as the counter electrode and a silver wire as the pseudo reference electrode. In order to probe the electrochemical characters of polymers, the monomers M1 and M2 were electrochemically polymerized by cyclic voltammetry (CV) in Figure 3.1. The CV was performed on indium tin oxide (ITO) coated glass slides with 0.1 M acetonitrile (ACN) /dichloromethane (CH_2Cl_2) (95/5, v/v) solution at a scan rate of 100 mV/s. Since the monomers had poor solubility in acetonitrile, dichloromethane was used to obtain a homogeneous solution. Sodium perchlorate

($NaClO_4$) and lithium perchlorate ($LiClO_4$) were used as the supporting electroytes during electropolymerization with repeated scan intervals between 0 V and 1.3 V for M1 and 0 V and 1.4 V for M2 as shown in Figure 3.2.

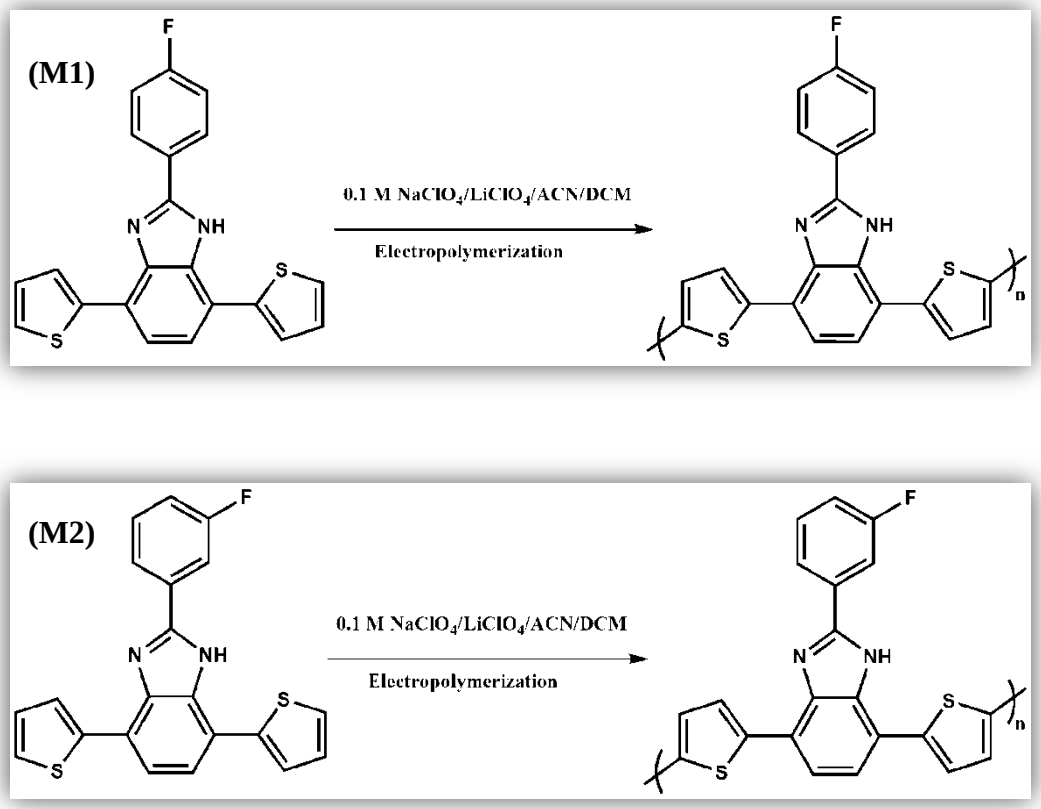

Figure 3.1 Electropolymerization of M1 and M2

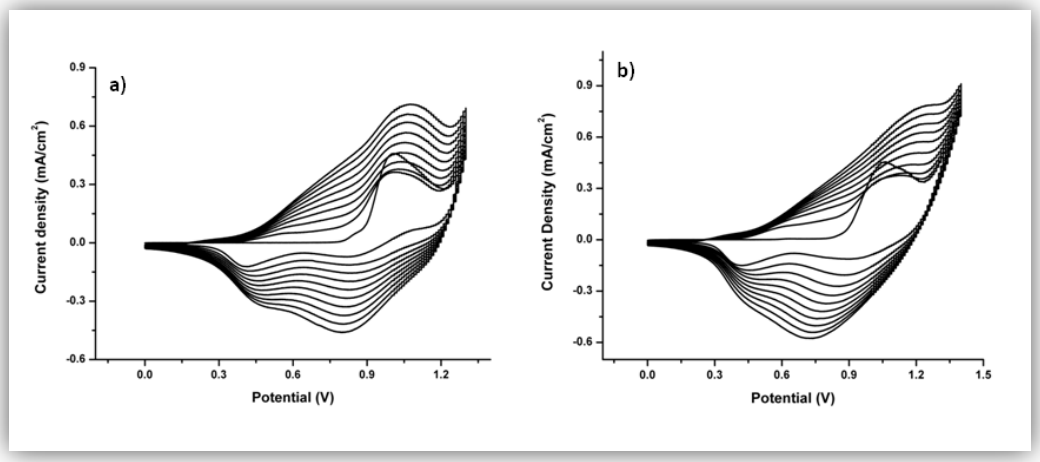

Figure 3.2 Repeated potential scan polymerization of (a) M1 and (b) M2 at 100 mV s^{-1} in 0.1 M $LiClO_4/NaClO_4$ CH_2Cl_2/ACN (5:95, v:v) solution on an ITO electrode

The irreversible monomer oxidation peaks were appeared in the first cycles at 1.0 V for M1 and at 1.05 V for M2. After the first cycle, observation of a new reversible redox couple with an increasing current intensity after each successive cycle proves the formation of electroactive polymer films P1 and P2 as seen in Figure 3.3. Electrochemically synthesized polymers were subjected to CV in a monomer free solution in order to investigate the p-type and n-type doping properties of the polymers. In 0.1 M $LiClO_4/NaClO_4$/ACN solution both polymers are p-dopable with a reversible redox couple at 0.97 V/ 0.78 V for P1 and at 1.1 V/ 0.84 V for P2 versus the Ag wire pseudo reference electrode as shown in Figure 3.3.

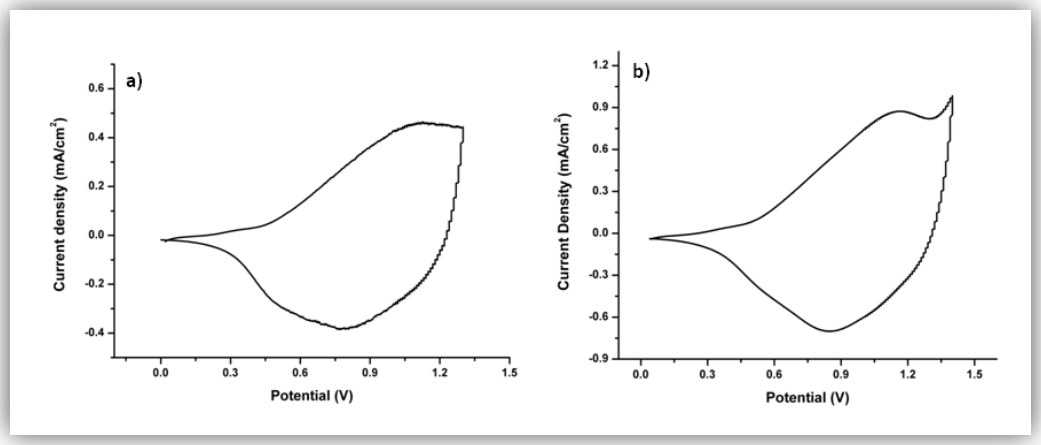

Figure 3.3 Single scan cyclic voltammograms of (a) P1 and (b) P2 in a monomer free 0.1 M $LiClO_4$/$NaClO_4$ ACN solution

The HOMO energy levels of each polymers were calculated from onset of the corresponding oxidation potentials vs. Fc/Fc^+ reference electrode (Figure 3.3). Both polymers have only p-doping property hence, LUMO energy levels were calculated by using optical band gap values. As seen in Table 3.1 the HOMO levels were reported as -5.46 eV (P1) and -5.54 eV (P2) respectively. The HOMO levels differ from each other slightly, this difference indicates the ease of oxidation of polymer films in this electrolytic medium. This behavior can be explained by position of fluorine atom. Changing the position of fluorine unit from para- to meta- on the phenyl ring has a tremendous effect on kinetic properties as depicted in Table 3.3. In addition, this position change affects electrochemical and spectroelectrochemical

properties significantly. Fluorine atom as a substituent has both inductive effect (electron-withdrawing) and mesomeric effect (electron-donating). Inductive effect will have the same influence for both positions whereas, mesomeric effect will be dominant over inductive effect in para- position [68]. In this case, depending upon the position of fluorine atom on the ring (para- or meta-) oxidation barriers will probably change. When resonance structures are considered, it is seen that para– substitued fluorine (P1) could stabilize the possible cationic charge. As a result of higher ring stabilization of para– substitued one (P1), its oxidation will be easier and its oxidation potential will be lower compared to meta– substitued derivative (P2) which supports our results (Table 3.1).

3.1.1.2 Scan rate dependence of M1 and M2

The scan rate dependence experiments were carried out via cyclic voltammetry so as to probe the electrochemical process in terms of whether it is diffusion controlled or not. The linear relation between scan rate and current intensities proved that polymer films were well adhered on ITO surface and the mass transfer in electrochemical processes were non-diffusion controlled during doping / dedoping. (Figure 3.4).

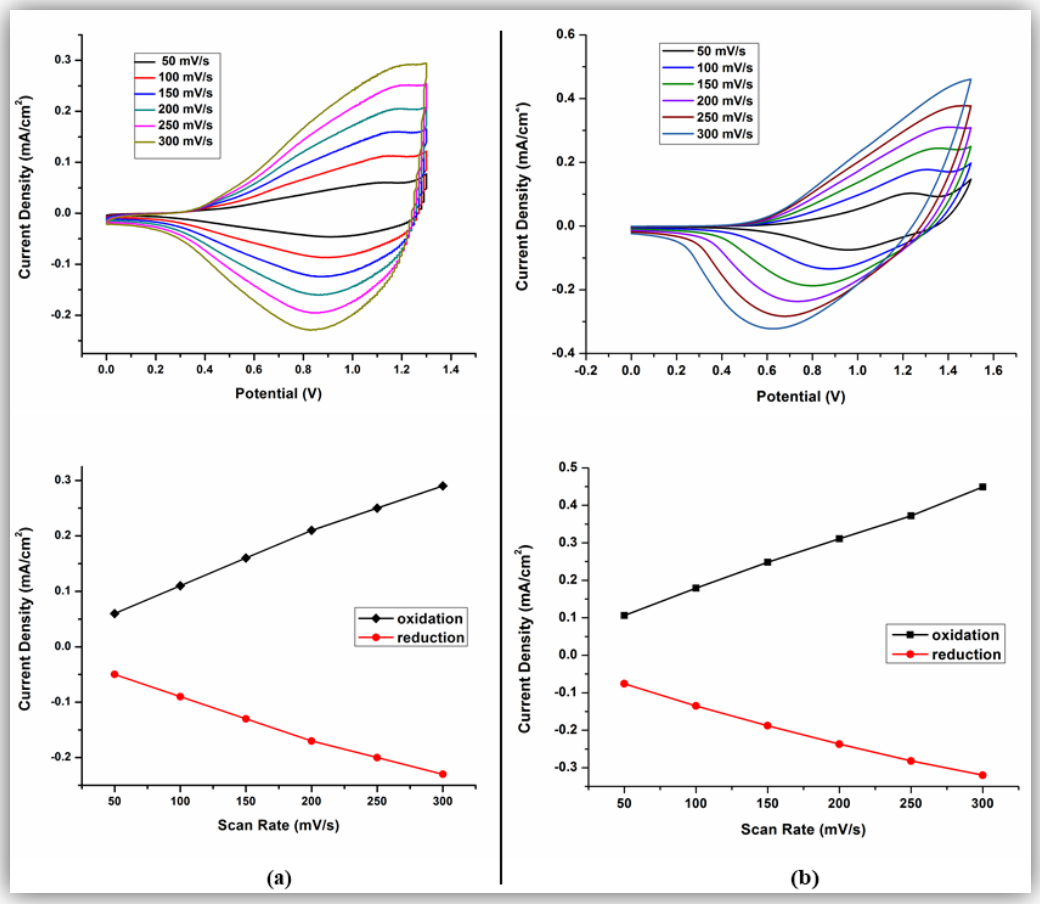

Figure 3.4 Scan rate dependence of (a) P1 film and (b) P2 film in a monomer free 0.1 M $NaClO_4$ - $LiClO_4$ / ACN solution at 50, 100, 150, 200, 250 and 300 $mV.s^{-1}$.

3.1.1.3 Spectroelectrochemical and Colorimetric Studies of P1 and P2

The optical changes upon stepwise doping and the electrochromic properties of conjugated polymers were investigated by conducting spectroelectrochemistry studies of P1 and P2. Both polymers were electrochemically synthesized on ITO and spectral changes were explored by UV–Vis-NIR spectrometer in a monomer-free 0.1 M $NaClO_4$–$LiClO_4$/ACN solution via incrementally increasing applied potential between 0.0 V and 1.2 V for P1 , 0.0 V and 1.15 V for P2. Initially, in order to remove any trapped charge and dopant ion during electrochemical polymerization, polymer coated ITO films were reduced to their neutral state, and then stepwise oxidation was performed. During oxidation while the absorption in the visible region reached a minimum value, new absorption bands (polaron, bipolaron bands) appeared in NIR which proves the formation of charge carriers. The normalized spectral changes occurring upon electrochemical oxidation of P1 and P2 were depicted in Figures 3.5 a and b in the range of 300−1650 nm.

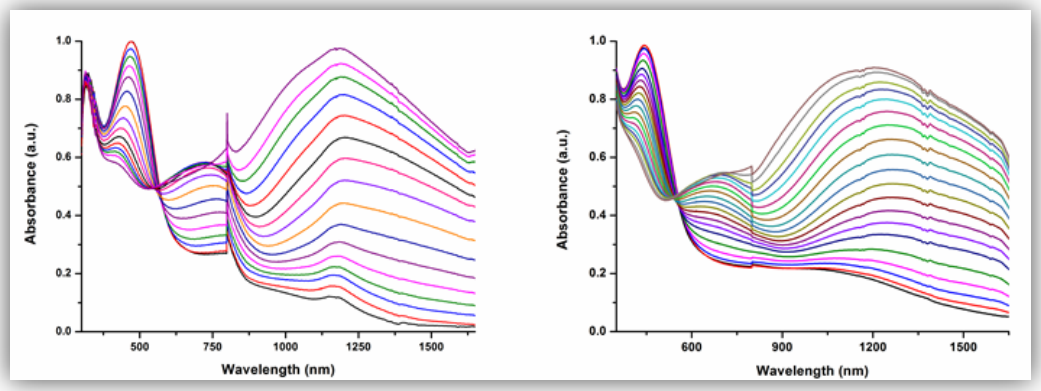

Figure 3.5 Electronic absorption spectra for (a) P1 and (b) P2 films in 0.1 M $NaClO_4$–$LiClO_4$/ACN solution between 0.0 V and 1.2 V for P1 , 0.0 V and 1.15 V for P2.

Table 3.1 Summary of electrochemical and spectroelectrochemical properties of P1 and P2

	HOMO (eV)	**LUMO (eV)**	**λ_{max} (nm)**	**E_g^{op} (eV)**
P1	-5.46	-3.55	471	1.91
P2	-5.54	-3.58	440	1.96

When the electronic absorption spectra of P1 and P2 were compared, the effect of position of fluorine atom on spectroelectrochemical properties can be seen. The difference on the λ_{max} values and optical band gaps can be explained by the parameters that affect absorption spectra of conjugated polymers. In literature, it is known that these properties are widely affected by effective conjugated length and packing of resulting polymers [69]. When the position of fluorine atom was changed from –meta to –para, better packing was achieved in the polymer backbone which causes a shift in absorption maxima from 440 nm to 471 nm. Optical band gaps (E_g^{op}) of the P1 and P2 were calculated from the onsets of lowest energy π–π* transitions as 1.91 eV and 1.96 eV, respectively. The λ_{max} of the P1 signifies 31 nm a red-shift when compared with λ_{max} of the P2. To sum up, better packing for P1 resulted in lower energy and higher λ_{max}.

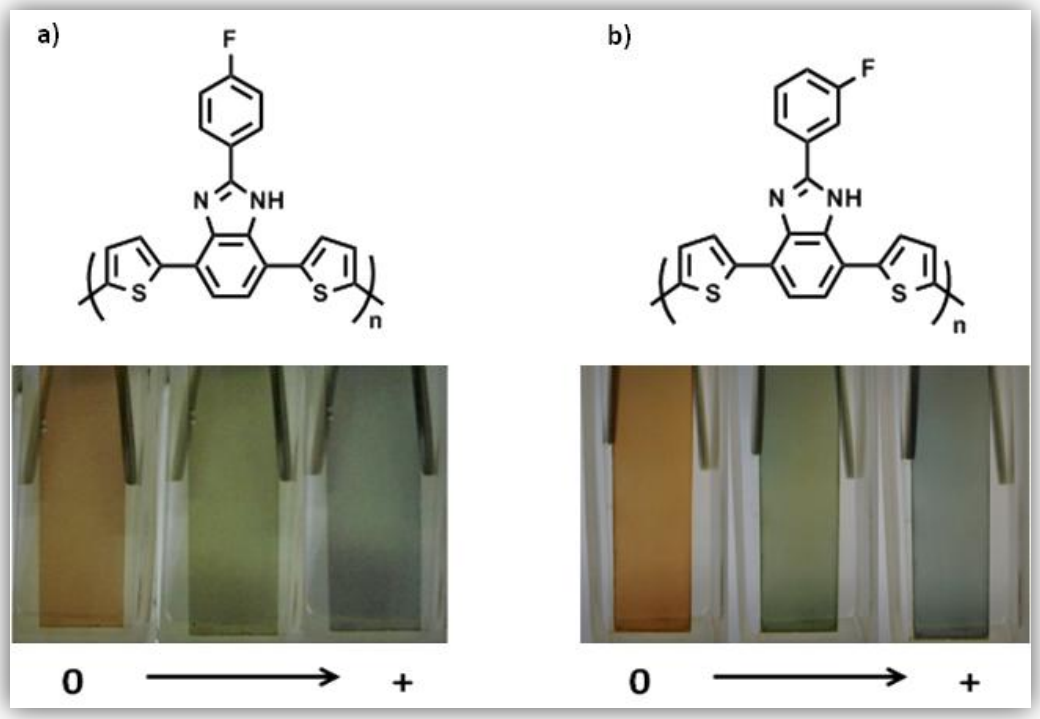

Figure 3.6 Structures of the polymers and their colors at their neutral and different oxidized states

In addition, spectroelectrochemical studies of the polymer films illustrate that the film's color changed during the p-doping (oxidation) processes. Structures of P1, P2 and their colors at their neutral and different oxidized states were demonstrated in Figures 3.6a and 5b. At the neutral state, both P1 and P2 have orange color. Following successive oxidation, intensity of absorption bands in the visible region steadily decrease while new absorption bands appear, and polymers have green color

during oxidation. Further oxidation results blue color for both polymers at fully oxidized state. As seen in Figure 3.6 there is little difference between the colors of P1 and P2, which means that the changing position of flourine atom from para– to meta – position has a little effect on colors of corresponding polymers. Furthermore, colorimetry experiments were carried out to determine the color of electrochemically synthesized polymers. In the CIE system; luminance (L), hue (a) and saturation (b) which are the attributes of color were recorded and reported in Table 3.2.

Table 3.2 Colorimetry results of P1 and P2

Polymer	Applied Potential	L	a	b
P1	**0.0 V**	57	-3	29
	0.8 V	57	-15	17
	1.4 V	59	-12	5
P2	**0.0 V**	80	-1	25
	1.0 V	79	-9	3
	1.5 V	57	-7	-5

3.1.1.4 Electrochromic contrast and switching studies of P1 and P2

The capability of a polymer to change its color rapidly between two states (neutral state and oxidized state) and illustrating a significant change are crucial properties for an electrochromic polymer. Switching time is defined as the period required for the color change of a material between its neutral and oxidized states.The percent transmittance changes and switching times of P1 and P2 between their fully oxidized and reduced states were investigated by applying potentials within 5 s time intervals. The kinetic studies were performed in a monomer free 0.1 M $NaClO_4$–$LiClO_4$/ACN solvent-electrolyte couple. The wavelengths at which kinetic studies performed were determined from the maximum absorbance at the spectra of polymer films.

As summarized in Table 3.3, P1 showed 41 % transmittance change upon doping/de-doping process at 1220 nm, 17 % at 685 nm and 16 % at 475 nm. P2 revealed 73 % transmittance at 1265 nm, 28 % at 770 nm and 29 % at 460 nm. Switching times were reported as 0.3 s, 0.4 s and 0.4 s for P1 and 1.7 s, 1.3 s and 0.7 s for P2 at corresponding wavelengths.

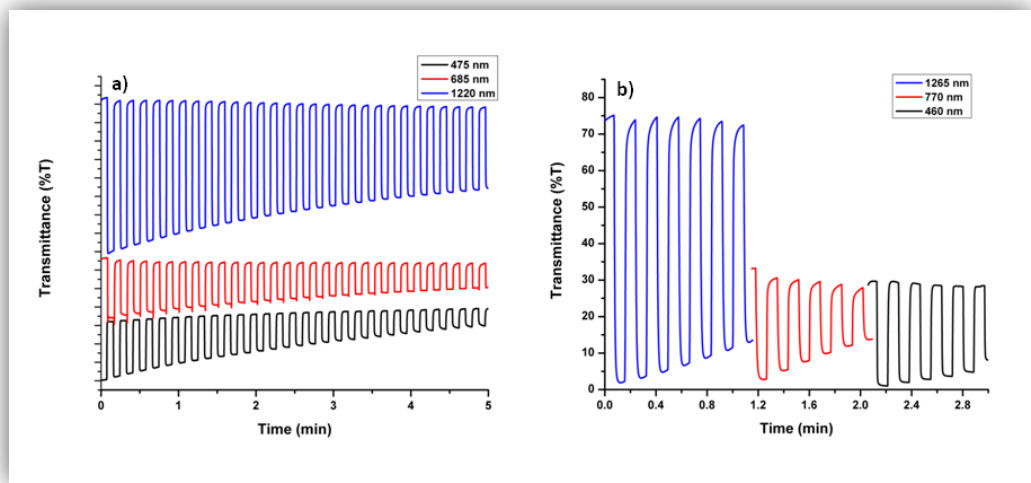

Figure 3.7 Optical contrasts and switching times monitored at different wavelengths for (a) P1 and (b) P2 in 0.1 M $NaClO_4$–$LiClO_4$/ACN solution

Kinetic studies strongly support the argument discussed in the electrochemical studies part. As explained before, para- substituted fluorine has more ring stabilization effect on this benzimidazole derivative when compared with meta–substituted one. This effect decreases the oxidation barrier of P1 and inreases its tendency to undergo a redox process which affects kinetic studies of the polymers significantly. As a result, switching times of P1 were really low compared to that of P2 in all wavelengths which is consistent with our argument (Table 3.3). In addition, when percent transmittance changes of P2 compared with those of other benzimidazole derivatives to best of our knowledge 73 % is the highest one in all. To

sum up, although stability of the polymers is not as good as other benzimidazole derivatives, swicthing times of P1 and precent transmittance of P2 are better compared to similar molecules [70, 71].

Table 3.3 Summary of kinetic and optic studies of P1 and P2

	Optical contrast (ΔT %)		**Switching times (s)**
P1	16 %	475 nm	0.4
	17 %	685 nm	0.4
	41 %	1220 nm	0.3
P2	29 %	460 nm	0.7
	28 %	770 nm	1.3
	73 %	1265 nm	1.7

3.1.2 Electrochemical and Optical Properties of M3 and M4

3.1.2.1 Electrochemical Polymerization of M3 and M4

In order to observe the electrochromic behaviors of polymers, the monomers M3 and M4 were polymerized electrochemically (Figure 3.8). For both monomers, the medium contained 0.1 M $NaClO_4$ - $LiClO_4$ / DCM / ACN (5:95, v:v). Since the monomers had poor solubility in acetonitrile, dichloromethane was used to obtain a homogeneous solution. The irreversible monomer oxidation potentials in the first cycle were found as 1.06 V for M3 and 0.92 V for M4 as shown in Figure 3.9.

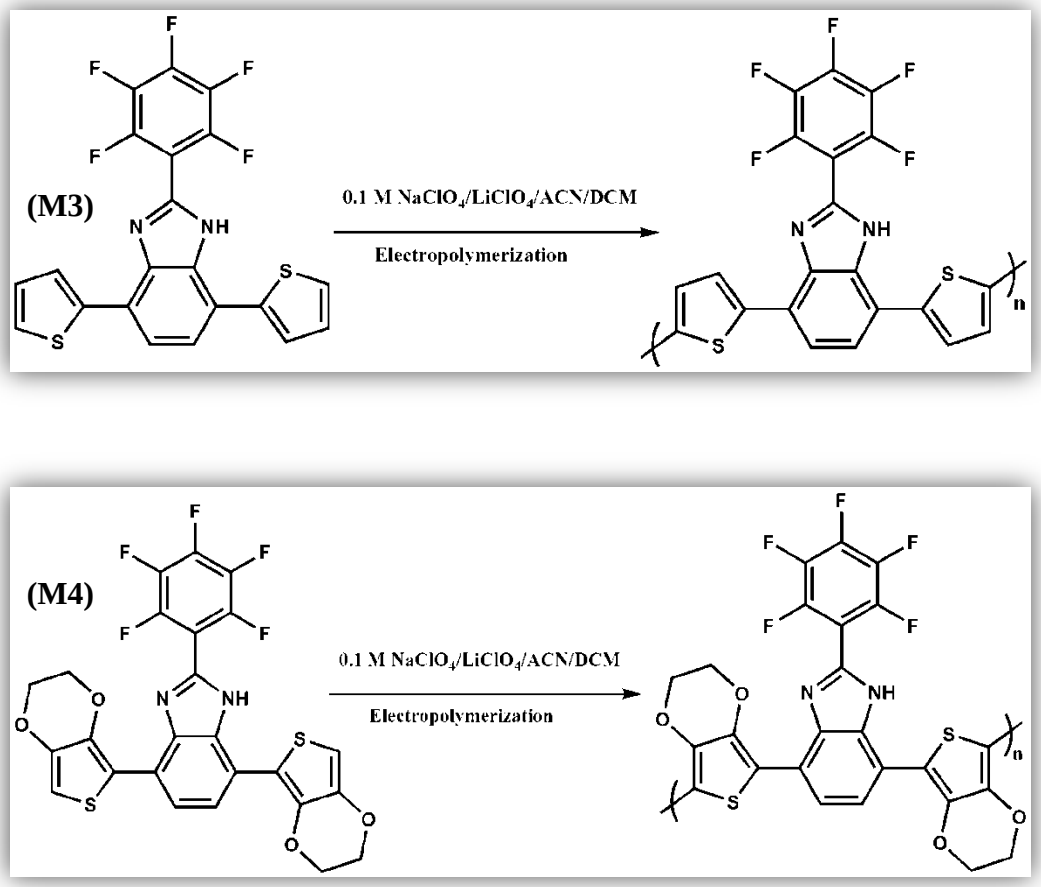

Figure 3.8 Electropolymerization of M3 and M4

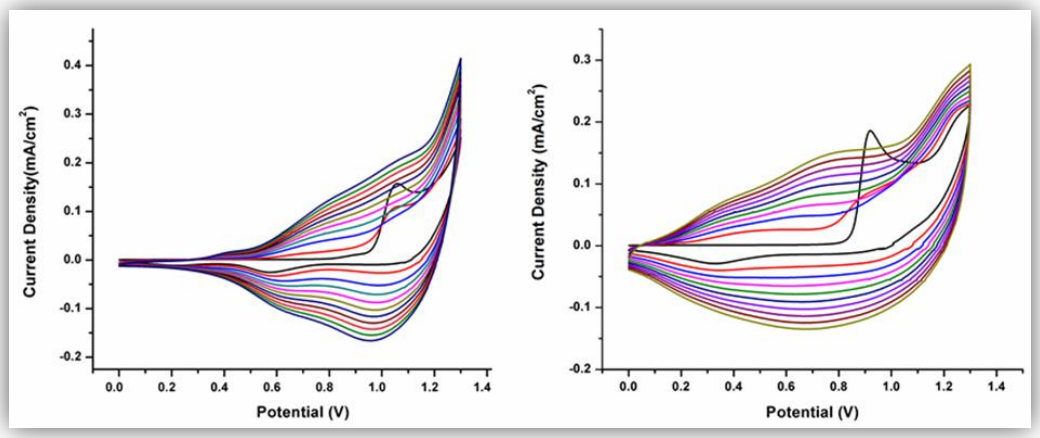

Figure 3.9 Repeated potential scan polymerization of (a) M3 and (b) M4 at 100 mV s^{-1} in 0.1 M $LiClO_4/NaClO_4$ CH_2Cl_2/ACN (5:95, v:v) solution on an ITO electrode

This difference can be explained with the high electron rich character of EDOT. Polymer redox peaks were observed at lower potentials than the monomer oxidation peaks. Current densities increased with increasing number of cycles. This proves that a polymer film was coated onto the ITO glass slide. So as to investigate the active layer of thin polymer films, single scan cyclic voltammograms of the P3 and P4 were performed in a monomer free 0.1 M $NaClO_4$ - $LiClO_4$ / ACN medium. As shown in Figure 3.10, both polymers have a p dopable character. The reversible redox couple for M3 was 0.95 V / 0.92 V and for M4 it was 0.72 V / 0.62 V.

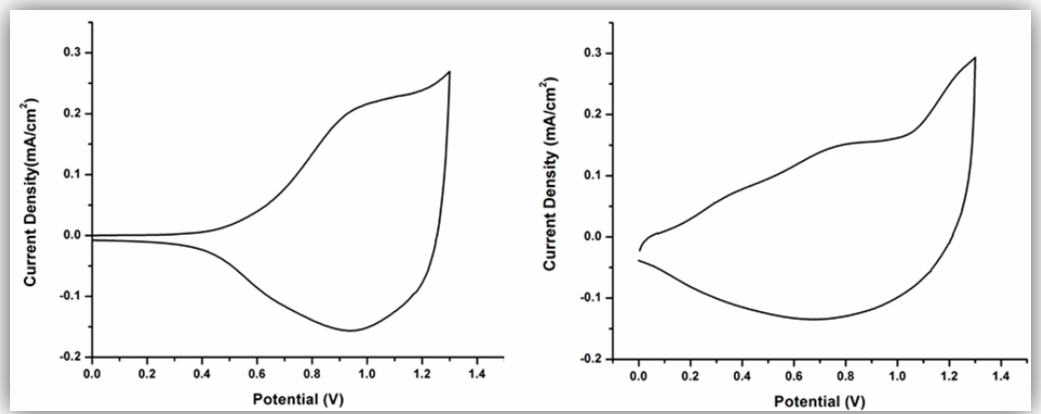

Figure 3.10 Single scan cyclic voltammograms of (a) P3 and (b) P4 in a monomer free 0.1 M $LiClO_4/NaClO_4$ ACN solution

The calculation of the HOMO energy level was done using the onset of the corresponding oxidation potentials vs. Fc/Fc^+ reference electrode by taking the value of SHE as -4.75 eV vs. vacuum (Figure 3.10 and Table 3.4). The LUMO energy level could not be calculated from the onset of the corresponding reduction potential since both polymers were not n dopable. They were calculated from the corresponding optical band gaps of the polymers. The HOMO energy levels were calculated as -5.75 eV for M3 and -5.57 eV for M4 in Table 3.4. Despite the fact that both polymers include same acceptor units, their HOMO energy levels were different from each other considerably. This difference can be explained with the presence of EDOT. As seen in Table 3.4, the LUMO energy level, reversible oxidation and

reduction potentials of P4 were lower than those of P3. This indicates that P4 provides more efficient donor – acceptor match than P3 on account of lower LUMO energy level.

3.1.2.2 Scan rate dependence of M3 and M4

The scan rate dependence experiments were performed by means of cyclic voltammetry in order to investigate the electrochemical process in terms of whether it is diffusion controlled or not. The linear relation between scan rate and current intensities indicated that polymer films were well adhered on ITO surface and the mass transfer in electrochemical processes were non-diffusion controlled (Figure 3.11).

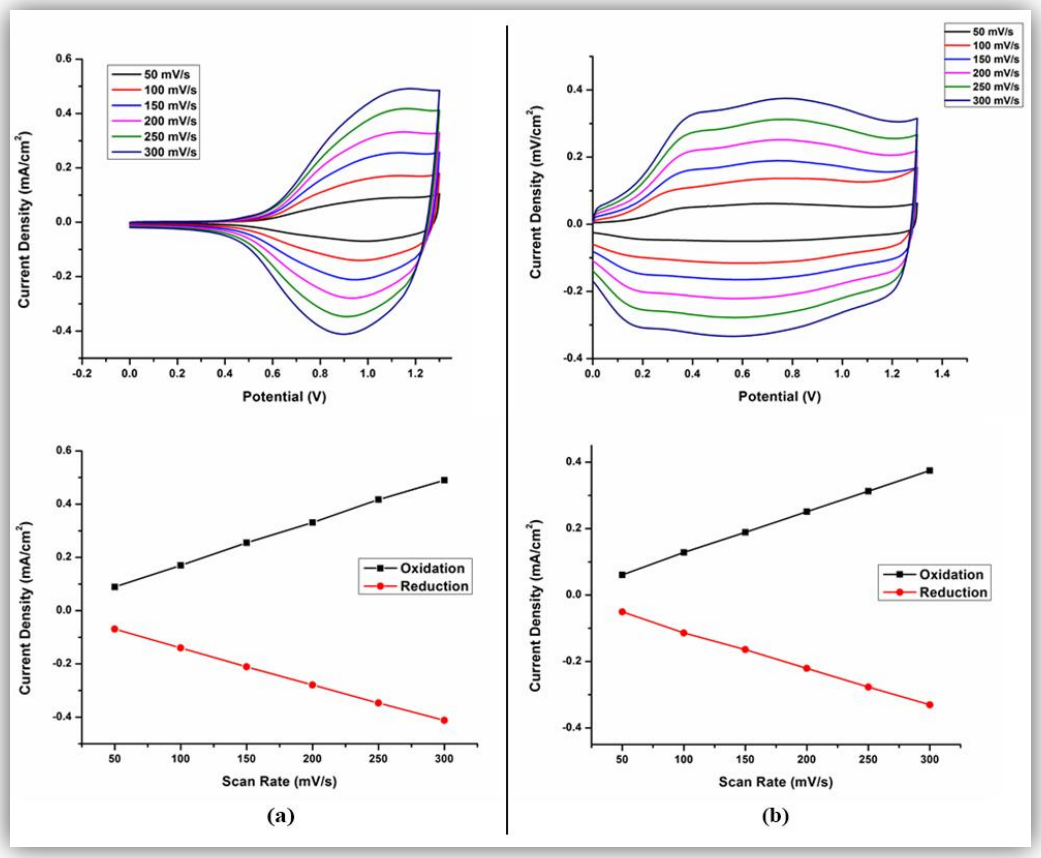

Figure 3.11 Scan rate dependence of (a) P3 film and (b) P4 film in a monomer free 0.1 M $NaClO_4$ - $LiClO_4$ / ACN solution at 50, 100, 150, 200, 250 and 300 $mV.s^{-1}$

3.1.2.3 Spectroelectrochemical and Colorimetric Studies of P3 and P4

To investigate the absorption behavior of electrochemically deposited polymer films, the spectroelectrochemical studies were performed. The polymer films onto ITO coated glass slide were exposed to doping via applied potentials in a monomer free

solution of 0.1 M $NaClO_4$ - $LiClO_4$ / ACN via UV-Vis-NIR spectrometer. These applied potentials were determined from the cyclic voltammograms of the polymers. The potential increments were 5 mV for P3 and 10 mV for P4 at each step as given in Figure 3.12. The absorption in the visible region decreased while the absorptions of polaron and bipolaron bands increased. The absorption of neutral state of P3 was observed at around 475 nm and its neutral state color was orange as seen in Figure 3.13 (a). Thus spectroelectrochemical studies and colorimetry results verified each other. The value of maximum absorption wavelength of P4 was at 575 nm and its neutral state color was blue as seen in Figure 3.13 (b). This situation proved that the red shift absorption was provided with P4 which contains EDOT moiety as the donor unit. Moreover, colorimetry experiments were done so as to determine the color of electrochemically synthesized polymers. In the CIE system; luminance (L), hue (a) and saturation (b) which are the attributes of color were recorded and reported in Table 3.5.

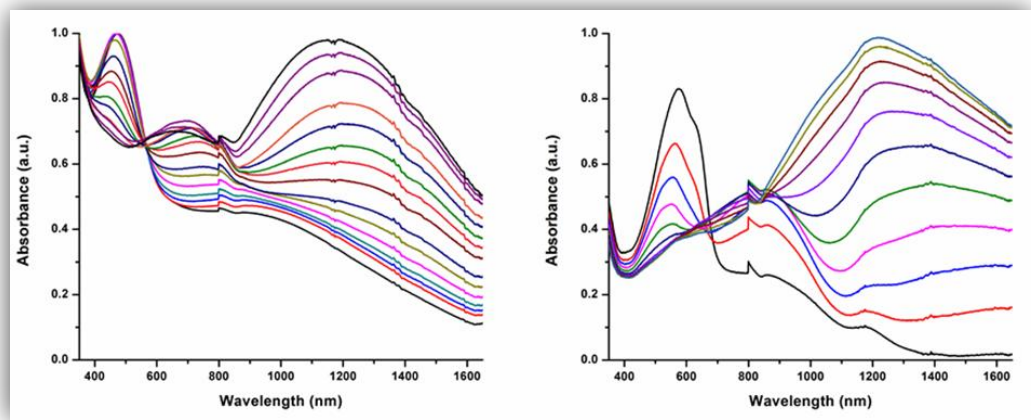

Figure 3.12 Electronic absorption spectra for (a) P3 and (b) P4 films in 0.1 M $NaClO_4$–$LiClO_4$ / ACN solution between 0.5 and 1.2 V for P3, 0.2 and 1.1 V for P4

The optical band gap was calculated from the onset of the absorption maxima in the visible region. The optical band gaps were found as 1.79 eV for P3 and 1.47 eV for P4. LUMO energy levels were calculated for both polymers using the optical band gaps and HOMO levels as -3.96 eV and -4.1 eV, respectively ((E_g^{op} = HOMO – LUMO)). For P3, polaronic and bipolaronic bands appear at 700 nm and 1210 nm, respectively. For P4, polaronic and bipolaronic bands appear at 840 nm and 1220 nm, respectively. With further oxidation, P3 had colors of green, blue and yellow and P4 was transparent as seen in Figure 3.13.

Table 3.4 Summary of electrochemical and spectroelectrochemical properties of P3 and P4

	HOMO (eV)	**LUMO (eV)**	**λ_{max} (nm)**	**E_g^{op} (eV)**
P3	-5.75	-3.96	480	1.79
P4	-5.57	-4.10	575	1.47

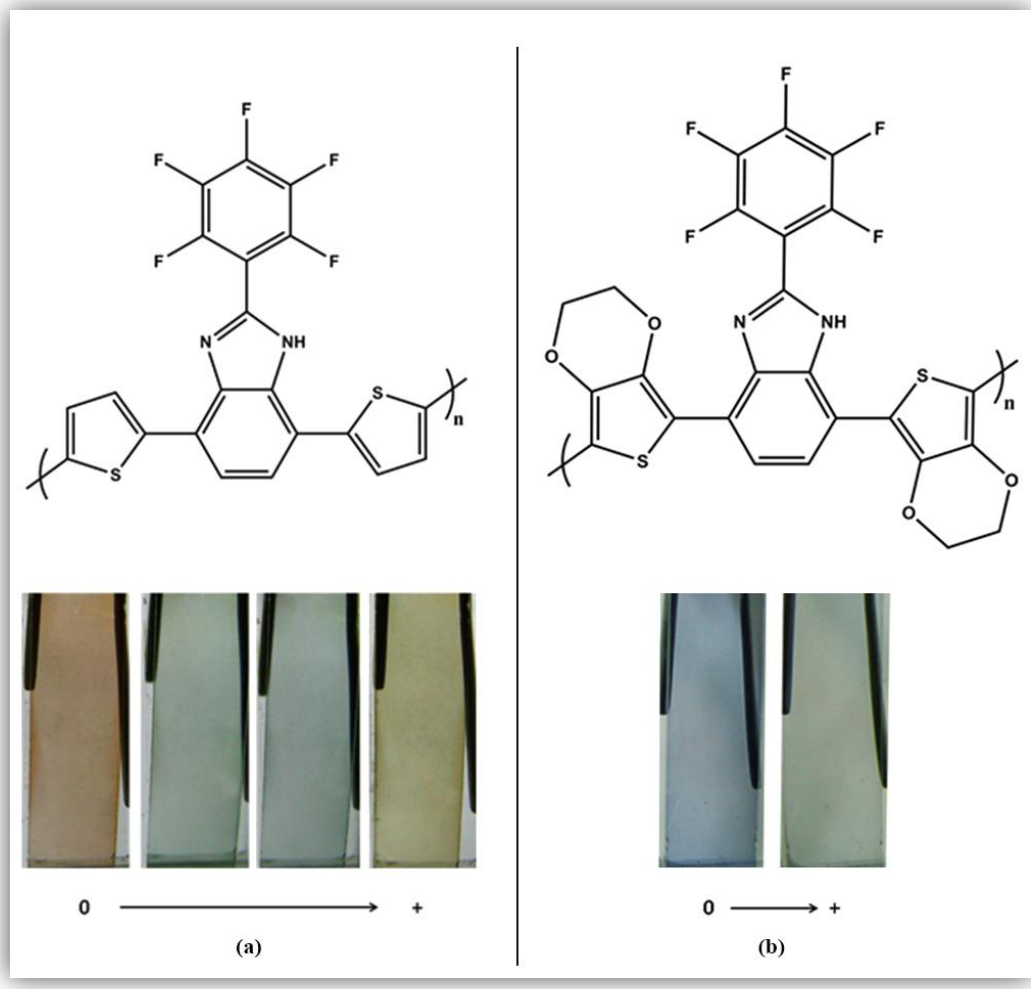

Figure 3.13 Structures of the polymers and their colors at their neutral and different oxidized states

Table 3.5 Colorimetry results of P3 and P4

Polymer	Applied Potential	L	a	b
P3	**0.0 V**	87	-7	12
	1.0 V	88	-11	7
	1.3 V	89	-11	4
	1.4 V	78	-7	11
P4	**0.0 V**	95	-10	-0.2
	1.4 V	85	-6	-6

3.1.2.4 Electrochromic contrast and switching studies of P3 and P4

The change of percent transmittance with respect to time and switching studies were measured by means of kinetic studies. After the determination of maximum wavelengths in three different regions from the spectroelectrochemical studies, potentials for 5 second time intervals were applied between polymers' neutral and fully oxidized states. Percent transmittance changes and switching time studies were determined in a monomer free 0.1 M $NaClO_4$–$LiClO_4$/ACN solution. Additionally, the switching times were calculated by means of kinetic studies in order to

investigate time required for 95% of full switches between colored and bleached states.

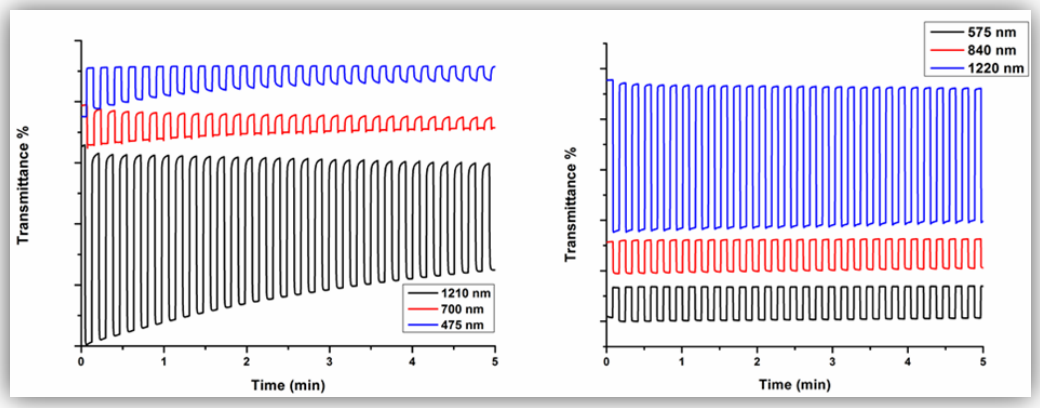

Figure 3.14 Optical contrasts and switching times monitored at different wavelengths for (a) P3 and (b) P4 in a monomer free 0.1 M $NaClO_4$–$LiClO_4$/ACN solution

As seen in Figure 3.14 and Table 3.6, P3 indicated 64% transmittance at 1210 nm, 12% at 700 nm and 14% at 475 nm. P4 showed 30% transmittance at 1220 nm, 7% at 840 nm and 7% at 575 nm. Switching times were calculated as 0.5 s, 0.1 s and 0.2 s for P3 and 0.3 s, 0.2 s and 0.1 s for P4 at suitable wavelengths respectively and reported in Table 3.6. The percent transmittance change of P3 in the visible region,

64%, was higher compared to other benzimidazole derivatives in the literature. Also P3 revealed 0.5 s switching time which is shorter with respect to the similar ones reported in literature [70, 72].

Table 3.6 Summary of percent transmittance changes and switching times of P3 and P4 at corresponding wavelengths

	Optical contrast (ΔT %)		**Switching times (s)**
P1	14 %	475 nm	0.2
	12 %	700 nm	0.1
	64 %	1210 nm	0.5
P2	7 %	575 nm	0.1
	7 %	840 nm	0.2
	30 %	1220 nm	0.3

CHAPTER 4

CONCLUSION

Fluorine containing D–A–D type monomers were synthesized via Stille coupling and characterized by means of Nuclear Magnetic Resonance and High Resolution Mass Spectroscopy. After the synthesis of monomers, the electrochemical polymerizations of monomers were carried out to obtain homopolymers of fluorine and benzimidazole bearing monomers on ITO coated glass slide. So as to probe the optical properties of electrochemically synthesized polymers, electrochemical, spectroelectrochemical and kinetic studies were performed. In the first part of thesis study, both para- and meta- substituted fluorine containing novel benzimidazole and thiophene based derivatives were designed to discuss the effect of position of substituents on electrochemical properties of polymers. Both polymer films have p-type doping property and showed electrochromic properties under applied different potentials. The HOMO levels were calculated from onsets of oxidation potentials of corresponding polymers as -5.46 and -5.54 eV for P1 and P2, respectively. The position of fluorine was changed from meta- to para- position, the oxidation of polymers was observed easily. Scan rate dependence experiments indicated that mass transfer in electrochemical processes were non-diffusion controlled during doping / dedoping. Optical band gaps of the polymers were calculated from the onsets of absorption maxima in the visible region with De Broglie equation as 1.91 eV for P1 and 1.96 eV for P2. Better packing property of para- substituted fluorine containing polymer, P1, caused a 31 nm red shift in absorption maxima. P1 resulted in lower energy and higher λ_{max} than that of P2. Since both polymers were not n- type dopable, the LUMO levels were calculated from the optical band gaps and found as -3.55 eV for P1 and -3.58 eV for P2. At neutral state, both polymers had orange color.

Following successive oxidation, both polymers were green in color. At fully oxidized state, they had blue color. As a result, both polymers possessed multichromic property. In addition, optical contrasts were enhanced by changing the position of fluorine from para- to meta- which was attributed to the better ring stabilization effect of para-substituted one. P1 showed 41% transmittance change upon doping/dedoping process at 1220 nm, 17% at 685 nm and 16% at 475 nm. P2 revealed 73% transmittance at 1265 nm, 28% at 770 nm and 29% at 460 nm. Switching times were reported as 0.3 s, 0.4 s and 0.4 s for P1 and 1.7 s, 1.3 s and 0.7 s for P2 at corresponding wavelengths. Switching times of P1 were really lower than that of P2 due to high conductivity. When percent transmittance changes of P2 compared with other benzimidazole derivatives from the literature to best of our knowledge 73% was the highest one. Reported results exhibited that fluorine containing benzimidazole derivatives were multipurpose materials due to improved kinetic results and band gaps.

This study was published in Electrochimica Acta in 2013 [67].

Furthermore, in the second part of thesis study, perfluorophenyl containing novel benzimidazole and thiophene, EDOT based derivatives were designed in order to investigate the donor effect between thiophene and EDOT moieties. Both polymers were p- type dopable. Oxidation potentials were found as 0.95 and 0.72 V for P3 and P4, respectively. Despite the fact that both polymers contained same acceptor units, their HOMO energy levels were different from each other considerably. The HOMO levels were calculated as -5.75 eV for P3 and -5.57 eV for P4. This difference was explained with the presence of EDOT. Scan rate dependence experiments exhibited that mass transfer was non-diffusion controlled during doping / dedoping process. Optical band gaps of the polymers were calculated as 1.79 eV for P3 and 1.47 eV for P4. LUMO levels were calculated as -3.96 and -4.10 eV for P3 and P4, respectively. P4 provides more efficient donor – acceptor match than P3 on account of lower LUMO energy level. The absorption of neutral state of P3 was observed at around

475 nm and its neutral state color was orange. The maximum absorption wavelength of P4 was at 575 nm and its neutral state color was blue. This proved that the red shift absorption was provided with P4 which contains EDOT moiety as the donor unit. Following oxidation, P3 possessed green, blue and yellowish color and P4 was transparent. Both polymers were multichromic property. Additionally, the switching times were calculated with kinetic studies to investigate time required for 95% of full switches between colored and bleached states. P3 indicated 64% transmittance at 1210 nm, 12% at 700 nm and 14% at 475 nm. P4 showed 30% transmittance at 1220 nm, 7% at 840 nm and 7% at 575 nm. Switching times were calculated as 0.5 s, 0.1 s and 0.2 s for P3 and 0.3 s, 0.2 s and 0.1 s for P4 at suitable wavelengths, respectively. The percent transmittance change of P3 in the visible region, 64%, was higher compared to other benzimidazole derivatives in the literature. The electrochemical and optical characterizations of the electrochemically synthesized polymer containing EDOT unit as the donor showed that EDOT is a stronger donor than thiophene.

This study was submitted to Smart Materials and Structures in 2014.

REFERENCES

[1] Thompson, B. C., Schottland, P., Zong, K., & Reynolds, J. R. (2000). In Situ Colorimetric Analysis of Electrochromic Polymers and Devices. *Chemistry of Materials*, *12*(6), 1563.

[2] Dyer, A. L., Craig, M. R., Babiarz, J. E., Kiyak, K., & Reynolds, J. R. (2010). Orange and Red to Transmissive Electrochromic Polymers Based on Electron-Rich Dioxythiophenes. *Macromolecules*, *43*(10), 4460.

[3] Sapp, S. A., Sotzing, G. A., & Reynolds, J. R. (1998). High Contrast Ratio and Fast-Switching Dual Polymer Electrochromic Devices. *Chemistry of Materials*, *10*(8), 2101.

[4] Sonmez, G., Sonmez, H. B., Shen, C. K. F., Jost, R. W., Rubin, Y., & Wudl, F. (2005). A Processable Green Polymeric Electrochromic. *Macromolecules*, *38*(3), 669.

[5] Letheby, H. (1862). XXIX.-On the production of a blue substance by the electrolysis of sulphate of aniline. *Journal of the Chemical Society*, *15*, 161.

[6] Shirakawa, H., Louis, E. J., MacDiarmid, A. G., Chiang, C. K., & Heeger, A. J. (1977). Synthesis of electrically conducting organic polymers: halogen derivatives of polyacetylene, $(CH)_x$. *Journal of the Chemical Society, Chemical Communications*, (16), 578.

[7] Heeger, A. J. (2001). Semiconducting and metallic polymers: the fourth generation of polymeric materials. *Synthetic Metals*, *125*(1), 23.

[8] Shirakawa, H. (2001). The discovery of polyacetylene film. *Synthetic Metals*, *125*(1), 3.

[9] MacDiarmid, A. G. (2001). Synthetic metals: a novel role for organic polymers. *Synthetic Metals*, *125*(1), 11.

[10] Unur, E., Beaujuge, P. M., Ellinger, S., Jung, J.-H., & Reynolds, J. R. (2009). Black to Transmissive Switching in a Pseudo Three-Electrode Electrochromic Device. *Chemistry of Materials*, *21*(21), 5145.

[11] Balan, A., Baran, D., & Toppare, L. (2011). Benzotriazole containing conjugated polymers for multipurpose organic electronic applications. *Polymer Chemistry*, *2*(5), 1029.

[12] Ozdemir, S., Sendur, M., Oktem, G., Doğan, Ö., & Toppare, L. (2012). A promising combination of benzotriazole and quinoxaline units: A new acceptor moiety toward synthesis of multipurpose donor–acceptor type polymers. *Journal of Materials Chemistry*, *22*(11), 4687.

[13] Xu, C., Zhao, J., Yu, J., & Cui, C. (2013). Ethylenedioxythiophene derivatized polynapthalenes as active materials for electrochromic devices. *Electrochimica Acta*, *96*(96), 82.

[14] Xu, C., Zhao, J., Wang, M., Wang, Z., Cui, C., Kong, Y., & Zhang, X. (2012). Electrosynthesis and characterization of a neutrally colorless electrochromic material from poly(1,3-bis(9H-carbazol-9-yl)benzene) and its application in electrochromic devices. *Electrochimica Acta*, *75*, 28.

[15] Du, Q., Mi, S., Zheng, J., & Xu, C. (2013). A comparative study of the electrochemical behavior of complementary polymer electrochromic devices based on different counter-electrodes. *Smart Materials and Structures*, *22*(12), 125025.

[16] Günes, S., Neugebauer, H., & Sariciftci, N. S. (2007). Conjugated polymer-based organic solar cells. *Chemical Reviews*, *107*(4), 1324.

[17] Kularatne, R. S., Magurudeniya, H. D., Sista, P., Biewer, M. C., & Stefan, M. C. (2013). Donor-acceptor semiconducting polymers for organic solar cells. *Journal of Polymer Science Part A: Polymer Chemistry*, *51*(4), 743.

[18] Li, Z., Zhou, D., Li, L., Li, Y., He, Y., Liu, J., & Peng, Q. (2013). Synthesis and characterization of copolymers based on benzotriazoles and different atom-bridged dithiophenes for efficient solar cells. *Polymer Chemistry*, *4*(8), 2496.

[19] Bijleveld, J. C., Zoombelt, A. P., Mathijssen, S. G. J., Wienk, M. M., Turbiez, M., de Leeuw, D. M., & Janssen, R. A. J. (2009). Poly(diketopyrrolopyrrole-terthiophene) for ambipolar logic and photovoltaics. *Journal of the American Chemical Society*, *131*(46), 16616.

[20] Tsai, J.-H., Chueh, C.-C., Chen, W.-C., Yu, C.-Y., Hwang, G.-W., Ting, C., … Meng, H.-F. (2010). New thiophene-phenylene-thiophene acceptor random conjugated copolymers for optoelectronic applications. *Journal of Polymer Science Part A: Polymer Chemistry*, *48*(11), 2351.

[21] Ekiz, F., Oğuzkaya, F., Akin, M., Timur, S., Tanyeli, C., & Toppare, L. (2011). Synthesis and application of poly-SNS-anchored carboxylic acid: a novel functional matrix for biomolecule conjugation. *Journal of Materials Chemistry*, *21*(33), 12337.

[22] Demirci, S., Emre, F. B., Ekiz, F., Oğuzkaya, F., Timur, S., Tanyeli, C., & Toppare, L. (2012). Functionalization of poly-SNS-anchored carboxylic acid with Lys and PAMAM: surface modifications for biomolecule immobilization/stabilization and bio-sensing applications. *The Analyst*, *137*(18), 4254.

[23] McQuade, D. T., Pullen, A. E., & Swager, T. M. (2000). Conjugated polymer-based chemical sensors. *Chemical Reviews*, *100*(7), 2537.

[24] Horie, M., Majewski, L. A., Fearn, M. J., Yu, C.-Y., Luo, Y., Song, A., Turner, M. L. (2010). Cyclopentadithiophene based polymers—a comparison of optical, electrochemical and organic field-effect transistor characteristics. *Journal of Materials Chemistry*, *20*(21), 4347.

[25] Chua, L.-L., Zaumseil, J., Chang, J.-F., Ou, E. C.-W., Ho, P. K.-H., Sirringhaus, H., & Friend, R. H. (2005). General observation of n-type field-effect behaviour in organic semiconductors. *Nature*, *434*(7030), 194.

[26] Zuniga, C., Barlow, S., & Marder, S. (2011). Approaches to Solution-Processed Multilayer Organic Light-Emitting Diodes Based on Cross-Linking. *Chemistry of Materials*, *23*(3), 658.

[27] Tsuji, H., Mitsui, C., Sato, Y., & Nakamura, E. (2009). Bis(carbazolyl)benzodifuran: A High-Mobility Ambipolar Material for Homojunction Organic Light-Emitting Diode Devices. Advanced Materials, 21(37), 3776.

[28] Bredas, J. L., & Street, G. B. (1985). Polarons, bipolarons, and solitons in conducting polymers. *Accounts of Chemical Research*, *18*(10), 309.

[29] Yang, S., Olishevski, P., & Kertesz, M. (2004). Bandgap calculations for conjugated polymers. *Synthetic Metals*, *141*(1-2), 171.

[30] Okamoto, K., & Luscombe, C. K. (2011). Controlled polymerizations for the synthesis of semiconducting conjugated polymers. *Polymer Chemistry*, *2*(11), 2424.

[31] Toshima, N., & Hara, S. (1995). Direct synthesis of conducting polymers from simple monomers. *Progress in Polymer Science*, *20*(1), 155.

[32] Yoshino, K., Hayashi, S., & Sugimoto, R. (1984). Preparation and Properties of Conducting Heterocyclic Polymer Films by Chemical Method. *Japanese Journal of Applied Physics*, *23*(Part 2, No. 12), L899.

[33] McCullough, R. D. (1998). The Chemistry of Conducting Polythiophenes. *Advanced Materials*, *10*(2), 93.

[34] Malinauskas, A. (2001). Chemical deposition of conducting polymers. *Polymer*, *42*(9), 3957.

[35] Yamamoto, T., Sanechika, K., & Yamamoto, A. (1980). Preparation of thermostable and electric-conducting poly(2,5-thienylene). *Journal of Polymer Science: Polymer Letters Edition*, *18*(1), 9.

[36] Lin, J. W.-P., & Dudek, L. P. (1980). Synthesis and properties of poly(2,5-thienylene). *Journal of Polymer Science: Polymer Chemistry Edition*, *18*(9), 2869.

[37] Zotti, G., Schiavon, G., Berlin, A., & Pagani, G. (1993). Thiophene oligomers as polythiophene models. 1. Anodic coupling of thiophene oligomers to dimers: a kinetic investigation. *Chemistry of Materials*, *5*(4), 430.

[38] Audebert, P., & Hapiot, P. (1995). Fast electrochemical studies of the polymerization mechanisms of pyrroles and thiophenes. Identification of the first steps. Existence of π-dimers in solution. *Synthetic Metals*, *75*(2), 95.

[39] Diaz, A. F., & Bargon, J. (1986). Handbook of Conducting Polymers. ed. T. J. Skotheim, Marcel Dekker, New York, 81.

[40] Osagawara, M., Funahashi, K., Demura, T., Hagiwara, T., & Iwata, K. (1986). Enhancement of electrical conductivity of polypyrrole by stretching. *Synthetic Metals*, *14*(1-2), 61.

[41] Mortimer, R. J. (1997). Electrochromic materials. *Chemical Society Reviews*, *26*(3), 147.

[42] Somani, P. R., & Radhakrishnan, S. (2003). Electrochromic materials and devices: present and future. *Materials Chemistry and Physics*, *77*(1), 117.

[43] Rowley, N. M., & Mortimer, R. J. (2002). New electrochromic materials. *Science Progress*, *85*(Pt 3), 243.

[44] Ak, M., Cirpan, A., Yilmaz, F., Yagci, Y., & Toppare, L. (2005). Synthesis and characterization of a bifunctional amido-thiophene monomer and its copolymer with thiophene and electrochemical properties. *European Polymer Journal*, *41*(5), 967.

[45] Sonmez, G., Shen, C. K. F., Rubin, Y., & Wudl, F. (2004). A red, green, and blue (RGB) polymeric electrochromic device (PECD): the dawning of the PECD era. *Angewandte Chemie (International Ed. in English)*, *43*(12), 1498.

[46] Sonmez, G., & Wudl, F. (2005). Completion of the three primary colours: the final step toward plastic displays. *Journal of Materials Chemistry*, *15*(1), 20.

[47] Chen, H.-Y., Yeh, S.-C., Chen, C.-T., & Chen, C.-T. (2012). Comparison of thiophene- and selenophene-bridged donor–acceptor low band-gap copolymers used in bulk-heterojunction organic photovoltaics. *Journal of Materials Chemistry*, *22*(40), 21549.

[48] Lin, Y., Li, Y., & Zhan, X. (2012). Small molecule semiconductors for high-efficiency organic photovoltaics. *Chemical Society Reviews*, *41*(11), 4245.

[49] Salzner, U. (2002). Does the Donor−Acceptor Concept Work for Designing Synthetic Metals? 1. Theoretical Investigation of Poly(3-cyano-3‘-hydroxybithiophene). *The Journal of Physical Chemistry B*, *106*(36), 9214.

[50] Dutta, P., Park, H., Lee, W.-H., Kim, K., Kang, I. N., & Lee, S.-H. (2012). Naphtho[1,2-b:5,6-b′]dithiophene-based conjugated polymer as a new electron donor for bulk heterojunction organic solar cells. *Polymer Chemistry*, *3*(3), 601.

[51] Gustafsson-Carlberg, J. C., Inganäs, O., Andersson, M. R., Booth, C., Azens, A., & Granqvist, C. G. (1995). Tuning the bandgap for polymeric smart windows and displays. *Electrochimica Acta*, *40*(13-14), 2233.

[52] Camurlu, P., & Gültekin, C. (2012). Utilization of novel bithiazole based conducting polymers in electrochromic applications. *Smart Materials and Structures*, *21*, 025019.

[53] Thompson, B. C., Kim, Y.-G., McCarley, T. D., & Reynolds, J. R. (2006). Soluble narrow band gap and blue propylenedioxythiophene-cyanovinylene polymers as multifunctional materials for photovoltaic and electrochromic applications. *Journal of the American Chemical Society*, *128*(39), 12714.

[54] Cheng, Y.-J., Yang, S.-H., & Hsu, C.-S. (2009). Synthesis of conjugated polymers for organic solar cell applications. *Chemical Reviews*, *109*(11), 5868.

[55] Beaujuge, P. M., & Reynolds, J. R. (2010). Color control in pi-conjugated organic polymers for use in electrochromic devices. *Chemical Reviews*, *110*(1), 268.

[56] Kukalenko, S. S., Bovykin, B. A., Shestakova, S. I., & Omel'chenko, A. M. (1985). Metal-containing Complexes of Lactams, Imidazoles, and Benzimidazoles and Their Biological Activity. *Russian Chemical Reviews*, *54*(7), 676.

[57] Barker, H. A., Smyth, R. D., Weissbach, H., Toohey, J. I., Ladd, J. N., & Volcani, B. E. (1960). Isolation and properties of crystalline cobamide coenzymes containing benzimidazole or 5, 6-dimethylbenzimidazole. *The Journal of Biological Chemistry*, *235*, 480.

[58] Ragno, G., Risoli, A., Ioele, G., & De Luca, M. (2006). Photo- and thermal-stability studies on benzimidazole anthelmintics by HPLC and GC-MS. *Chemical & Pharmaceutical Bulletin*, *54*(6), 802.

[59] Rodríguez-Rodríguez, C., Sánchez de Groot, N., Rimola, A., Alvarez-Larena, A., Lloveras, V., Vidal-Gancedo, J., González-Duarte, P. (2009). Design, selection, and characterization of thioflavin-based intercalation compounds with metal chelating properties for application in Alzheimer's disease. *Journal of the American Chemical Society*, *131*(4), 1436.

[60] Kim, S. J., & Kool, E. T. (2006). Sensing metal ions with DNA building blocks: fluorescent pyridobenzimidazole nucleosides. *Journal of the American Chemical Society*, *128*(18), 6164.

[61] Goodwin, K. D., Lewis, M. A., Tanious, F. A., Tidwell, R. R., Wilson, W. D., Georgiadis, M. M., & Long, E. C. (2006). A high-throughput, high-resolution strategy for the study of site-selective DNA binding agents: analysis of a "highly twisted" benzimidazole-diamidine. *Journal of the American Chemical Society*, *128*(24), 7846.

[62] Da Silveria Neto, B.A., SantAna, A.L., Ebeling, G., Goncalves, S.R., Costa, E.V.U., Quina, H.F., & Dupont, J. (2005). Photophysical and electrochemical properties of π-extended molecular 2,1,3-benzothiadiazoles. *Tetrahedron*, 61, 10975.

[63] Tsubata, Y., Suzuki, T., Miyashi, T., & Yamashita, Y. (1992). Single-component organic conductors based on neutral radicals containing the pyrazino-TCNQ skeleton. *The Journal of Organic Chemistry*, *57*(25), 6749.

[64] Balan, A., Baran, D., Gunbas, G., Durmus, A., Ozyurt, F., & Toppare, L. (2009). One polymer for all: benzotriazole containing donor-acceptor type polymer as a multi-purpose material. *Chemical Communications (Cambridge, England)*, (44), 6768.

[65] Zhu, S. S., & Swager, T. M. (1997). Conducting Polymetallorotaxanes: Metal Ion Mediated Enhancements in Conductivity and Charge Localization. *Journal of the American Chemical Society*, *119*(51), 12568.

[66] Bahrami, K., Khodaei, M. M., & Naali, F. (2008). Mild and highly efficient method for the synthesis of 2-arylbenzimidazoles and 2-arylbenzothiazoles. *The Journal of Organic Chemistry*, *73*(17), 6835.

[67] Ileri, M., Hacioglu, S. O., & Toppare, L. (2013). The effect of para- and meta-substituted fluorine on optical behavior of benzimidazole derivatives. *Electrochimica Acta*, *109*, 214.

[68] Huang, Y., Zhang, M., Ye, L., Guo, X., Han, C. C., Li, Y., & Hou, J. (2012). Molecular energy level modulation by changing the position of electron-donating side groups. *Journal of Materials Chemistry*, *22*(12), 5700.

[69] Goedel, W. A., Somanathan, N. S., Enkelmann, V., & Wegner, G. (1992). Steric effects in 3-substituted polythiophenes: comparing band gap, nonlinear optical susceptibility and conductivity of poly(3-cyclohexylthiophene) and poly(3-hexylthiophene). *Die Makromolekulare Chemie*, *193*(5), 1195.

[70] Ozelcaglayan, A. C., Sendur, M., Akbasoglu, N., Apaydin, D. H., Cirpan, A., & Toppare, L. (2012). Synthesis and electrochemical properties of a new benzimidazole derivative as the acceptor unit in donor–acceptor–donor type polymers. *Electrochimica Acta*, *67*, 224.

[71] Nurioglu, A. G., Akpinar, H., Sendur, M., & Toppare, L. (2012). Multichromic benzimidazole-containing polymers: Comparison of donor and acceptor unit effects. *Journal of Polymer Science Part A: Polymer Chemistry*, *50*(17), 3499.

[72] Namal, I., Ozelcaglayan, A. C., Udum, Y. A., & Toppare, L. (2013). Synthesis and electrochemical characterization of fluorene and benzimidazole containing novel conjugated polymers: Effect of alkyl chain length on electrochemical properties. *European Polymer Journal*, *49*(10), 3181.

APPENDIX A

NMR SPECTRA OF SYNTHESIZED MONOMERS

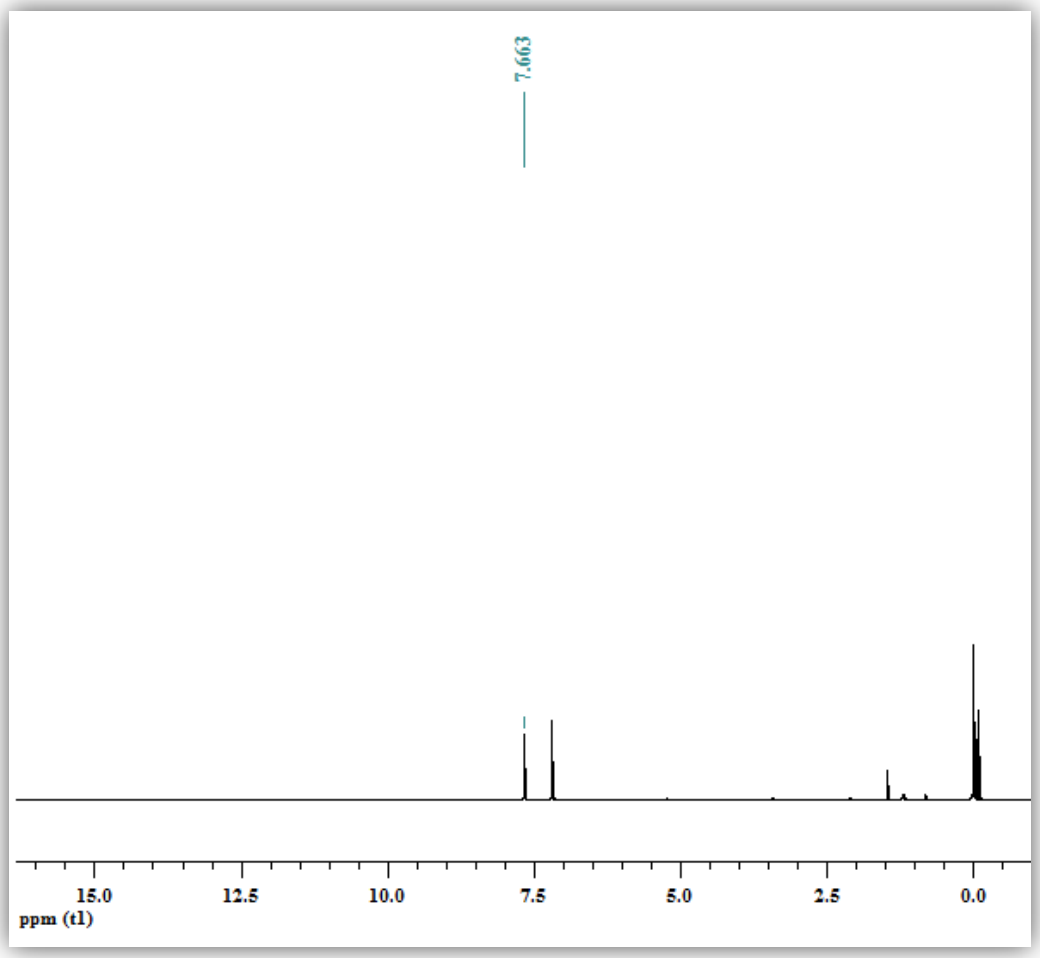

Figure A. 1 ^{1}H-NMR spectrum of 4,7-dibromobenzo[c][1,2,5]thiadiazole

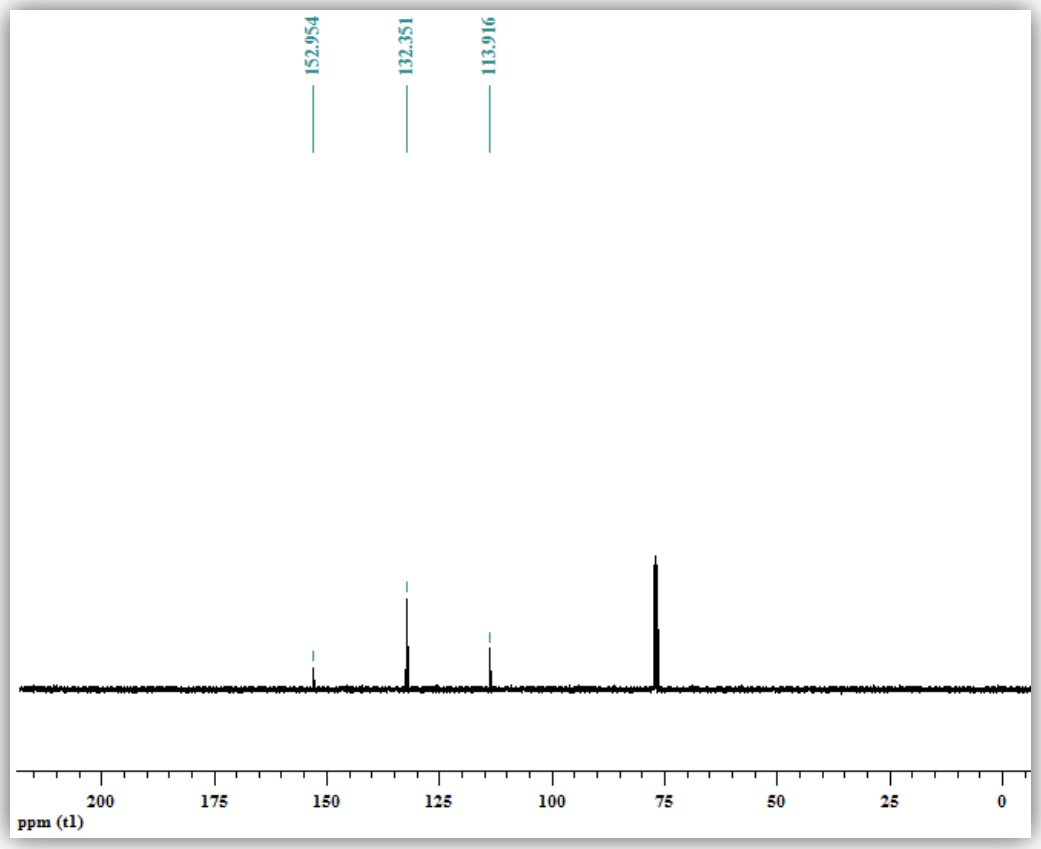

Figure A. 2 ^{13}C-NMR spectrum of 4,7-dibromobenzo[c][1,2,5]thiadiazole

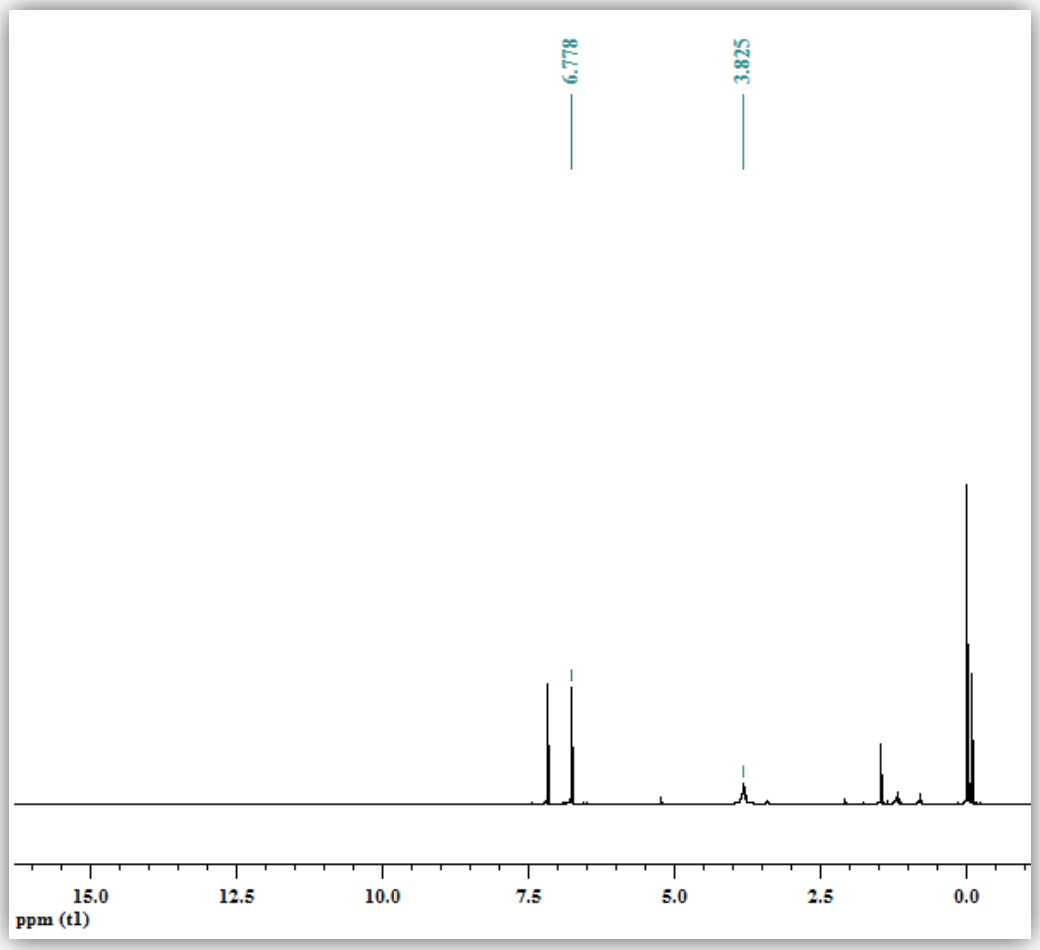

Figure A. 3 ^{1}H-NMR spectrum of 3,6-dibromo-1,2-phenylenediamine

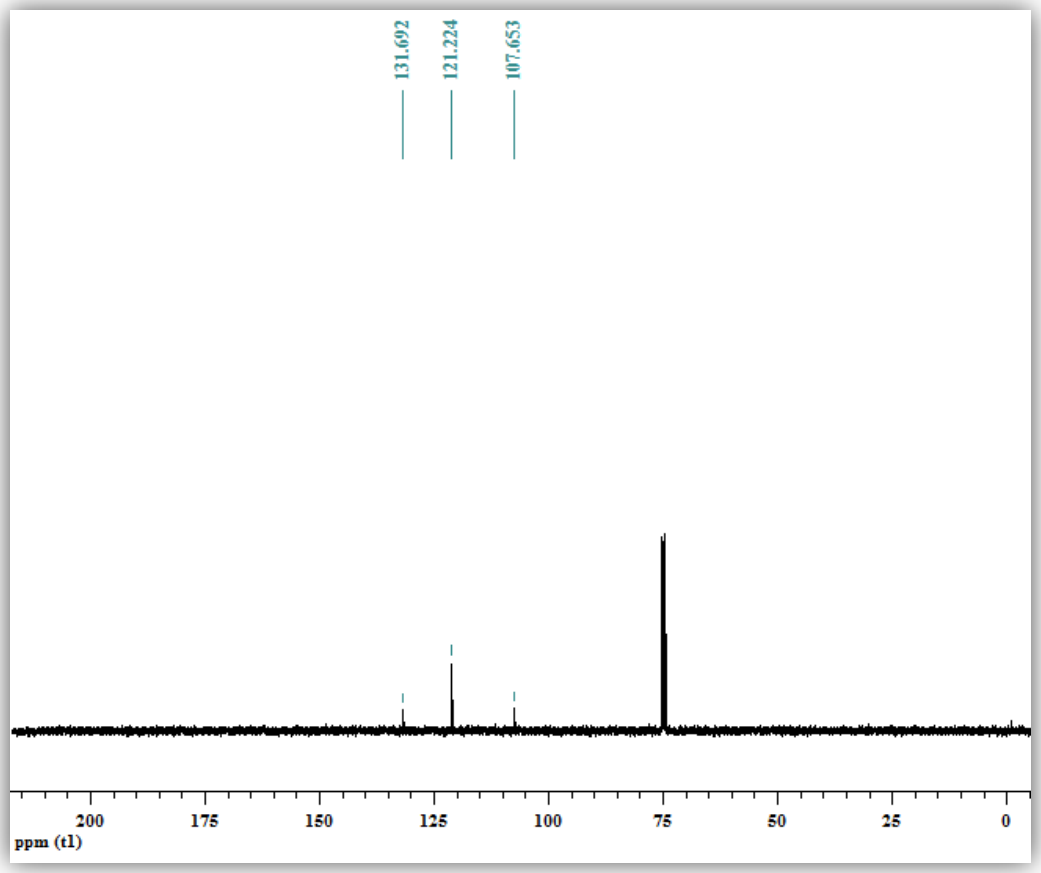

Figure A. 4 ^{13}C-NMR spectrum of 3,6-dibromo-1,2-phenylenediamine

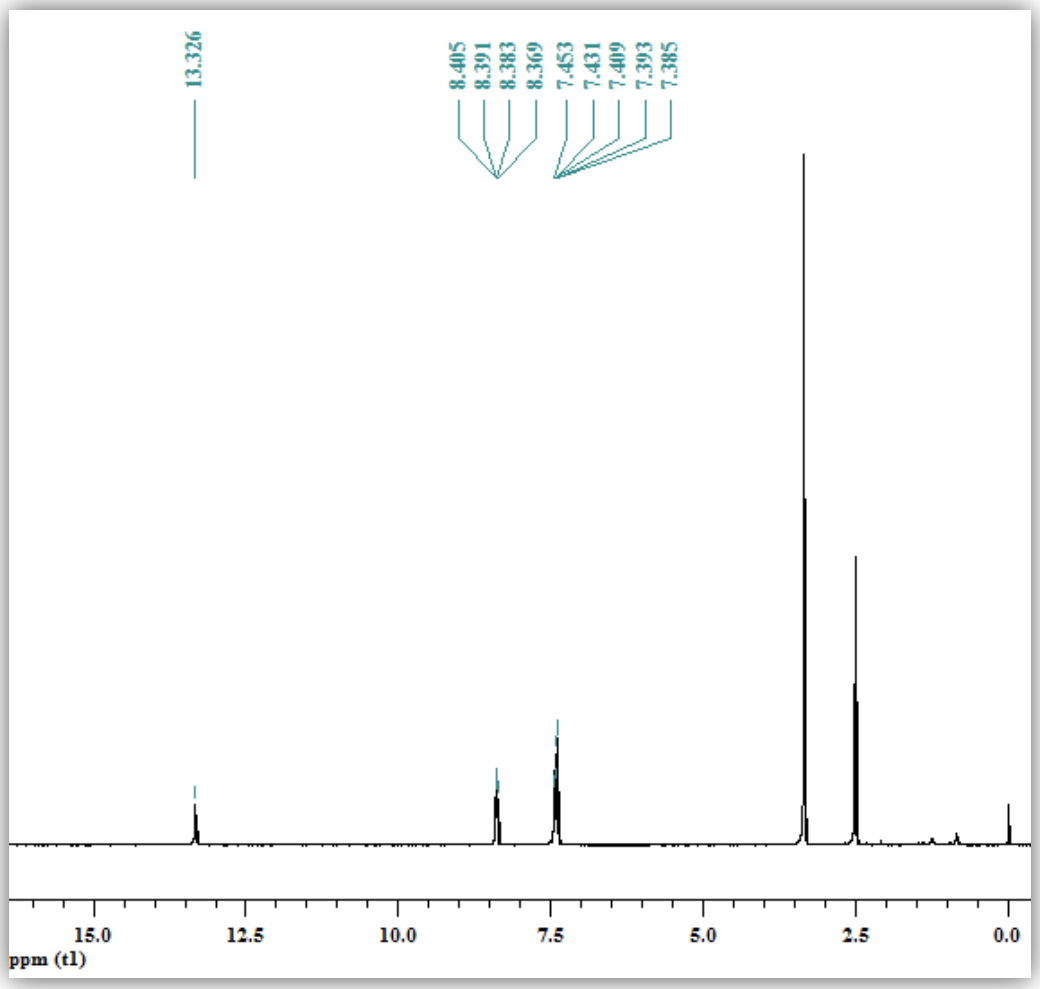

Figure A. 5 ^{1}H-NMR spectrum of 4,7-dibromo-2-(4-fluorophenyl)-1H-benzo[d]imidazole

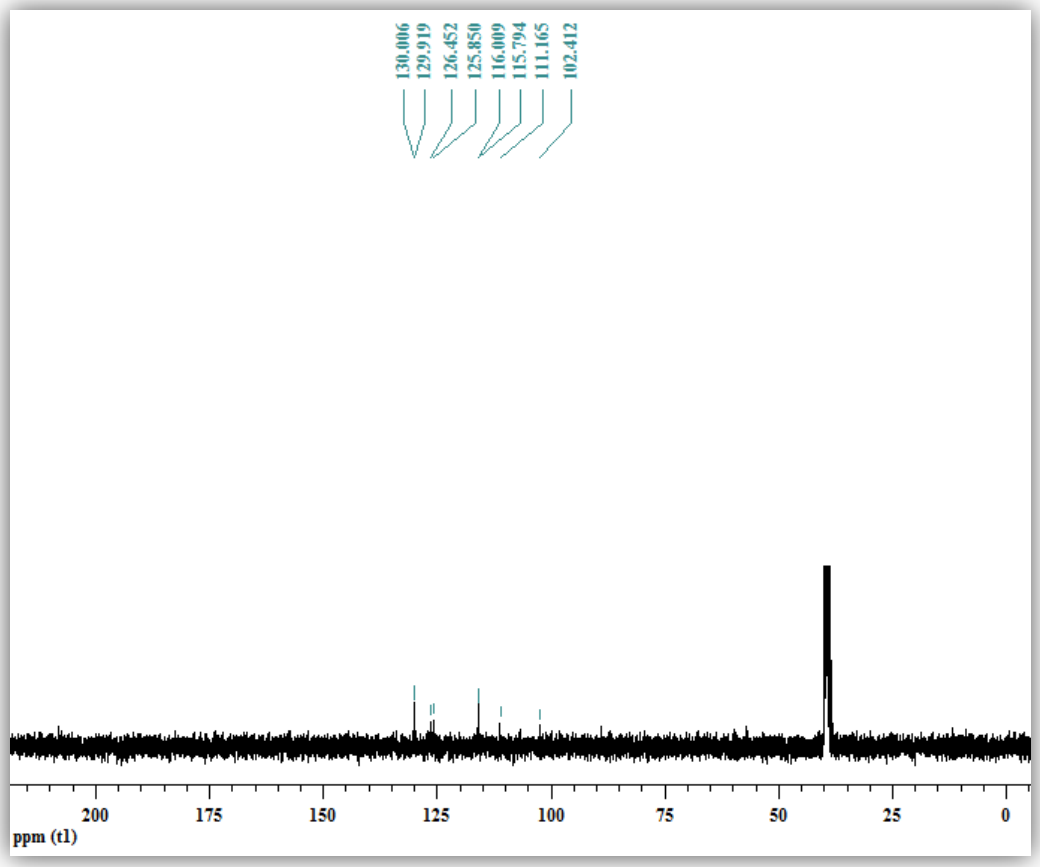

Figure A. 6 ^{13}C-NMR spectrum of 4,7-dibromo-2-(4-fluorophenyl)-1H-benzo[d]imidazole

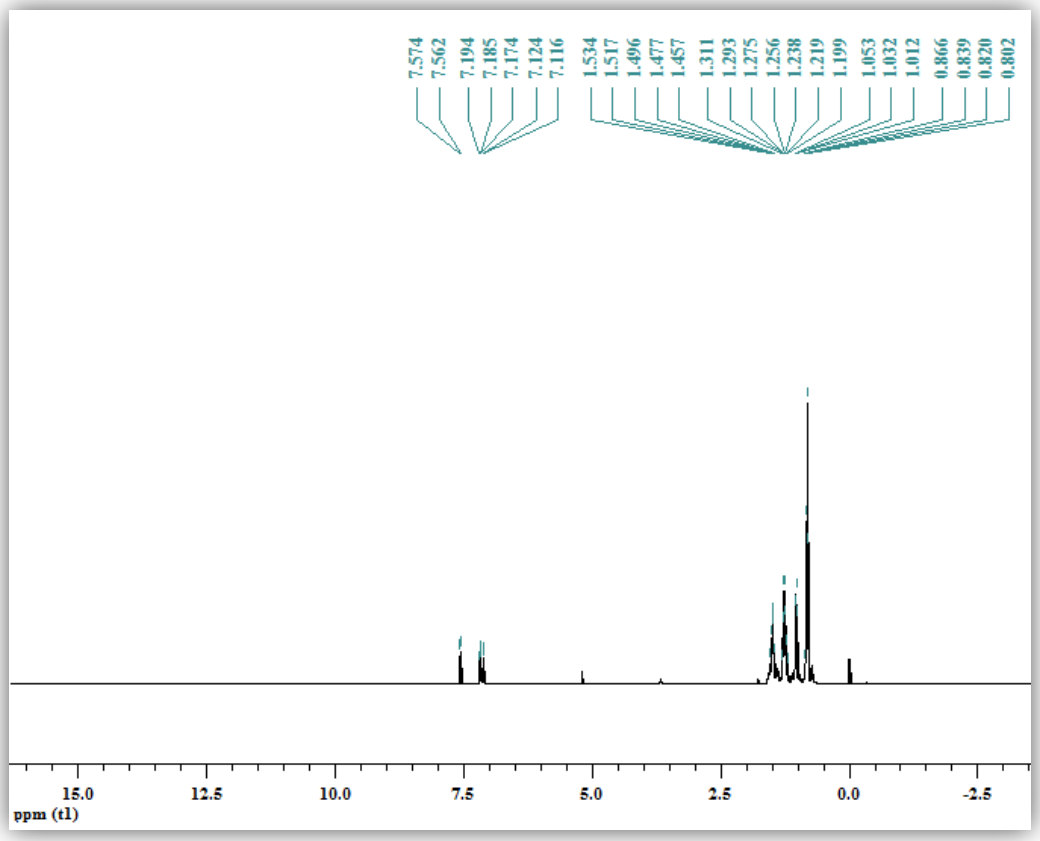

Figure A. 7 ^{1}H-NMR spectrum of tributyl(thiophene-2-yl)stannane

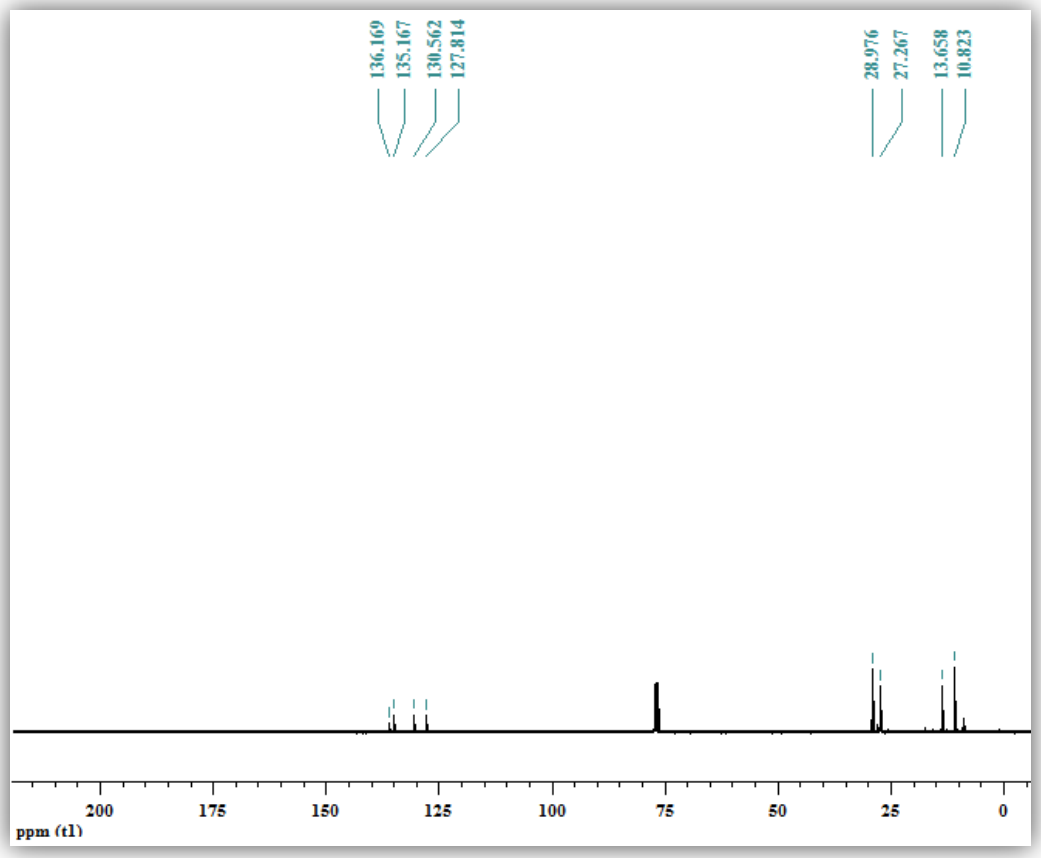

Figure A. 8 ^{13}C-NMR spectrum of tributyl(thiophene-2-yl)stannane

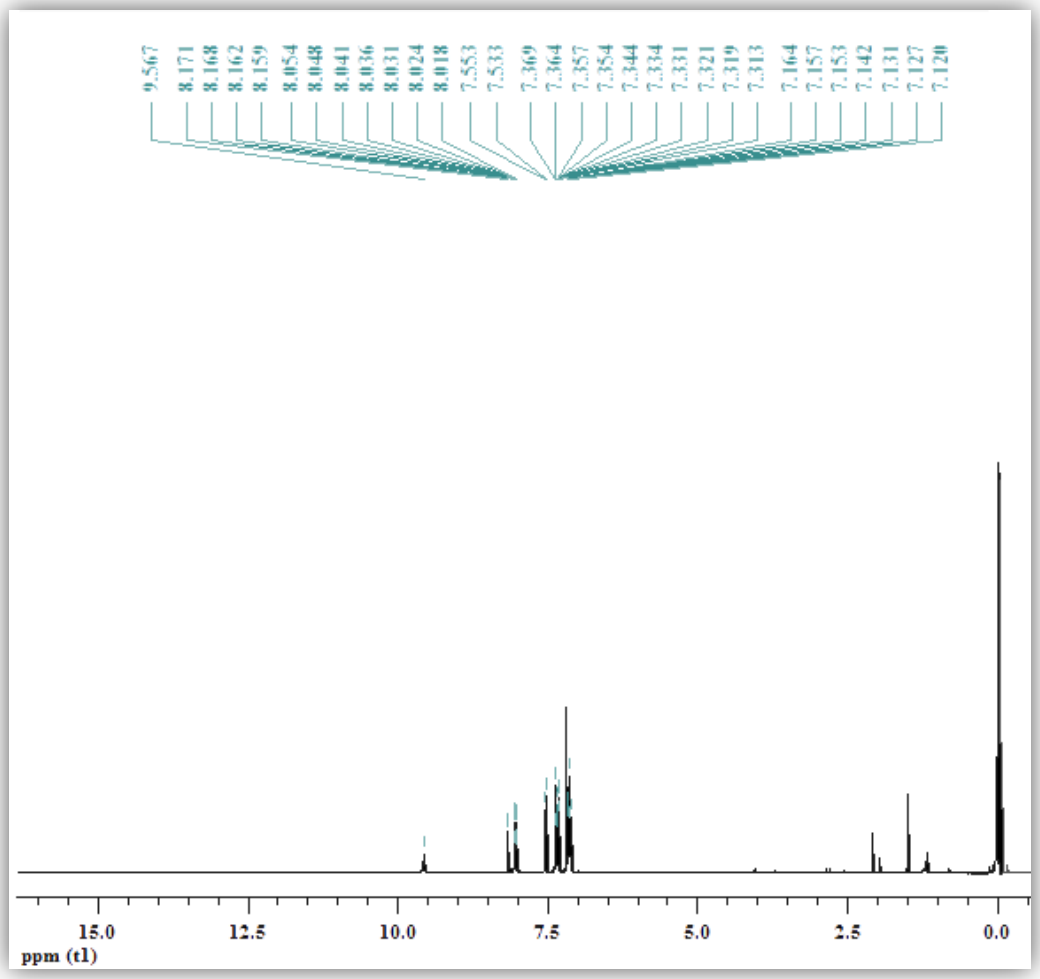

Figure A. 9 ^{1}H-NMR spectrum of 2-(4-fluorophenyl)-4,7-di(thiophen-2-yl)-1H-benzo[d]imidazole

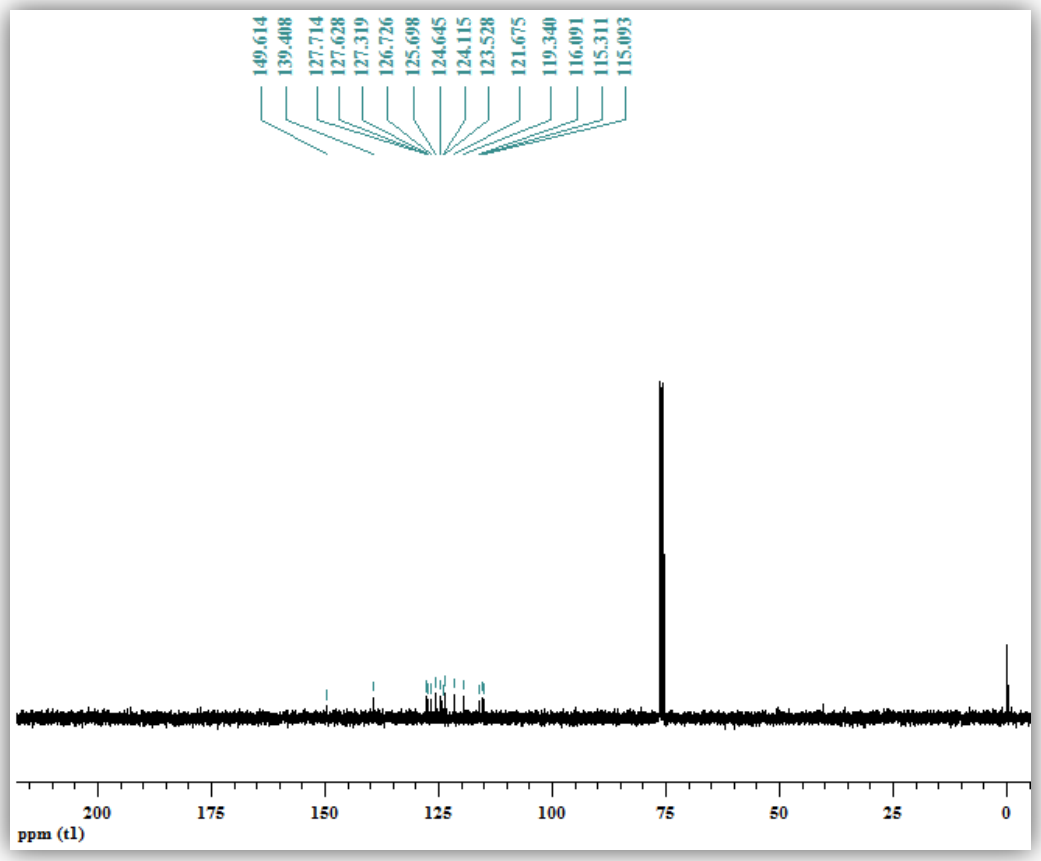

Figure A. 10 ^{13}C-NMR spectrum of 2-(4-fluorophenyl)-4,7-di(thiophen-2-yl)-1H-benzo[d]imidazole

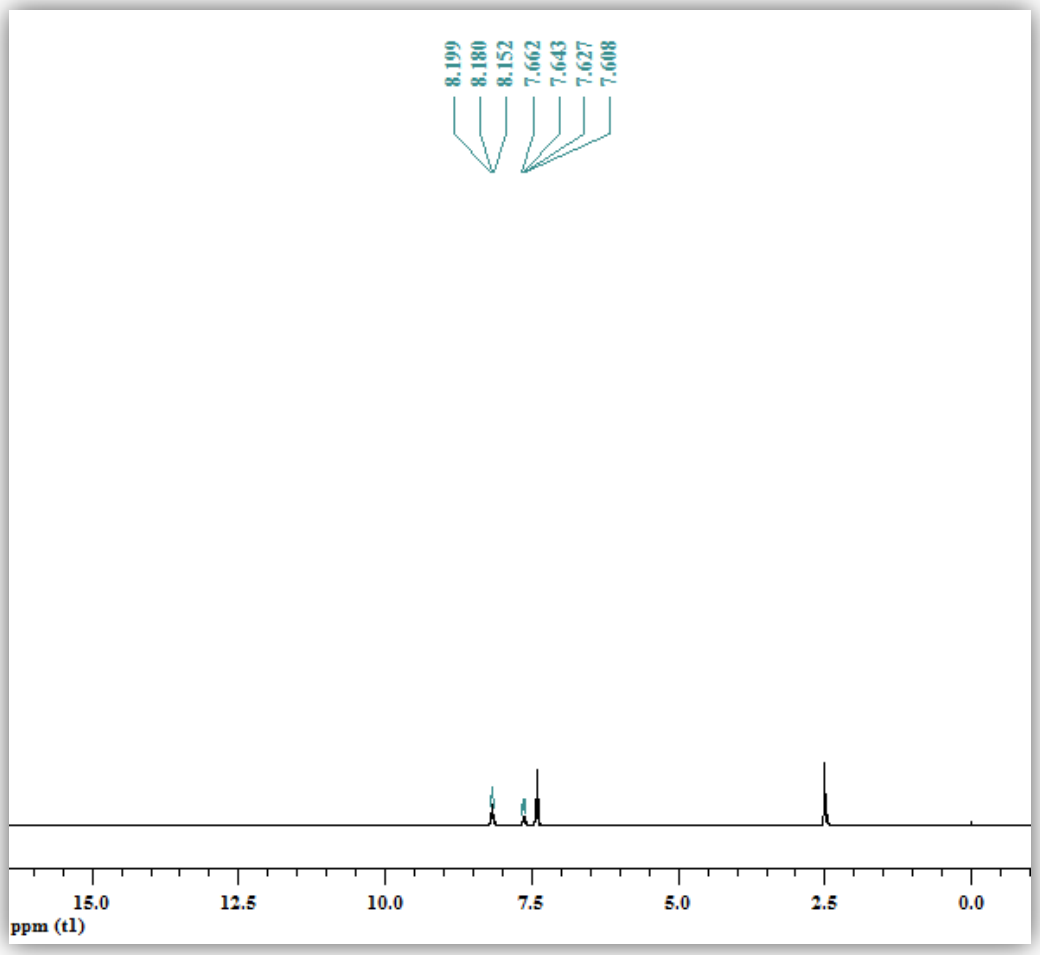

Figure A. 11 ^{1}H-NMR spectrum of 4,7-dibromo-2-(3-fluorophenyl)-1H-benzo[d]imidazole

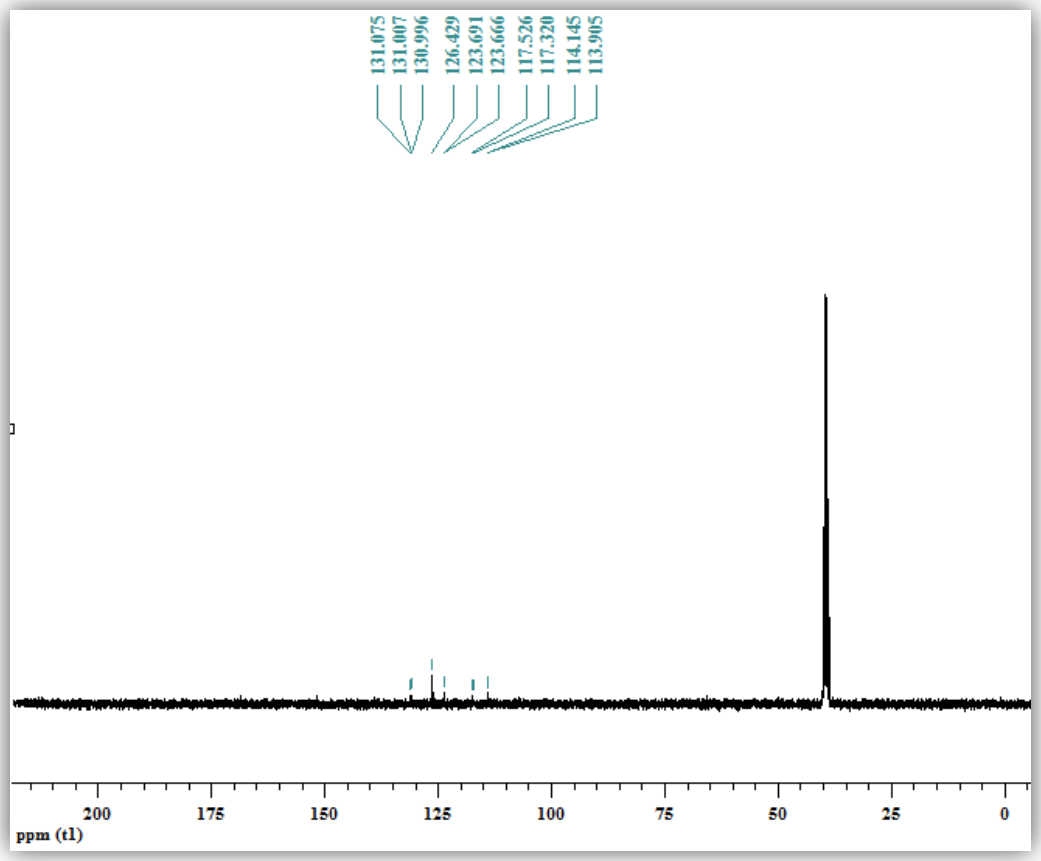

Figure A. 12 ^{13}C-NMR spectrum of 4,7-dibromo-2-(3-fluorophenyl)-1H-benzo[d]imidazole

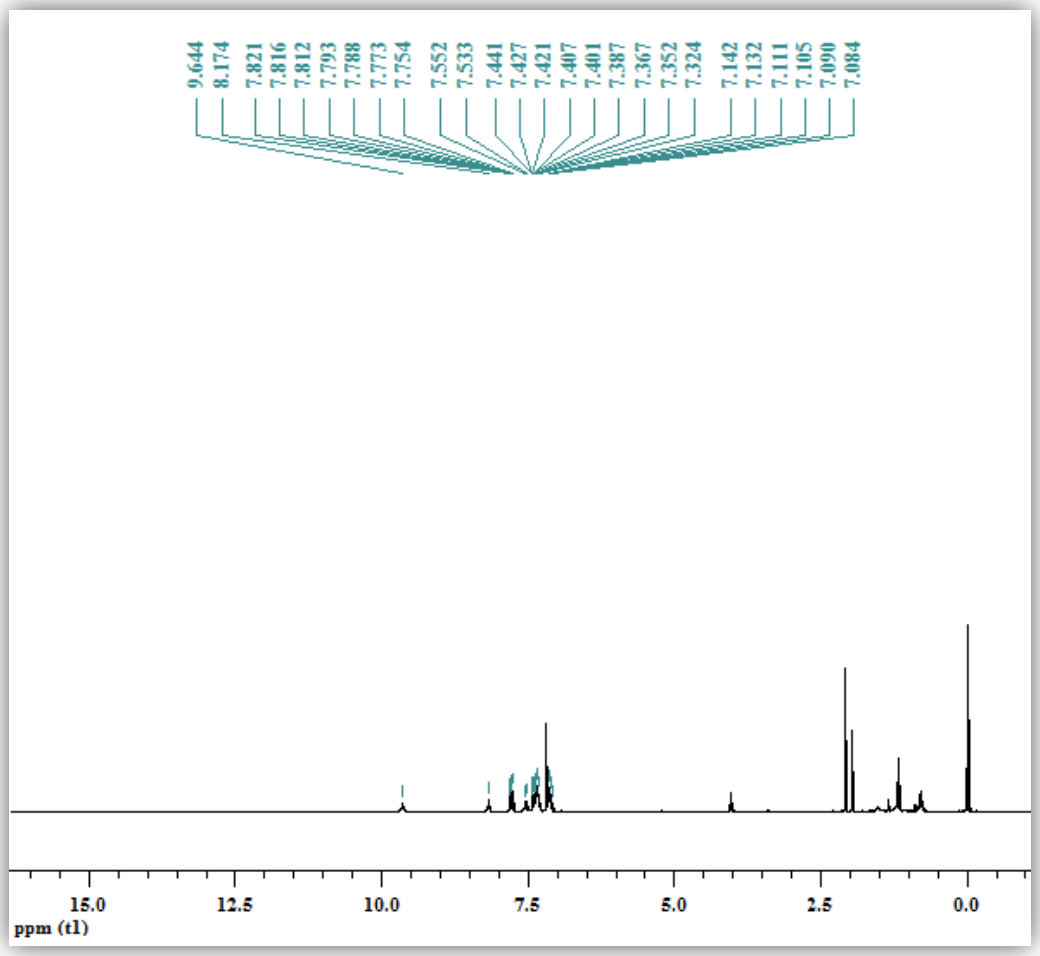

Figure A. 13 ^{1}H-NMR spectrum of 2-(3-fluorophenyl)-4,7-di(thiophen-2-yl)-1H-benzo[d]imidazole

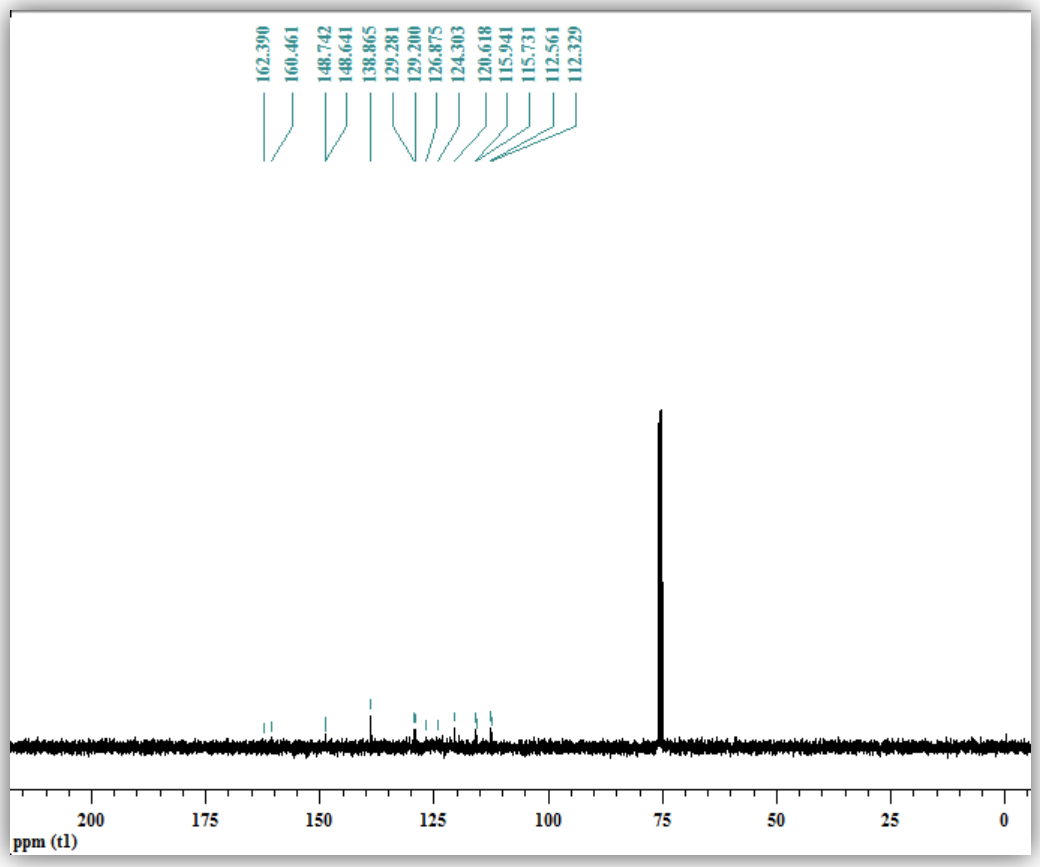

Figure A. 14 ^{13}C-NMR spectrum of 2-(3-fluorophenyl)-4,7-di(thiophen-2-yl)-1H-benzo[d]imidazole

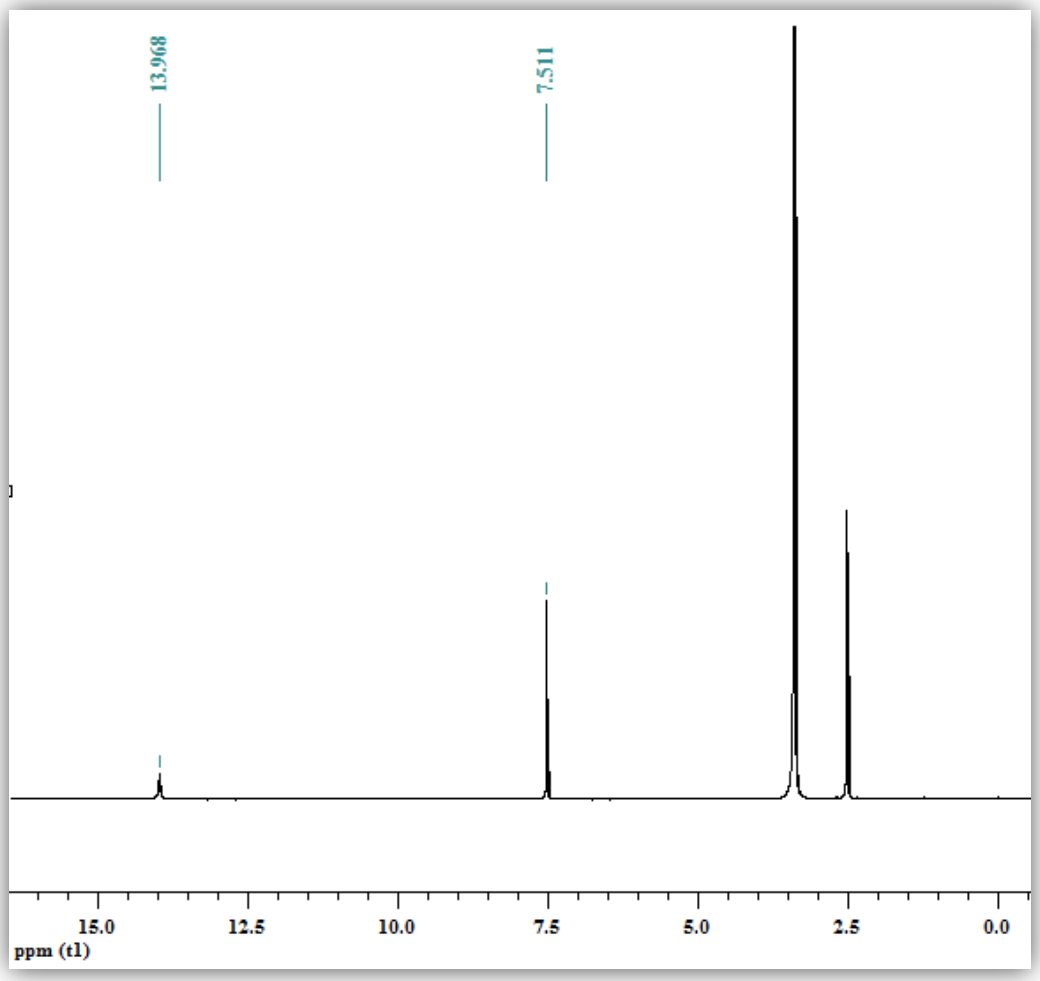

Figure A. 15 ^{1}H-NMR spectrum of 4,7-dibromo-2-(perfluorophenyl)-1H-benzo[d]imidazole

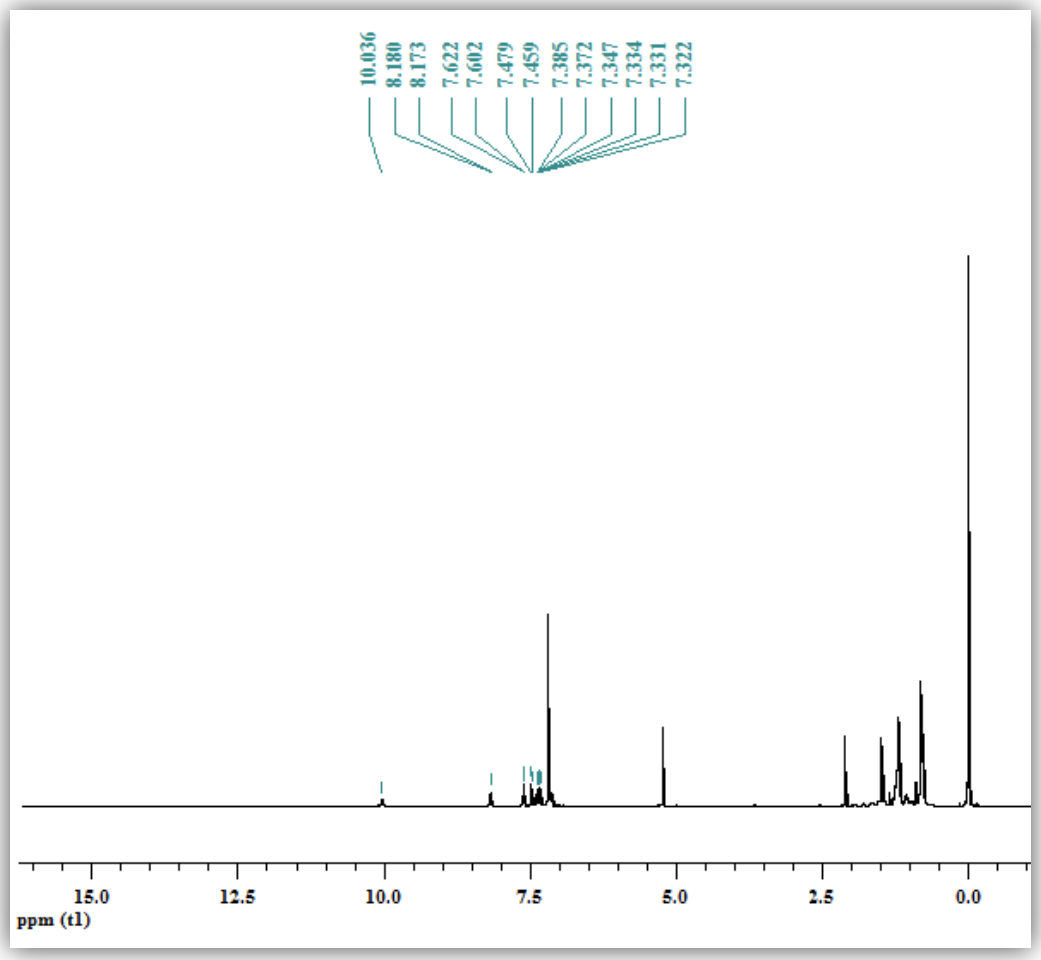

Figure A. 16 ^{1}H-NMR spectrum of 2-(perfluorophenyl)-4,7-di(thiophen-2-yl)-1H-benzo[d]imidazole

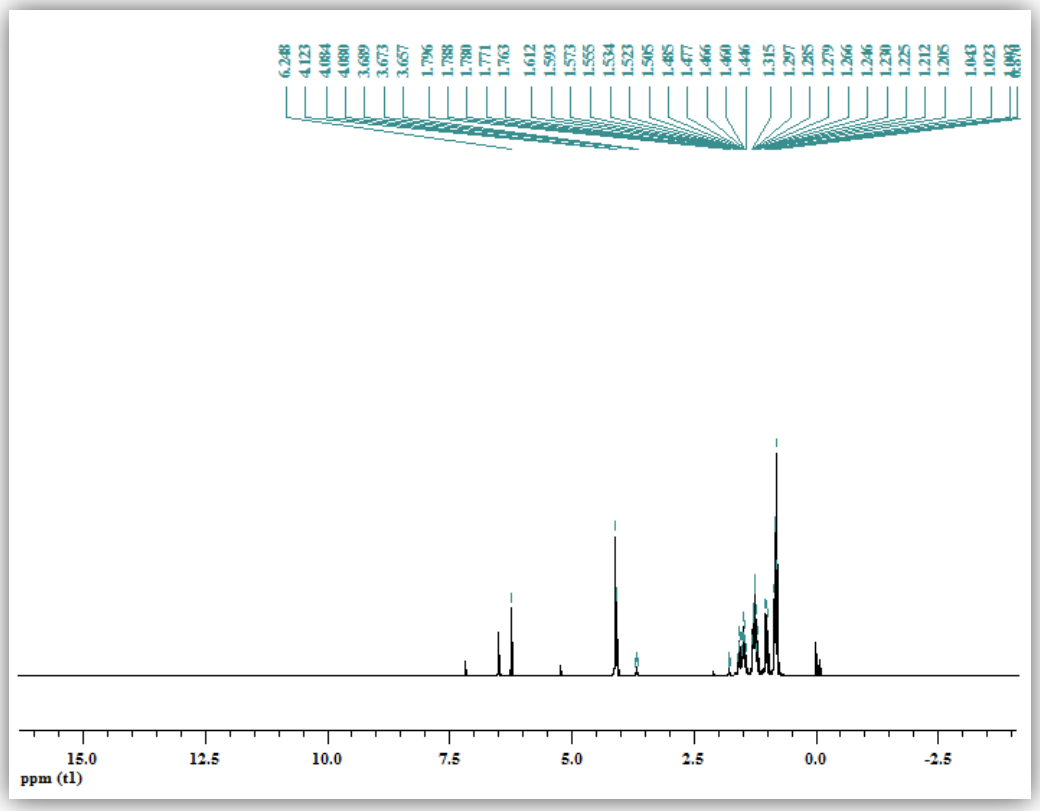

Figure A. 17 ^{1}H-NMR spectrum of tributyl(2,3-dihydrothieno[3,4-b][1,4]dioxin-5-yl)stannane

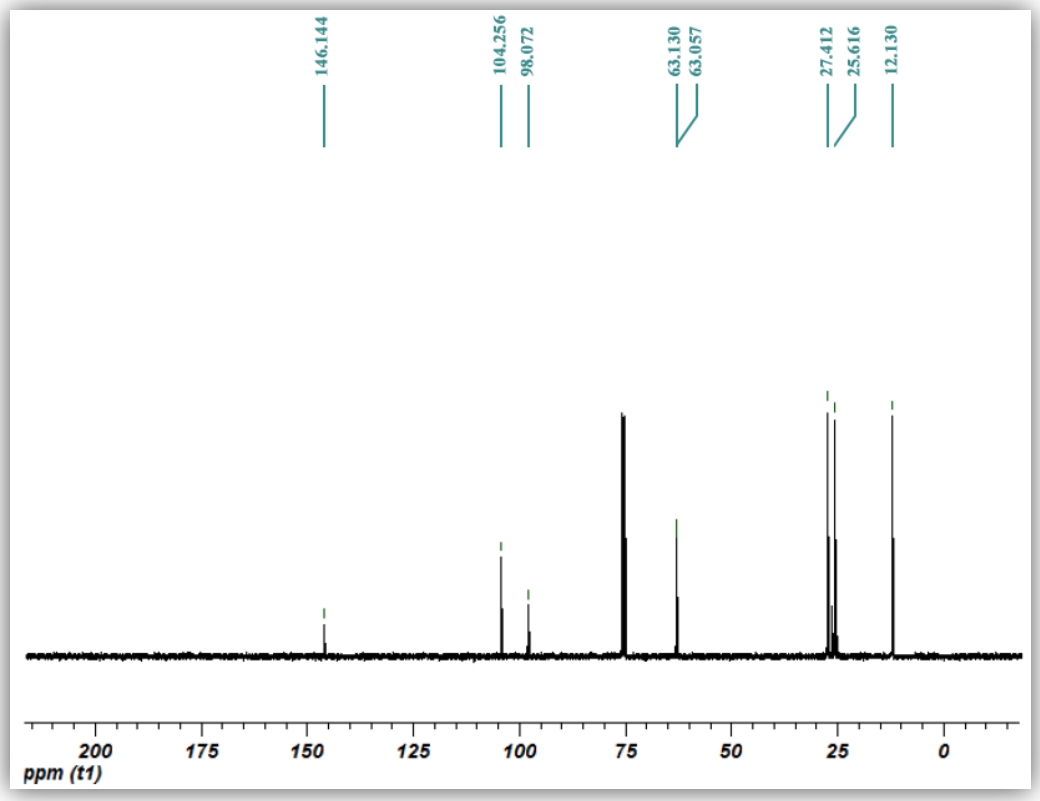

Figure A. 18 ^{13}C-NMR spectrum of tributyl(2,3-dihydrothieno[3,4-b][1,4]dioxin-5-yl)stannane

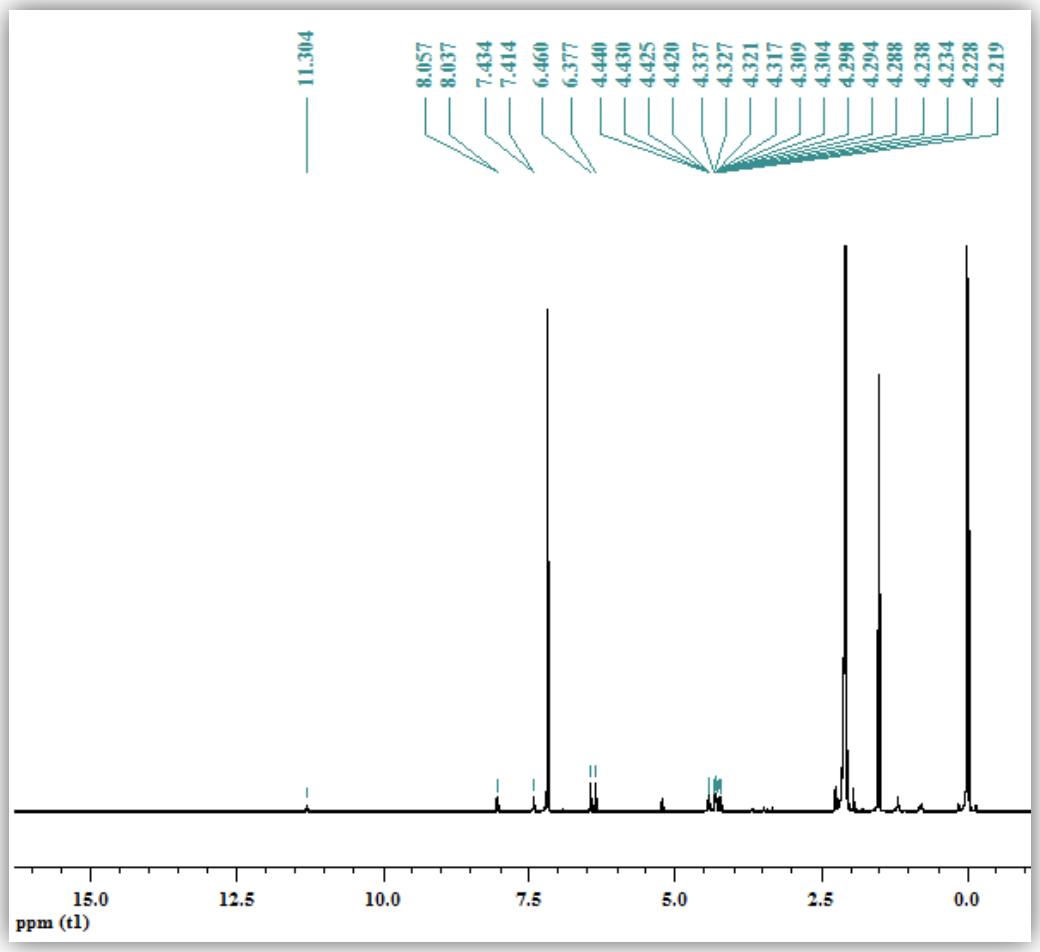

Figure A. 19 ^{1}H-NMR spectrum of 4,7-bis(2,3-dihydrothieno[3,4-b][1,4]dioxin-5-yl)-2-(perfluorophenyl)-1H-benzo[d]imidazole